X-752-72-438

PREPRINT

NASA TM X- 66118

ELLIPTICAL STORM CELL MODELING OF DIGITAL RADAR DATA

FREDERICK J. ALTMAN

MARCH 1972

GSFC

GODDARD SPACE FLIGHT CENTER

GREENBELT, MARYLAND

(NASA-TM-X-66118) ELLIPTICAL STORM CELL MODELING OF DIGITAL RADAR DATA F.J. Altman (NASA) Mar. 1972 86 p CSCL 04B

N73-12661

Unclas

G3/20 49152

X-752-72-438

ELLIPTICAL STORM CELL MODELING OF DIGITAL RADAR DATA

Frederick J. Altman

March 1972

GODDARD SPACE FLIGHT CENTER
Greenbelt, Maryland

ABSTRACT

A new model for spatial distributions of reflectivity in storm cells has been fitted to digital radar data from the National Severe Storms Laboratory (NSSL) in Oklahoma for May 1968 and from the MIT Lincoln Laboratory in Massachusetts for July 1970. The NSSL data were taken with a modified WSR-57 weather radar with 2.6-km resolution.

The NSSL data consisted of modified B-scan records on magnetic tape of storm cells tracked at 0° elevation for several hours. The Millstone Hill MIT L-band radar with 0.8-km resolution produced cross-section data on several cells at 1/2° elevation intervals. The model developed uses ellipses for contours of constant effective-reflectivity factor Z with constant orientation and eccentricity within a horizontal cell cross section at a given time and elevation. The centers of the ellipses are assumed to be uniformly spaced on a straight line, with areas linearly related to $\log Z$. This asymmetrical model can display the steep gradient in $\log Z$ at some cell aspect found by Shaw and others. All cross sections are similar at different heights (except for cell tops, bottoms, and splitting cells), especially for the highest reflectivities; wind shear causes some translation and rotation between levels. Goodness-of-fit measures and parameters of interest for 204 ellipses are considered. The model was found to be a good representation of the reflectivity and attenuation of intense storm cells, although more investigation is required of the problem of cell splitting.

ACKNOWLEDGMENT

The assistance of Peter Carlston and Scott Jones in programing and documentation is gratefully acknowledged. The former wrote section 4.2.

CONTENTS

CONTENTS (Continued)

Section 1
INTRODUCTION

1.1 GENERAL

This document is the final report on the storm modeling study performed by Computer Sciences Corp. (CSC) for NASA under contract NAS5-21638. The general problem is prediction of interference between space and terrestrial communication systems caused by precipitation scattering. Specifics of the problem and the approach to its solution are summarized in the following section, which includes a summary of previous work by CSC in the field and an indication of work to be done. Other sections present radar data, methodology, storm modeling, results, and conclusions. It may be noted that the storm models developed have application to studies of attenuation of radio waves as well as scattering, and also to various meteorological storm studies and hydrological simulations of the water cycle.

1.2 SUMMARY

To support the sharing of frequency bands by space and terrestrial radio communication services, the CCIR (International Radio Consultative Committee) has instituted Study Programme 5-1D-1/5, including the determination of the average distribution in time and space of observed values of effective scattering cross section per unit volume of precipitation as a function of height above ground, time of day, season, and climatic region. The observations used in the present study are digitized reflectivity-factor (Z) data from radars at the Massachusetts Institute of Technology Lincoln Laboratory (MIT-LL) and the National Severe Storms Laboratory (NSSL). The data are essentially horizontal sections through storm cells. (See table 1-1.)

Table 1-1.—Radar and Data Characteristics

Source	NSSL	MIT-LL
Area	Oklahoma	New England
Date	May 1968	July 1970
Time	1735 to 2020	2310 to 0003
3-dB beamwidth	2.0°	0.7°
Range resolution	2.6 km	0.8 km
Tilt	0°	1° to 5°

The approach used was to assume a model, fit it to the data, and compute the error of fit. The basic model for a contour of constant reflectivity is an ellipse of the same area, as suggested by Rogers and Rao (ref. 1) as well as Amorocho (ref. 2). The former authors assumed ellipses all of the same orientation, with those in a set for a given cell and height concentric but with different eccentricities. The model used here assumes different orientations for different sets, but the same orientation and eccentricity within a set. Furthermore, the ellipse centers of a set are assumed uniformly spaced on a straight line. As suggested by previous work and that of Hudlow (ref. 3), the square roots of the areas within a set are considered a linear function of $\log Z$. This asymmetrical model can display the discontinuity in reflectivity at some cell aspect found by Shaw (ref. 4) and Donaldson.[1]

The assumed model was found to represent the contours of a storm cell cross section at a given height very well in general. A median error E of 25 percent was found in fitting individual ellipses to 204 contours:

$$E = 100\,\frac{U - X}{U}$$

where

U = union, area within either ellipse or contour

X = intersection, area within both ellipse and contour

The median additional error resulting from the constraints of the above assumptions on ellipses within a set was less than 5 percent. It was found that three horizontal sets, for heights of about 5, 6, and 7 km, could be well represented by the same set model, so that the proposed cell model consists of nested, vertical elliptical cylinders, displaced or rotated at some heights by wind effects, with rounded or plumed tops and flattish bottoms. A typical horizontal cross section, with $\log Z$ considered as a third dimension, is an asymmetrical elliptical paraboloid.

In spite of displacement and rotation of the basic cylinder at some heights, the peak reflectivity Z_0 and the slope of the fitted linear profile, $\log Z_0$/(max area), varied very slowly spatially from height to height with the MIT-LL data, or from time to time at a given height with the NSSL data. The samples were too small to establish appropriate storm cell classes or characteristic parameters for each. However, it appears that the data resolution was adequate and that the model is accurate and general enough to describe the intense cells, which seem to be the most definitely structured. The chief problem encountered was incipient or actual splitting of a single cell at one or more levels.

A comparison was made of the attenuation along paths through the centers of five horizontal sections of one cell (MIT-LL cell A) as observed and as modeled by ellipse sets. The agreement at three of the levels was excellent, but at two levels it was degraded because the orientation of the core $\log Z = 4$ ellipse remained relatively constant with height, whereas the average rotated counterclockwise (ccw). It may therefore improve the model for some

[1] Ralph J. Donaldson (Air Force Cambridge Research Labs.), personal communication, Nov. 1970.

purposes to use the core orientation for the ellipse set instead of the average of the individual orientations.

Many more storm cells should be processed to verify the model parameters derived and to suggest appropriate methods for treating splitting cells, or at least to indicate the magnitude of the problem.

Section 2
OVERVIEW OF STORM MODELING

2.1 INTRODUCTION

In section 1 the broad problem was stated to be prediction of precipitation-scatter interference. More specifically, it is to predict distributions of effective scattering cross section per unit volume as functions of time and space in two scales with different orders of magnitude. Permissible interference is defined in terms of very small fractions of an hour, and precipitation is known to vary considerably in distances less than a kilometer. So on the one hand, distributions with resolutions of seconds and meters are of interest; on the other, these distributions are wanted as functions of season and climate, with scales of months and hundreds of kilometers. It is not surprising that the solution of this problem is not yet at hand.

2.2 APPROACH

One possible type of solution is experimental, the measurement of enough known configurations in enough places for sufficient time. As will be shown, this is impractical even in a rather trivial case. A more fruitful approach is analytic, to study the nature of the distributions of interest with a view to relating them to some broad existing data base. The only available data useful for this approach are radar reflectivity and surface rainfall. Only weather radars specially equipped for digital storage can provide useful resolution in time and space, including height, and useful quantities of storm records. (See sec. 4.1.1.) Thus, for a first approach, Rayleigh scattering is assumed and radar backscatter data are used. Second, the only data base broad enough in the large scales of space and time is found in the world's rainfall archives of approximately a hundred years. Not every country, however, can match the U.S. hourly precipitation data from gages spaced about 50 km (30 n. mi.) apart in many areas. Fortunately, the United States is subject to a wide variety of climates, so that results found should not be difficult to extrapolate to similar climatic regions elsewhere. Therefore, the problem is resolved into a study of the characteristics of reflectivities aloft using radar data, of rainfall on the surface, and determining their correlations so that one may be predicted from the other.

Studies of reflectivity and rainfall require reduction of large volumes of data to a small number of characterizing parameters. This process can be based on assumption and evaluation of models. (See sec. 4.1.) These models may ultimately be somewhat sophisticated, like the one for storm cells proposed and given preliminary evaluation in this report. A simple, yet powerful model developed in earlier work is the linear storm profile stressed in this section. In general, a profile is a plot of one variable as a function of another, but such a curve

may require many parameters or the plot itself for storage and manipulation. It is much more convenient if appropriate scales can be found for the quantities of interest so that the profile is, with acceptably small error, a straight line. Two numbers, a slope and intercept or two intercepts, then characterize the function for efficient storage and simplified usage. The finding of such useful models is stressed. It will be noted by reference to the literature that only models involving extensive averaging in time and space, and hence of limited application, have been available, and that those found in the previous work (secs. 2.4 and 2.5) and only recently confirmed by others are in some ways still ahead of the state of the art. Two applications seem to merit particular attention. The first is the use of a field of rain gages as a sort of low-resolution radar with hourly scans to provide area sampling that, from preliminary results, would avoid the pitfalls of sampling sparse data at one point only and provide profiles analogous to those found with radar data. The second interesting application of the linear profile is to use radar data quantized to a few levels to characterize about a 60-dB range in reflectivity, to derive peak values with a useful degree of accuracy.

2.3 EXPERIMENT VERSUS ANALYSIS

It would seem that storm models could be developed either by experiment or by study, or perhaps by an optimal combination of studies checked by experiments. However, there is an inherent danger in relying on experiments based on insufficient sampling of rare events. This is well brought out by the reluctance of a British expert, E. G. Bilham, to rely on even 50 years of point-rainfall records. He indicates that even decades without intense rains in a small area are more likely due to chance than to climate and states (ref. 5) that "the really intense rains lasting no more than an hour or two seem to be distributed without regard to the annual average rainfall." The principle involved is not, of course, to avoid experiment, but rather to avoid reliance on too little data to warrant the conclusions desired. It will be seen below that this problem is overcome by use of radar or rainfall data from a circle of about 185-km (100 n. mi.) radius; i.e., area rather than point sampling.

2.4 SUMMARY OF PREVIOUS WORK

2.4.1 Composite Radar Profiles

The earliest extensive body of rainfall reflectivity data was taken at X-band with an AN/CPS-9 radar at Montreal Airport by McGill University's Stormy Weather Group from May to September 1963. CSC Report 453340 (ref. 6), prepared under NASA contract NASW-1216, used this data base and appropriate geometry, often approximate, to develop the preliminary results for intersecting beams that are reported in CCIR Report 339. Monthly profiles included all types of rainfall and the underlying assumption was made that the reflectivity was uniformly distributed; i.e., equally likely to occur anywhere in the 185-km (100-n. mi.) circle of observation or in the worst month of observation. In spite of some obvious possibilities for error, this was a useful first approach. Unfortunately, McGill's present radar is not appropriately equipped to produce digitized data, and early radar data of NSSL were not satisfactory, although some of those data are considered below and more should be processed for additional information.

2.4.2 Hourly Radar Profiles

Even though the early NSSL data were not accurate, the errors were apparently systematic so that many relationships were preserved; the data were used in CSC Report 6012-1 (ref. 7) to derive characteristics of height and reflectivity profiles which have proven useful as bases for later work. The data used were taken by NSSL using a modified WSR-57 radar at Norman, Okla., from April to June 1966. As detailed in reference 7, the S-band data were quantized in square units 2.6 km (1.4 n. mi.) on a side in steps of 10 dBZ (dBZ = 10 log Z) and were used to produce profiles of height versus the square root of the fractional area covered by effective reflectivity factor Z above some value, and of log Z versus the same abscissa. On the scales indicated, the profiles were surprisingly linear and constant in slope for several consecutive hours. More or less well-separated high- and low-slope categories were found and tentatively labeled for convenience as convective or continuous, respectively. Useful correlations were found between the slopes and other parameters of the height and log Z profiles and in particular between the intercepts of the log Z profiles and the simultaneous radar tops (highest echoes within about 185 km (100 n. mi.) at a quarter before each hour) observed at the Oklahoma City radar of the National Weather Service network. These findings gave hope that a commonly assumed Z-R relationship, where R = rainfall rate in millimeters per hour, would provide log Z profiles from surface data, so that with the heights derived from radar tops and use of two classes of slopes or modes, improved predictions would be possible.

Accordingly, the next stage of the work concentrated on surface rainfall, but two other matters should be noted before leaving the radar study. First, correlations were found, in a separate study, between radar tops all over the United States and hourly rainfalls having an expected 25-yr return period, as found in standard publications. These correlations provide bases for useful criteria as to minimum permissible heights for intersections of beams of space and terrestrial communication systems. Second, selected storm cells from similar 1968 NSSL data were used for development of an ellipse-fitting technique, to be covered in more detail. It was found that the linear profiles of the type mentioned were spurious in convective cases involving only single or closely similar cells. The simplified early method of line fitting had obscured a maximum-height cutoff found by another method and recognized as applicable to single cells.

2.4.3 Rainfall Profiles

In CSC Report 6012-2 (part of Report RC-10245 to the FCC; ref. 8) several types of rainfall profiles were considered, using standard hourly precipitation data from 30 stations fairly uniformly distributed within a 220-km (120-n. mi.) radius of Norman, Okla. It was shown that straight lines generally resulted from plotting cumulative log R distributions versus the square root of fractional time, or area, or area-time product, such as for 30 stations during 20 hr in a month. Such area sampling in terms of N, the number of stations reporting more precipitation than R mm hr^{-1}, exhibited a smoothing tendency explained by two-dimensional extension of the Nyquist sampling theorem and the relatively stable nature of the storms as they pass over one station after another. Not only were linearity and stability

found as with radar data, but also the high and low classes of slope. A study of the literature found agreement with the results of Huff (ref. 9) and Hudlow (ref. 3) as to the suitability of the log R to the square root of area relationship for durations up to a few hours. However, Huff used a gage spacing of only about 5.5 km (3 n. mi.) instead of the ordinary widely spaced data used here. Also, his smaller network with sides 37 km (20 n. mi.) long did not completely cover the widespread low-slope continuous rain configurations. In Report 6012-2 (ref. 8) one storm that evidently consisted of only a single cell in the whole circle of gages was found to have the same linear profile against area found from single-cell radar data. Because of the poor sampling resolution, this profile was relatively inaccurate. The profile was not checked nor compared with the radar data for the same period.

2.5 STORM CELL CHARACTERISTICS

The elemental storm unit to be modeled is the cell. A basic postulate was assumed from observation that even though rainfall may be found in any and all configurations, the high-intensity, high-extent cells of most importance result from organized activity, such as in the supercell discussed by Browning (ref. 10) and others. Thus order may be found where it is of most interest. The ellipse was assumed for the basic shape of a contour of constant reflectivity, in the horizontal plane, as was done by Rogers and Rao (ref. 1), providing more flexibility than the circles used by Dennis (ref. 11). The assumptions used here regarding relationships between contours are related to those of Rogers and Rao as shown below:

Assumption	*Rogers and Rao*	*Altman*
Elliptical shape	Yes	Yes
Same eccentricity	No	Yes
Same orientation	All	All in a set
Same centers	Yes	No

Although Rogers and Rao assumed concentric ellipses, in this report the centers of the ellipses in a set for different values of Z at a given time and elevation are assumed to be uniformly spaced on a straight line. This is in agreement with the data and results of Shaw (ref. 4) and of Amorocho (ref. 2).

The remaining factor required to define the model is the relationship of the area within a contour versus log Z at the contour, which gives linear profiles. It was noted previously that the general relationship found in CSC Report 6012-1 was linear for log Z versus the square root of the area. However, for single cells, the abrupt changes of log Z normally found at one aspect of the cell in the raw data, and confirmed by meteorologists experienced in the field, could only imply linearity of log Z versus area, or length squared, a parabolic function. This was also found, as noted, with rainfall data in the case of a single-cell storm. Therefore, it has been concluded that isolated cells or complexes of closely similar cells exhibit profiles linear with area, and that aggregates of dissimilar cells exhibit profiles linear with square root of area. The synthesis of an aggregate from individual cell profiles has not been, but should be, attempted.

The data bases used for the present study of cell characteristics have been given in table 1-1. Results from NSSL data were obtained by the author in a previously unreported study. The study reported here, based on a small amount of data from these two sources, showed the utility of the model assumed and validated its correctness for a set of ellipses at a given time or tilt angle. But the limited data provide only preliminary notions as to the nature of time or space ensembles. It appears, reasonably, that the ellipse parameters vary only slowly from time to time at a given elevation, but vary considerably with height in a single cell because of the change with height of the winds aloft. At present, the best cell model appears to be one of substantially vertical elliptical cylinders, with portions displaced and rotated somewhat by wind shear, and with rounded tops and flat bottoms. Configurations at cell birth, death, and splitting will require more data and study.

2.6 WORK TO BE DONE

Now that radar reflectivity, surface rainfall profiles, and cell characteristics have been studied separately, it is important to establish the relationship between peak surface rainfalls and peak reflectivities aloft. This relationship—

(1) Is complex because rain may not fall until late in the storm life cycle and will then be strongly localized in time and space

(2) Has been obscured by the usual averaging in time and space

(3) Should be studied with profile technique using both slopes and intercepts, which is more powerful than using averages alone

NSSL radar data and Agricultural Research Service (ARS) rainfall data from the same area in Oklahoma are at hand for April and May of 1969 and available for the same period of 1970. The radar outputs have a resolution of 1.85 km (1 n. mi.), with tilted antenna data to indicate vertical structure. The ARS network comprises about 200 stations on about 5.5-km (3-n. mi.) centers, providing an unusually large, dense system. The profile techniques already developed, and described above, should be used to establish detailed space and time correlations between peak surface rainfall and peak reflectivity aloft to facilitate prediction of precipitation scatter interference.

As the CCIR sharing criteria permit harmful interference no more than about 0.01 percent of the worst month, it is clear that rare events such as storms associated with floods are included, so that methods used in their prediction should be of value. In fact, Bilham and other U.K. and U.S. hydrologists use statistics of extreme values. It is not generally realized that extremes can be more valuable predictors than medians. Further study in this area may be profitable.

Several items suggested by work done in previous studies were noted previously and are summarized here:

(1) The linear $\log R$ to the square root of the area cell profile found in CSC Report 6012-2 (ref. 8) should be checked for accuracy against radar data and the exercise

repeated for other similar data to establish the utility of surface data from normal widespread low-resolution gage networks. If the ARS-NSSL comparison proposed above is performed, the high-resolution ARS network can be progressively degraded by omission of alternate stations to produce even more valuable results.

(2) The synthesis of aggregate profiles from individual cell profiles should be studied to confirm the compatibility of the two profile relationships found in previous studies.

(3) The data base of cell characteristics should be extended far beyond the few cells considered here, which are too few to support any sound conclusions. Because it has been found that useful accuracy can be obtained from coarse data by the profile technique, several years of NSSL April-May data should be processed to insure that the assumptions used here apply to at least the most intense cells and in unusual circumstances. The incidence of splitting should be noted, and if it is found statistically frequent, attempts should be made to model it usefully. Cell sorting could be automated, and statistical summaries of parameters of most interest should be programed.

Section 3
DIGITIZED RADAR DATA

3.1 INTRODUCTION

Before describing in detail the two types of digitized radar data used for this study, it is necessary to establish a uniform nomenclature. This is done with reference to figure 3-1. A *header* line carries a date-time group and other items, followed by a data sequence, a term used loosely here. The data lines are called *records*, made up of *boxes*, each containing a single-digit value of reflectivity factor Z. As the digit may represent Z linearly or logarithmically, the term "intensity" is used for the digit in general. The contiguous group of records making up a cell, or occasionally two cells or a configuration about to split or otherwise irregular, is called a *block*. A group of blocks for a given time and tilt, such as the top two in the figure, is designated a *quadrangle* or *quad.*

3.2 NSSL DATA

The weather radar data system at the NSSL has been described by Wilk et al. (ref. 12). It is based on the WSR-57, the standard weather radar of the National Weather Service, which has the following characteristics–

Wavelength	10 cm
Peak power	450 kW
Pulse length	4 μs
Pulse repetition frequency	164 s^{-1}
Minimum detectable signal	-110 dBmW
Beamwidth	2°
Antenna gain	38.5 dB
Azimuthal scan rate	2 rpm for PPI displays
	0.4 rpm for magnetic tape recording

It has been modified by addition of digital video processing equipment including the Lhermitte integrator developed at NSSL. Lines with reflectivity of log $Z = 4$ or greater from the data recorded on magnetic tape, provided by Kathryn Gray of NSSL, are displayed in figure 3-2. Each sequence starts with a month-day-year-time group and initial range, incremental range, and tilt angle in degrees. The reflectivity data follow in rotated B-scan format (bearing vertical, range horizontal). The first three digits of each line are the azimuth of the 2°-wide antenna beam. The following 77 digits 0 to 5 represent the average log Z in "boxes" 2° wide and 2.624 km (1 range unit (RU) or 1.417 n. mi.) long. The 77 RU's extend from 26.28 to 228.4 km (14.19 to 123.3 n. mi.). Angles are computed on a grid with spacings of 1° by 1 RU, so they are true at about 150 km (80 n. mi. or 50 RU), near the center of the

range. On the printout grid, distances in the azimuth direction are true at about 125 km (67 n. mi. or 41 RU). It should be noted that the B-scan or polar grid is treated as rectangular, as this is closely true for the small cells considered. The raw data are culled to reduce computational load and noise by removing–

(1) Fixed echoes within certain azimuths and ranges

(2) Azimuths containing only 1's

(3) Strings of 1's and single 2's, isolated within an azimuth

(4) Isolated azimuths

(5) Strings of 1's and single 2's, isolated within a range slot

The resulting preprocessed data then appear as in figure 3-1, ready for ellipse fitting, with a header for each quad and a separator after each block to define its range limits.

3.3 MIT DATA

The MIT data are from the Millstone Hill L-band radar of MIT-LL, furnished by Dr. Robert Crane. Table 3-1 tabulates the radar characteristics and table 3-2 shows factors

Table 3-1.–MIT-LL Radar Characteristics

Frequency	1.295 GHz (23.2-cm wavelength)'
Antenna	26-m (84-ft) parabola with Cassegrainian feed
Antenna gain	46.7 ± 0.3 dB ("new" subreflector)
Beamwidth	0.7° between half-power points
Polarization	Right-hand circular transmitted Left-hand circular received
Transmitted power	3.3-MW peak (continuously monitored)
Pulse length	12.4 μs
Pulse repetition rate	120 s^{-1}
Receiver bandwidth	80.5 kHz (12.4-μs matched predetection filter)
Resolution volume	1° by 1.9 km
Data processing	Analog-to-digital conversion of sine and cosine channels every 10 μs
Computer sampling rate	20 s^{-1}
Detection	Square law by computer operations
Dynamic range	80 dB accomplished by combining the output from two receivers
System noise temperature	280 K (includes atmospheric and ground effects averaged over 0° to 30° elevation angle)
Overall system line losses	2.8 dB for receiver 1 43.5 dB for receiver 2
Matched filter processing loss	1.1 dB
Single-pulse value for unity signal-to-noise ratio	−30 dBZ at 100 km

Table 3.2.–MIT-LL Measurement Accuracy

Measurement	Absolute accuracy, maximum, dB	Calibration repeatability, maximum, dB	Sample fluctuation, rms, dB
Transmitter:			
Power monitor[a]	0.2	0.1	0.1
Line loss	.1	–	–
Antenna:			
Transmit and receive gain	.6	–	–
Pattern integration	.1	–	–
Receiver:			
Noise tube	.3	.1	–
Calibrate source:[a]			
Power monitor	.2	.1	–
Attenuator setting	–	.1	–
Line loss	.1	–	–
Estimation error for Rayleigh process	–	–	.7
Measurement of received-to-transmitted power ratio	.7	.2	.7

[a]Includes line loss error (maximum) used to transfer readings to reference points.

affecting radar measurement accuracy. Figure 3-3 outlines the region scanned southwest of the radar in the hour just before midnight of July 29, 1970, during a thunderstorm. The quads of interest are indicated, as well as typical blocks. Echoes in part of the lower left-hand quad and part of the one above it are shown with dBZ values in figures 3-4(a) to (i). The headers show radar tilts or elevation angles from 1° to 5° in 1/2° steps at times from 2310 to 2357 hr. The echoes of most interest are marked A, B, C1, and C2 on figure 3-4(c), showing a scan where all appear.

The computer preprocessing of the MIT-LL magnetic tape record is summarized in figure 3-5. Briefly, the original tape is reblocked as it is copied and quad maps of log Z are prepared. From the latter, blocks of most interest are selected. These are mapped as in figure 3-6. The boxes are 0.7813 km on a side, with intensities given as log Z to one significant figure, so that a 4 is used for $4 \leqslant \log Z \leqslant 5$. The line or record numbering is arbitrary. On the corresponding punched cards it is multiplied by 2 for compatibility with the ellipse-fitting program and the 2° azimuths of the NSSL data. Individual cells in a block are selected and extraneous points are rejected. As shown in figure 3-5, maps and cards are prepared with intensities quantized on linear thresholds as well as logarithmic. The linear thresholds are based on the maximum block intensity M as follows:

Digit	*Fraction of maximum intensity* M
5	0.8 to 1
4	.6 to .8
3	.4 to .6
2	.2 to .4
1	.1 to .2
0	0 to .1

Arbitrary values of M can also be inserted when a storm cell appears on two quads.

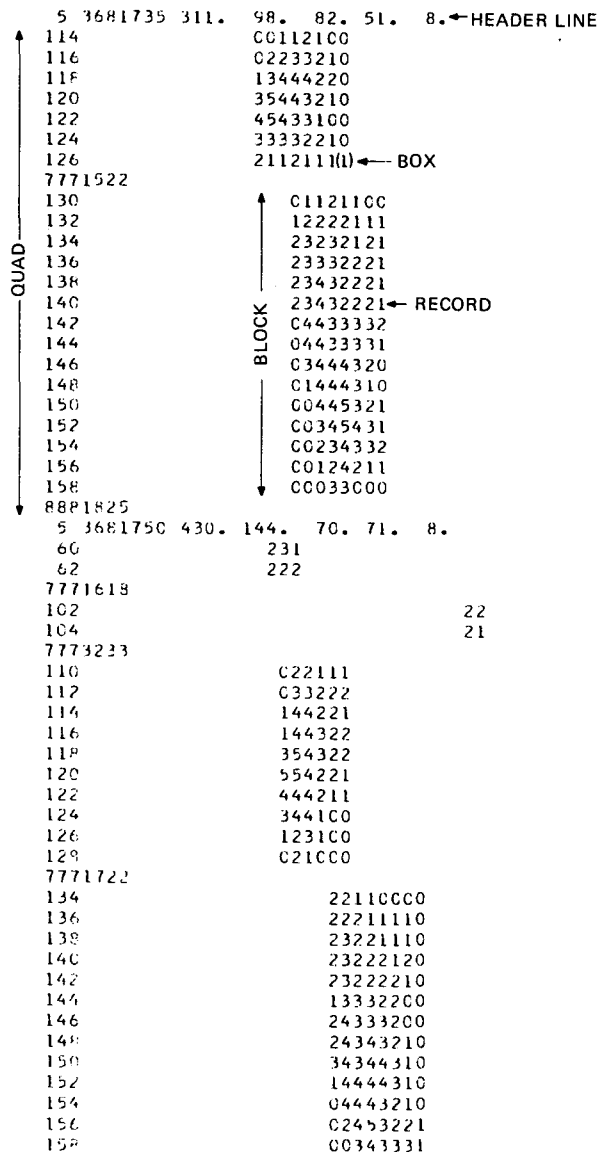

Figure 3-1.—NSSL data blocks.

```
 4  2 68      2001     R1#14.19029     DR#1.417004     ELEV#   0
               262 000000C000000000000C000000000000000000000000000000000000000000000000000000000011223444

ARS NET COUNT#  1
 AREAS FOR EACH Z LEVEL      202.7       63.6       23.6       18.0        0.0

 4  2 68      2015     R1#14.19029     DR#1.417004     ELEV#   0
               264 C000000000000000C000000000000000C000000000000000000000000000000000000000123344342
               266 0000000000000000000000000000000000000000000000000000000000000000000122223343222

ARS NET COUNT#  2
 AREAS FOR EACH Z LEVEL      400.7       93.6       53.6       23.4        0.0

 4  2 68      2030     R1#14.19029     DR#1.417004     ELEV#   0
               268 C000000000000000000C000000000000000000000000000000000000000000000012344433321 11

ARS NET COUNT#  1
 AREAS FOR EACH Z LEVEL      532.5      169.7       62.5       16.5        0.0

 4  2 68      2045     R1#14.19029     DR#1.417004     ELEV#   0
               262 000000C000000000000C000000000000000000000000000000000000000000000000000001344310
               264 000000000000000000000000000000000000000000000000000000000000000000000123444330
               266 000000C000000000000000000000000000000000000000000000000000000000000001233334210
               268 000000000000000C000C000000000000C000000000000000000000000000000000001234332221 00
               270 0000000000000000000C000000000000000000000000000000000000000000000013334442321 1000
               272 000000C000000000000000000000000000000000000000000000000000000000011223443121 01000

ARS NET COUNT#  6
 AREAS FOR EACH Z LEVEL      823.6      267.4      140.9       67.4        0.0

 4  2 68      2100     R1#14.19029     DR#1.417004     ELEV#   0
               264 000000000000000000000000000000000000000000000000000000000000000000001344320100 00
               266 000000000000000000000000000000000000000000000000000000000000000000012444210000 00
               268 000000000000000000000000000000000000000000000000000000000000000000123444312100 00
               270 0000000000000000000C000000000000000000000000000000000000000000000013432221100 0000
               272 000000C000000000000000000000000000000000000000000000000000000000014333420000 0000
               274 000000000000000000000000000000000000000000000000000000000000000010111344332100 0000
```

Figure 3-2.—NSSL raw data.

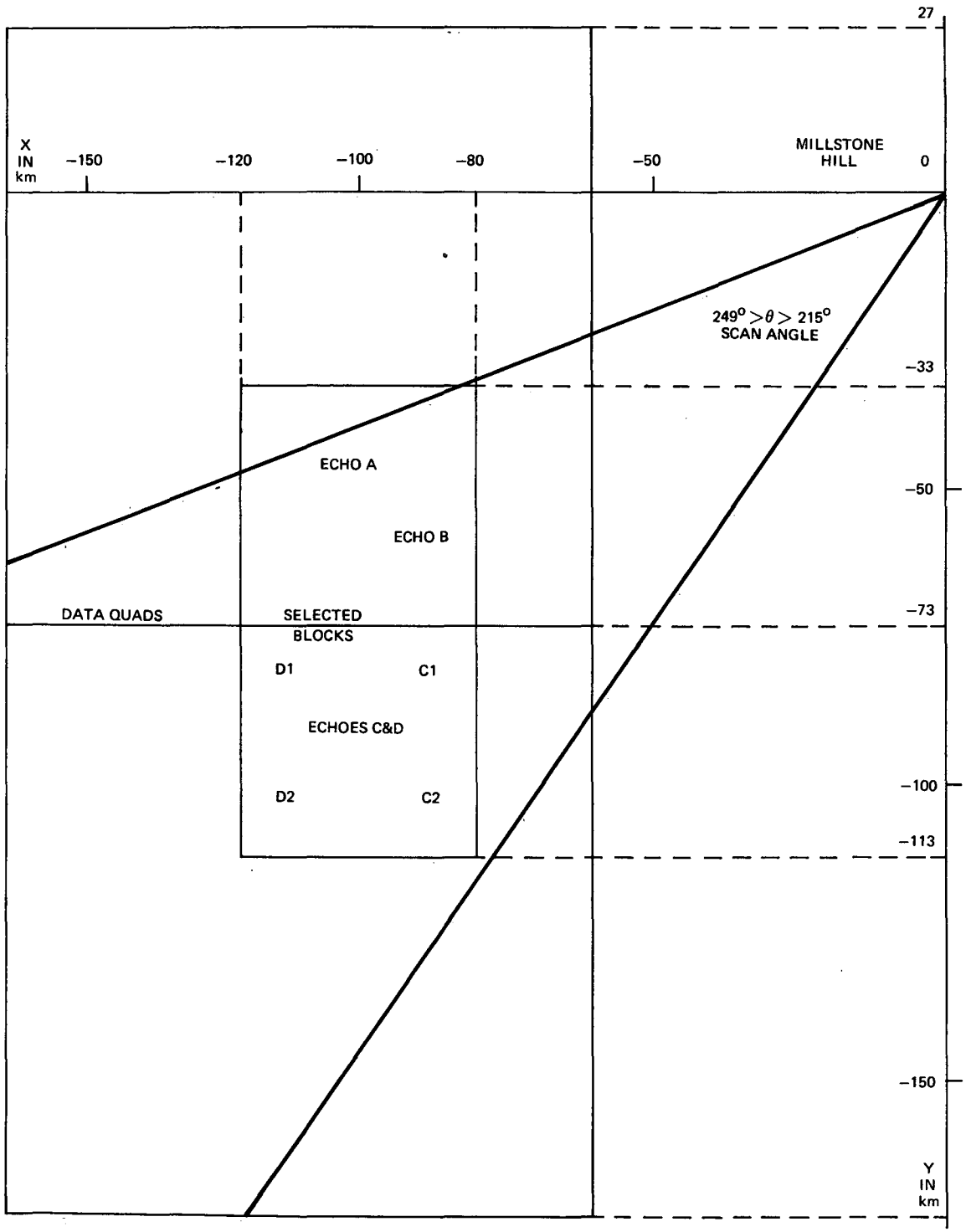

Figure 3-3.—MIT-LL radar scan.

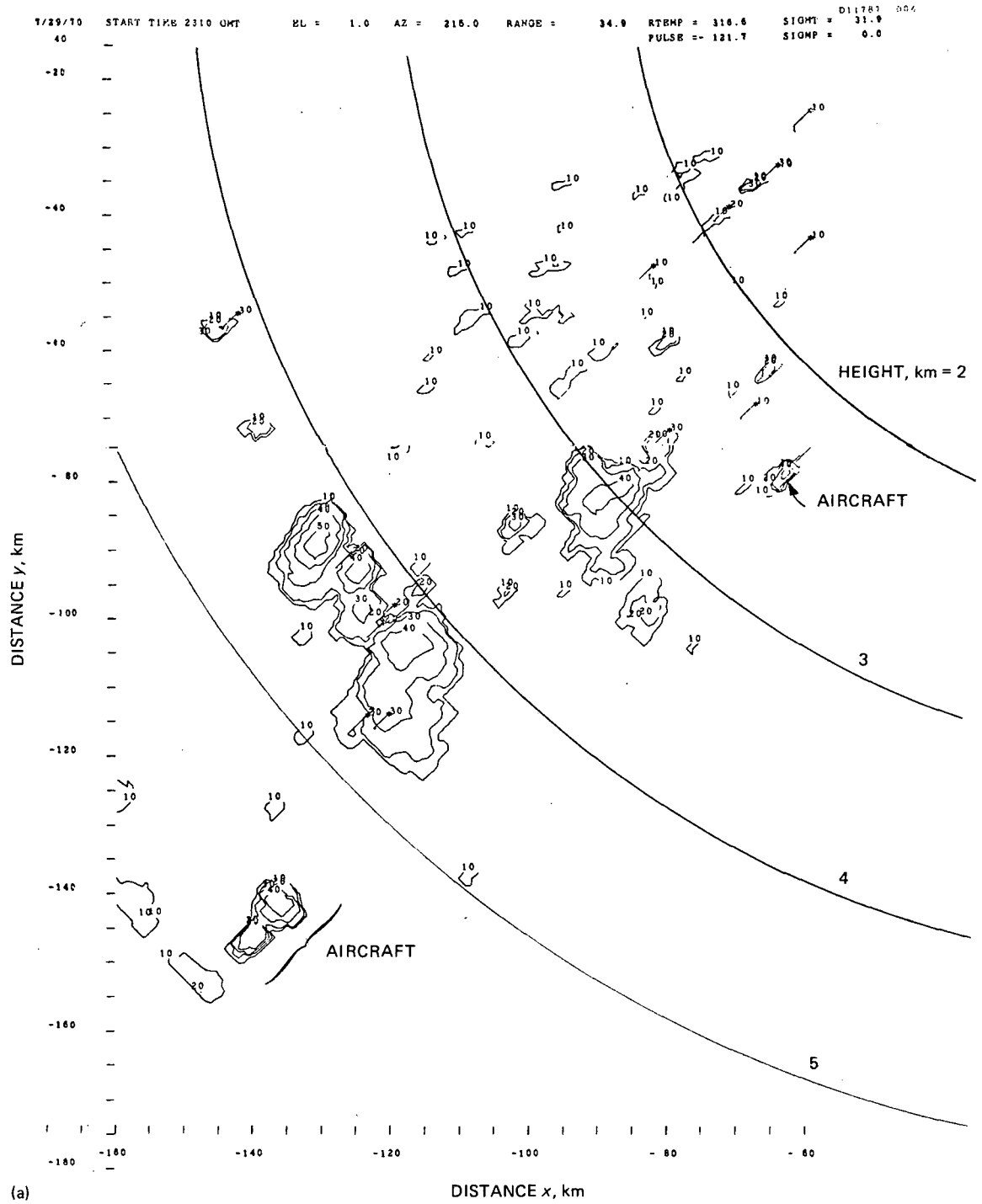

Figure 3-4.—MIT-LL July 29, 1970, radar map. (a) Time, 2310; elevation, 1.0°.

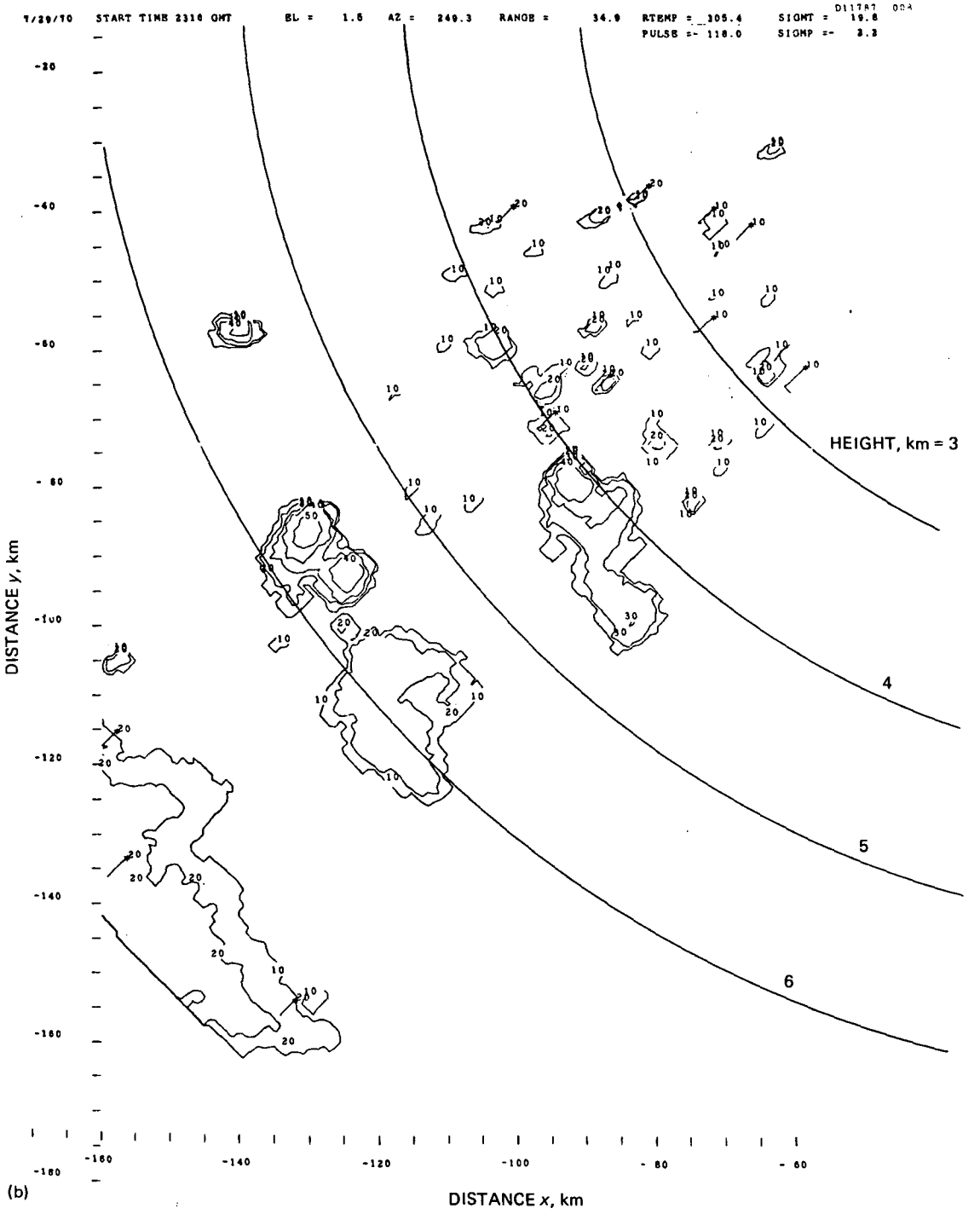

Figure 3-4 (continued).—(b) Time, 2316; elevation, 1.5°.

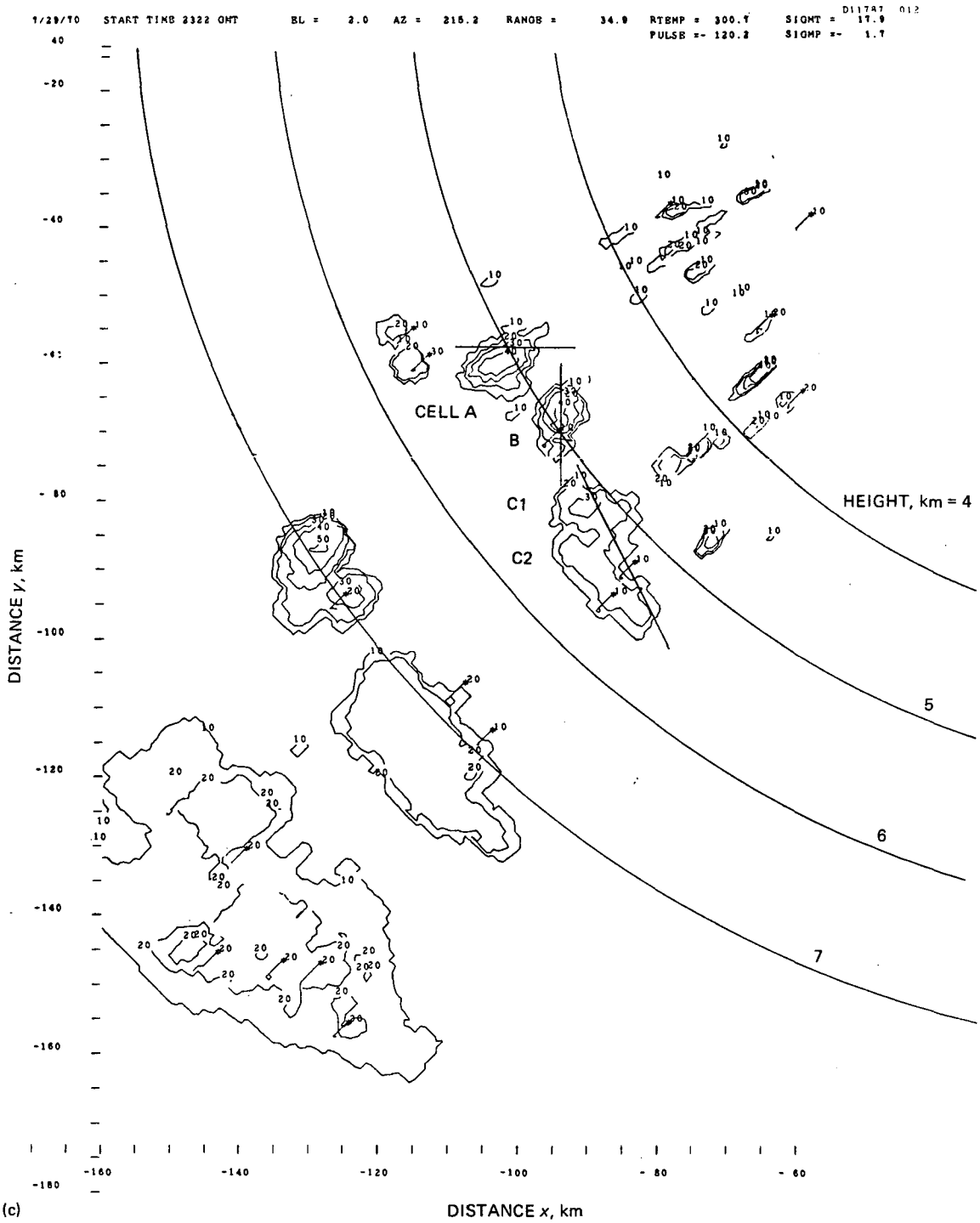

Figure 3-4 (continued).—(c) Time, 2322; elevation, 2.0°.

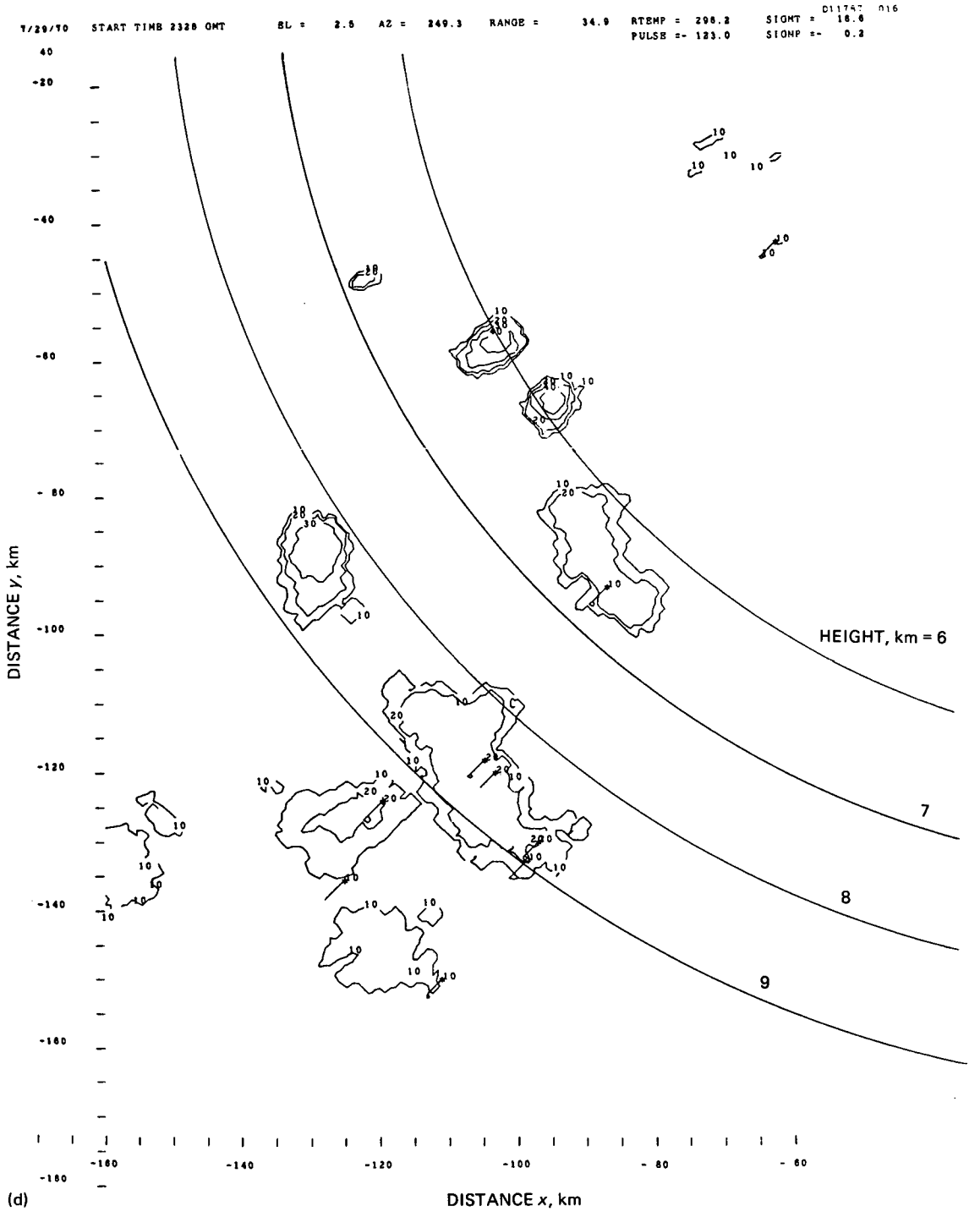

Figure 3-4 (continued).—(d) Time, 2328; elevation, 2.5°.

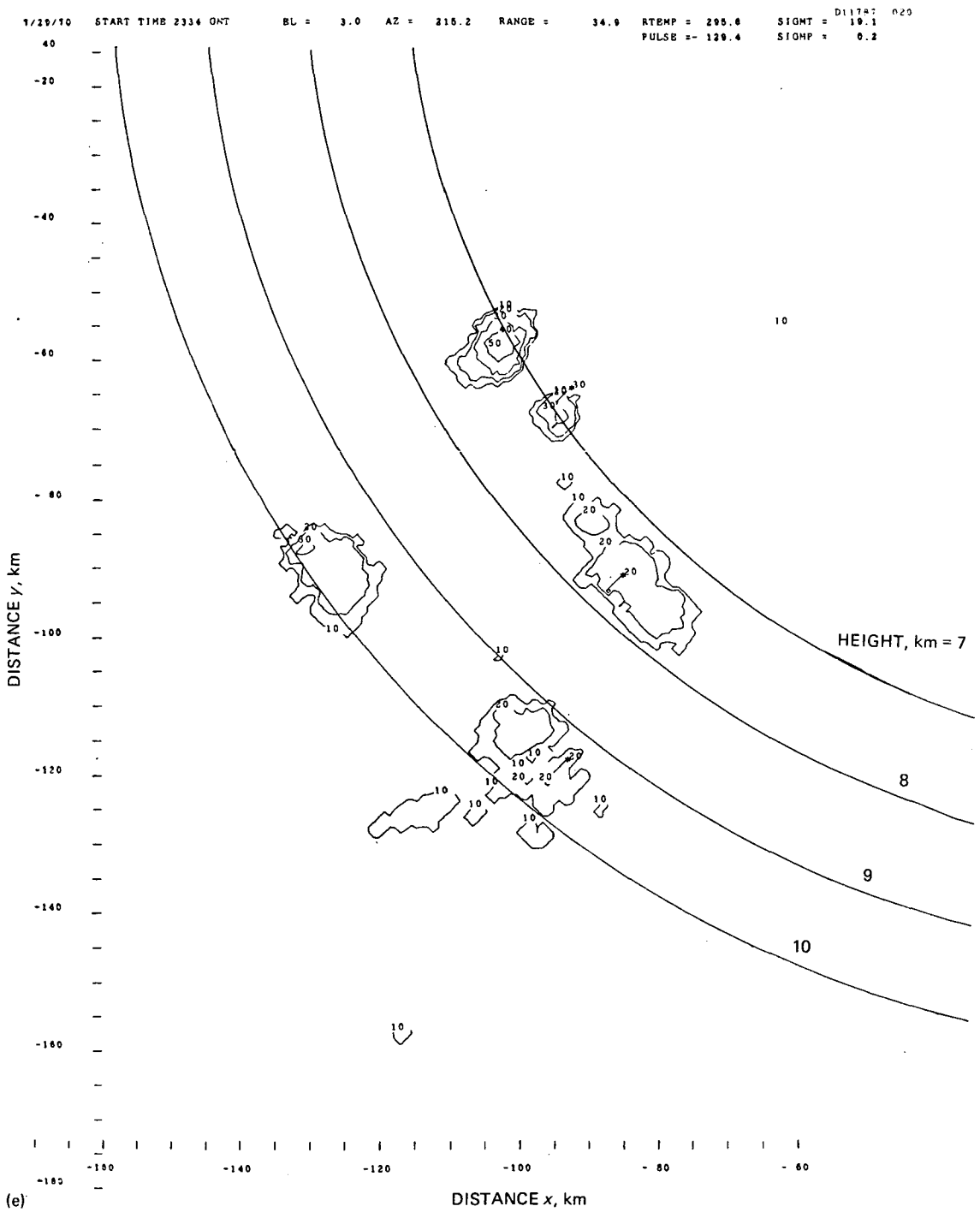

Figure 3-4 (continued).—(e) Time, 2334; elevation, 3.0°.

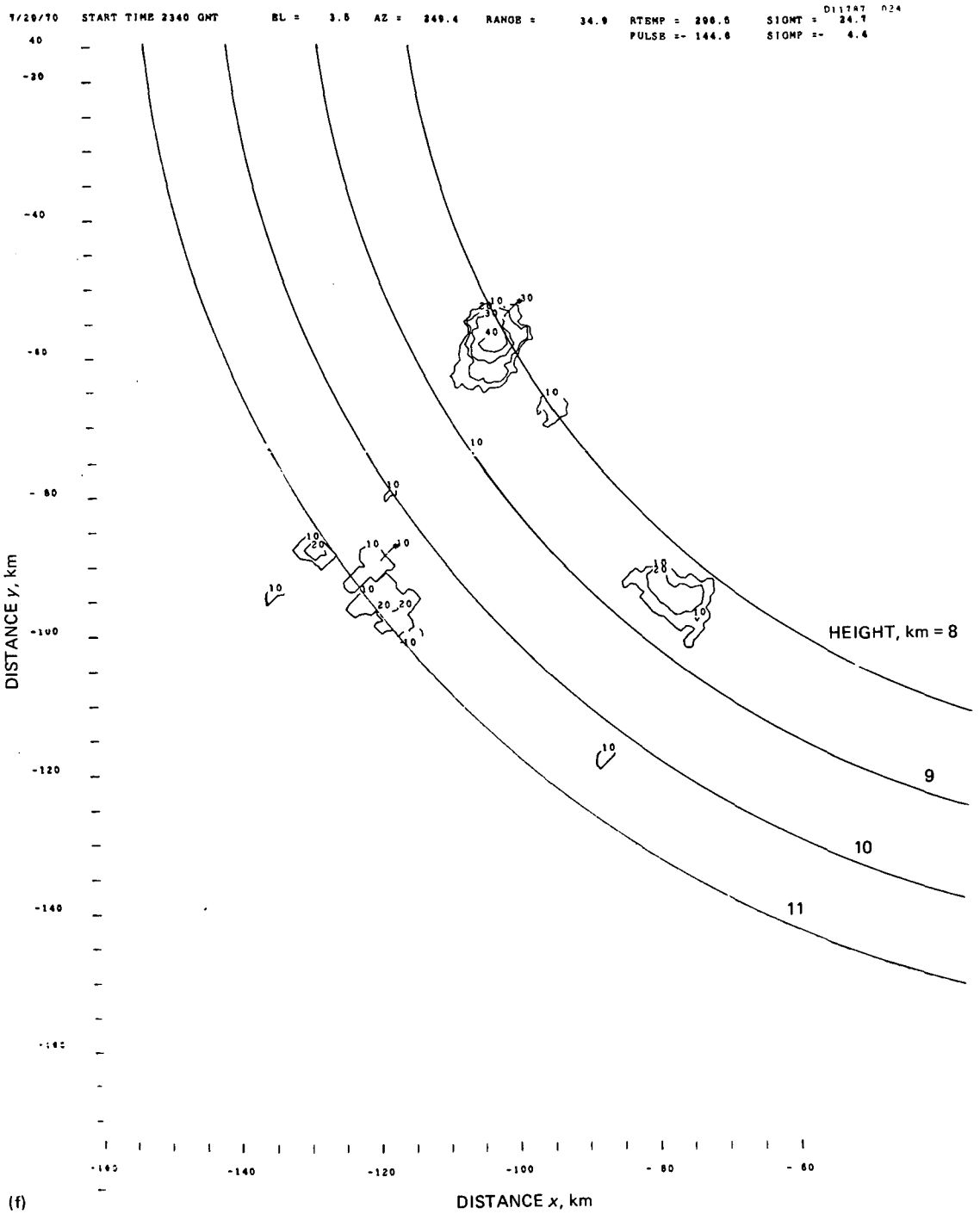

Figure 3-4 (continued).—(f) Time, 2340; elevation, 3.5°.

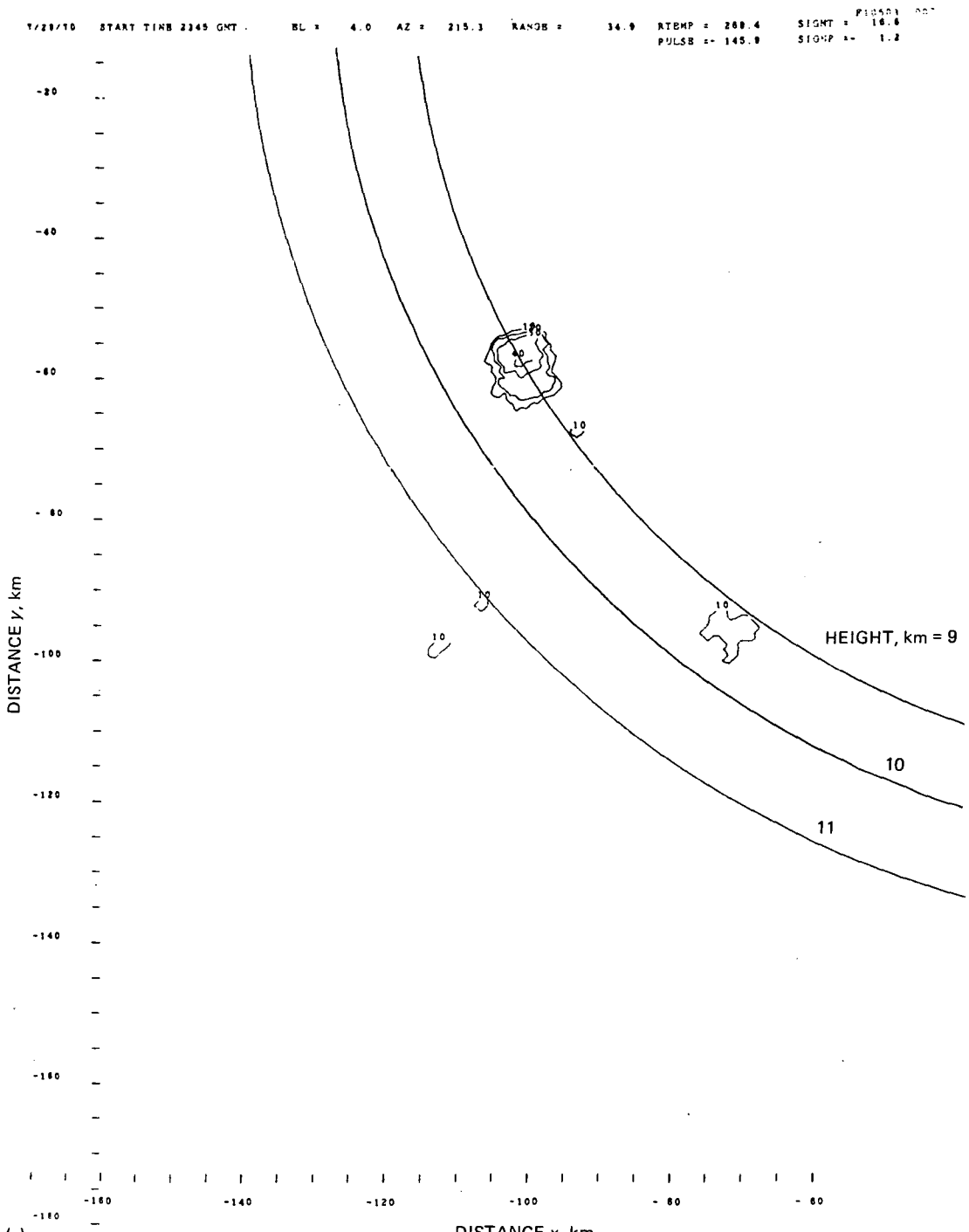

Figure 3-4 (continued).—(g) Time, 2345; elevation, 4.0°.

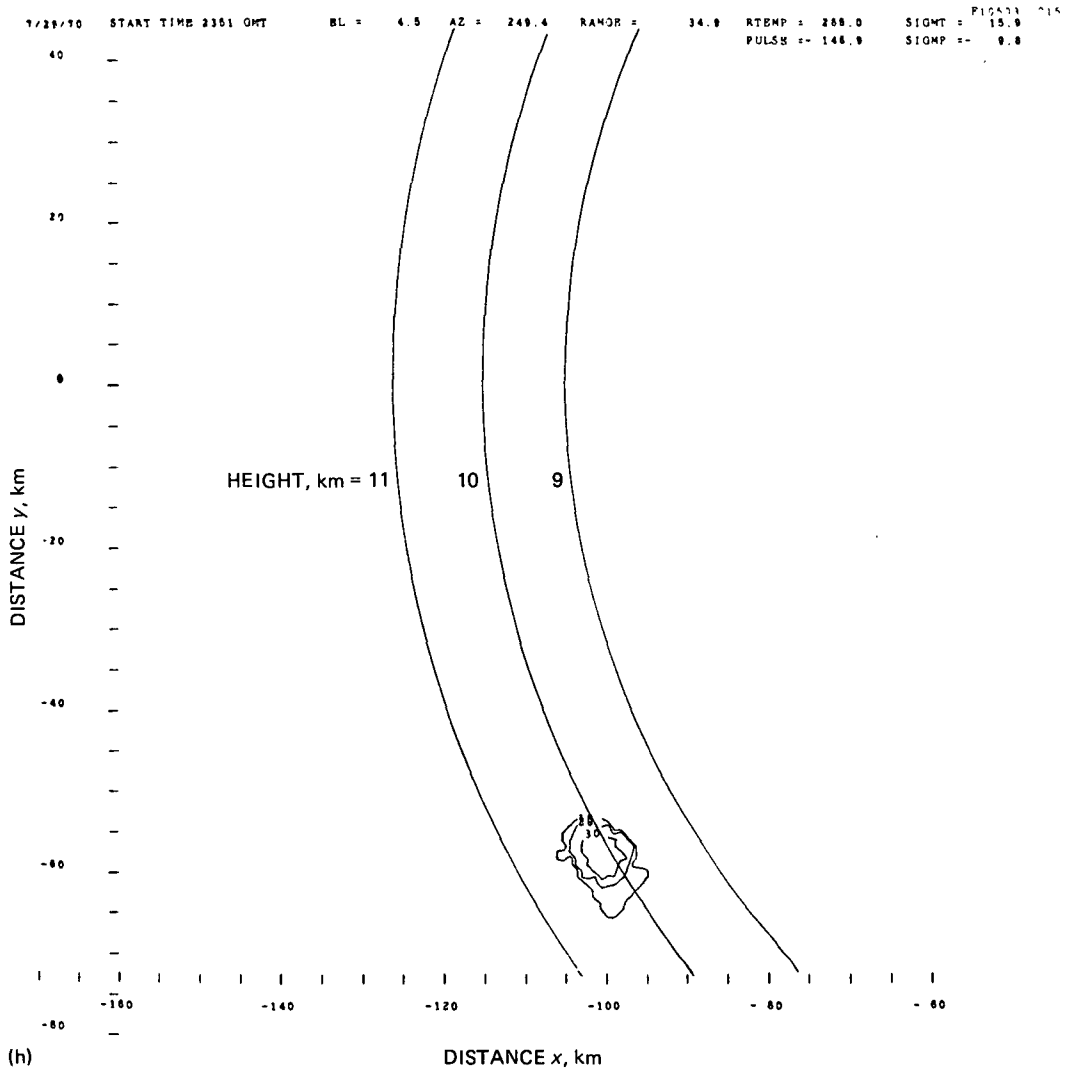

Figure 3-4 (continued).—(h) Time, 2351; elevation, 4.5°.

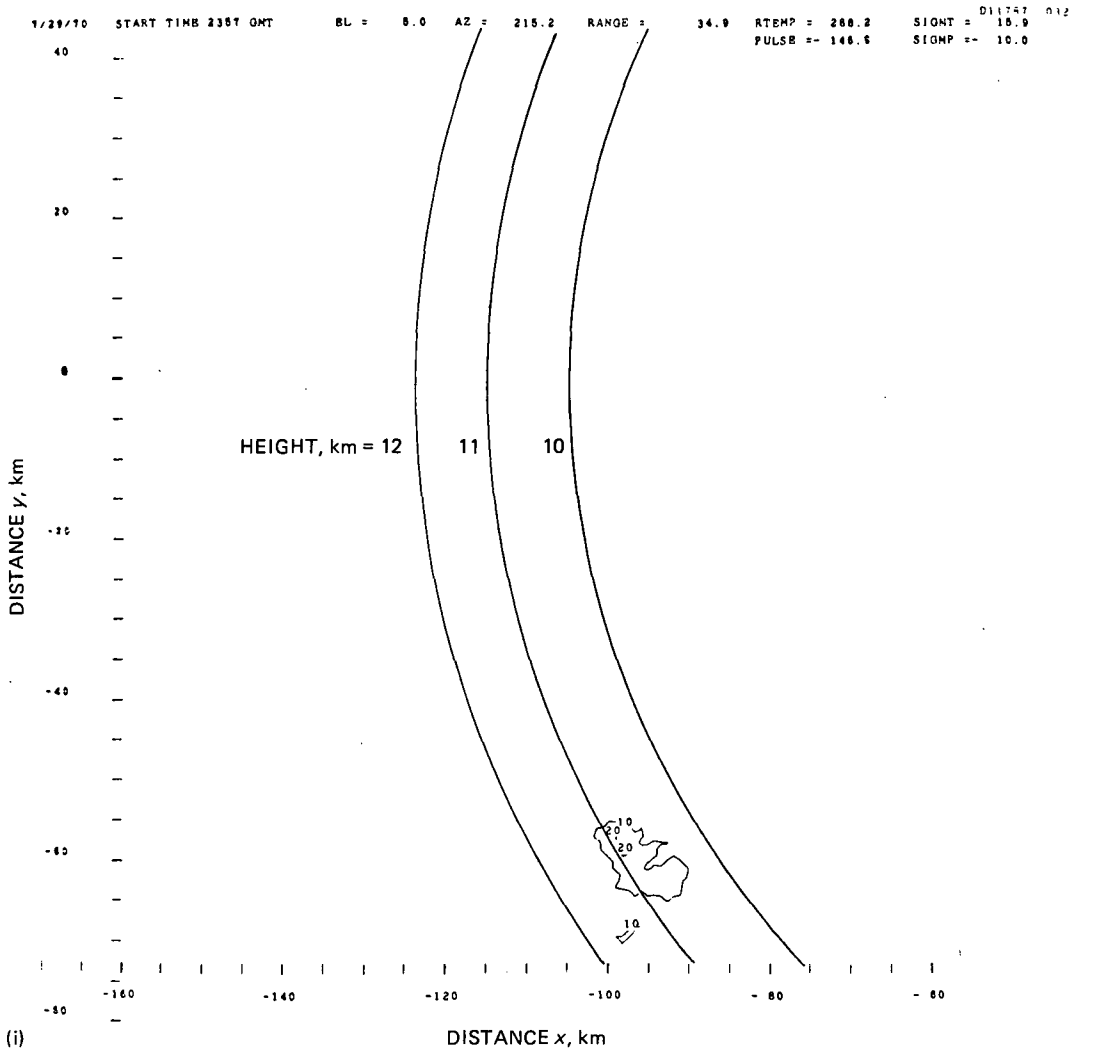

(i)

Figure 3-4 (concluded).—(i) Time, 2357; elevation, 5.0°.

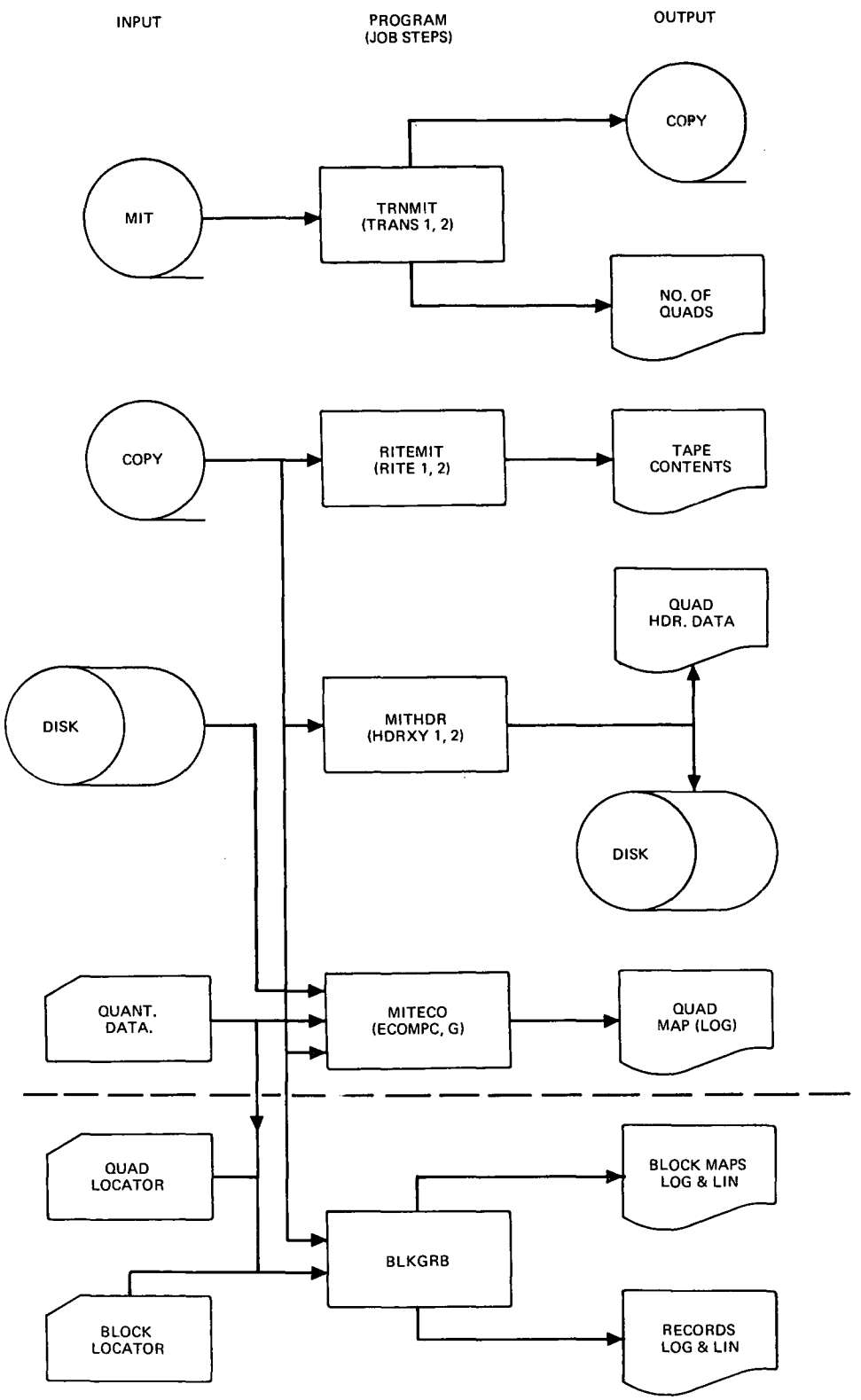

Figure 3-5.—MIT-LL data preprocessor diagram.

```
DATE  72970 TIME 2322BLOCK ORIGIN%X,Y<  -120.00,  -73.66
DELTA X .781 DELTA Y .781
QUAD ORIGIN%X,Y<  -160.00,  -73.10

 1 00000000000000000000000000000000000000000000000000000000
 2 00000000000000000000000000000000000000000000000000000000
 3 00000000000000000000000000000000000000000000000000000000
 4 00000000000000000000000000000000000000000000000000000000
 5 00000000000000000000000000000000000000000000000000000000
 6 00000000000000000000000000000000000000000000000000000010
 7 00000000000000000000000000000000000000000000000000000000
 8 00000000000000000000000000000000000000000000011100000000
 9 00000000000000000000000000000000000000000000111111000000
10 00000000000000000000000000000000000000000000111111000000
11 00000000000000000000000000000000000000000000111110000000
12 00000000000000000000000000000000000000000000010000000001
13 00000000000000000000000000000000000000000000000000000000
14 00000000000000000000000000000000000000000000000000110011
15 00000000000000000000000000000000000000000000000011000111
16 00000000000000000000000000000000000000000000000000000110
17 00000000000000000000100000000000000000000000000000000000
18 00000000000000000011100000000000000000000000000000000000
19 00000000000000000111000000000000000000000000000000000000
20 00000000000000000000000000000000000000000000000000011000
21 00000000000000000000000000000000000000000000000000111000
22 00000000000000000000000000000000000000000000000000110000
23 00000000000000000000000000000000000000000000000000000000
24 00000000000000000000000000000000000000000000000000000000
25 00110000000000000000000000000000000000000000000000000000
26 11111000000000000000000011000001000000000000000000000000
27 12222000000000000000000111110111000000000000000000000000
28 12222100000000000000000011001111000000000000000000000000
29 11211000000000000000010122211100000000000000000000000000
30 10101110000000000001111232322000000000000000000000000000
31 00011220000000000011233333322000000000000000000000000000
32 00022222000000000112333434331100000000000000000000000000
33 00222222000000001234444444320 CELL A 00000000000000000
34 00222222200000012344444443220 00000000000000000
35 00022232200000023444443321000000000000000000000000000000
36 00022221100000113333343221100000000000100000000000000000
37 00001010000000011223232222110000001011100000000000000000
38 00000000000000011211112222110000112211000000000000000000
39 00000000000000000011111110000123230000000000000000000000
40 00000000000000000001011000001233333000000000000000000000
41 00000000000000000000000000011334432200000000000000000000
42 00000000000000000000000001100223443322000000000000000000
43 00000000000000000000000111000133443331100000 CELL B 000000
44 00000000000000000000011000012333443221000000 000000
45 00000000000000000000000000002244443100000000000000000000
46 00000000000000000000000000000224433200000000000000000000
47 00000000000000000000000000000222220000000000000000000000
48 00000000000000000000000000001121112000000000000000000000
49 00000000000000000000000000001012211000000000000000000000
50 00000000000000000000000000000122210000000000000000000000
51 00000000000000000000000000000022100000000000000000000001
```

Figure 3-6.—MIT-LL block map.

Section 4
STORM MODELING METHODOLOGY

4.1 INTRODUCTION

4.1.1 General

Storms have been characterized by profiles that have been produced and used by hydrologists for many years, as discussed quite generally by Court (ref. 13). These profiles are usually averaged over many hours and are not accurate enough for more than rough calculations. As Eagleson (ref. 14) says on page 196 of *Dynamic Hydrology:*

> Except in the most simple cases, it is usually quite difficult to deduce an accurate lagrangian description (i.e., relative to the translating fluid) of a mesoscale disturbance from an array of eulerian (i.e., fixed-point) measurements. However, this lagrangian description is essential to the further understanding of storm structure and to the improvement of generalized methods for hydrologic forecasting. . . . Weather radar studies of storm structure should ultimately provide the desired lagrangian data.

As noted in the previous section, weather radar data are being used for this study. However, it is not just an accurate description that is being deduced but a model—a simplified description expressing a large quantity of data with a few parameters preserving the essential characteristics of the storm cells. The development of such a model can be considered as several separate problems.

4.1.2 Contour Model

The basic data configuration is the contour around the area within which the reflectivity is higher than some level, say $\log Z = 4$. The first problem, which is not considered here, is to isolate such contours from other contours of equal interest and from those of lesser interest which represent only computational noise. The second is to select the basic shape to fit a contour of interest. Dennis (ref. 11) used the circle as a useful first step. Court suggested (ref. 13) the ellipses of the bivariate normal distribution, followed recently by Amorocho (ref. 2). Rogers and Rao (ref. 1) used ellipses, as will be described. A sample of 151 ellipses fitted to $\log Z$ data is discussed in section 7.3.1, and the median error is found to be near 20 percent. Thus the selection of the ellipse seems justified. It also seems clearly preferable to the circle in view of the elongated shapes that were found, with minor/major axis ratios as low as 0.1.

4.1.3 Set Model

Fitting an ellipse is a two-dimensional problem, but each storm cell cross section or sequence may have up to five contours for different values of log Z, so fitting these may be considered a three-dimensional problem, with log Z as the third dimension. One objective is, of course, to find simple relationships between the ellipses to reduce the total number of descriptive parameters. The bivariate normal distribution suggested by Court is a possibility, but its spread at low values does not fit the data, so Amorocho (ref. 2) used only the upper portion. Rogers and Rao (ref. 1) also assumed concentric ellipses of constant orientation, but with variable ellipticity. The model assumed here and justified later uses constant ellipticity and orientation, but ellipse centers are uniformly displaced along a straight line. Two functional relations between Z and area have been tried, log Z versus area and log Z versus square root of area.

4.1.4 Four-Dimensional Models

The above models may add a fourth dimension in two ways considered here. The NSSL scans at 0°-tilt angle are repeated at intervals of 15 min. MIT-LL scans for several tilt angles in a single cell involve log Z or Z as a function of the usual three dimensions. Thus ellipsoids could be fitted, but the variations of wind with height would shear the ellipsoids so that a piecewise approach is preferable. It is found that several tilt sequences (roughly the same as heights) may be considered as identical, forming a family of approximately concentric elliptical cylinders with a different family above some height. Another reason for not using ellipsoids is the anomalous nature of the top and bottom of a cell, frequently with a plume at the top and an irregular bottom. One unsolved problem that should be mentioned is that of splits. Cells often split into two after developing a second nucleus, assuming intermediate configurations that are not well treated by arbitrary division into one or two cells. At the least, it must be decided by characterizing many more cells whether this phenomenon is statistically significant.

4.2 FITTING ELLIPSES

The problem of finding the best fit line to an irregular cluster of points, (x_i, y_i), $i = 1, n$, is an old one in the field of statistics. Usually the regression line of y on x, $y = ax + b$, is found. Suppose the regression of x on Y, $x = a'y + b'$, is also computed. By rearrangement

$$y = \frac{1}{a'} x - \frac{b'}{a'}$$

leading one to expect $a = 1/a'$ and $b = -b'/a'$, which is generally not the case. This is of little concern in the usual applications of regression lines, but when ellipse axes are being sought that will (in some sense) best fit the scatter of points, more symmetry is required than the regression lines are capable of giving.

It is known that any pair of coordinate axes (u, v) will exactly split the scatter plot into equal halves if their origin is the center of mass. The problem is determining which coordinate system will equalize the points among its quadrants. It is a fact that such a

coordinate system cannot have a regression line as one of its axes, so a different approach must be taken.

Consider the covariance matrix

$$\Gamma \equiv \begin{pmatrix} \sigma_{11} & \sigma_{12} \\ \sigma_{21} & \sigma_{22} \end{pmatrix} \equiv \begin{pmatrix} \sum x_i^2 & \sum x_i y_i \\ \sum y_i x_i & \sum y_i^2 \end{pmatrix}$$

in which $\sigma_{11} = \sigma_x^2$, $\sigma_{22} = \sigma_y^2$, and $\sigma_{21} = \sigma_{12}$. For an elongated, tilted scatter plot, there may be more points in the first and third quadrants than in the second and fourth. Hence, for

$$\sigma_{12} = \sum x_i y_i$$

there will be more products of like sign (yielding positive terms) than of unlike sign (yielding negative terms). Therefore, $\sigma_{12} \neq 0$. Clearly the coordinate system (u, v), to equalize the points in its quadrants, will have $\sigma'_{12} = \Sigma u_i v_i = 0$.

Expression of (u_i, v_i) in terms of a rotation of (x_i, y_i) yields

$$u_i = x_i \cos\theta + y_i \sin\theta$$

$$v_i = -x_i \sin\theta + y_i \cos\theta$$

Substitution into the expression for Γ gives the rotated matrix

$$\Gamma' \equiv \begin{pmatrix} \sigma'_{11} & \sigma'_{12} \\ \sigma'_{21} & \sigma'_{22} \end{pmatrix} \equiv \begin{pmatrix} \sum u_i^2 & \sum u_i v_i \\ \sum v_i u_i & \sum v_i^2 \end{pmatrix}$$

$$\Gamma' = \begin{pmatrix} \sigma_{11}\cos^2\theta + \sigma_{22}\sin^2\theta + \sigma_{12}\sin^2\theta & \tfrac{1}{2}(\sigma_{22} - \sigma_{11})\sin 2\theta + \sigma_{12}\cos 2\theta \\ \tfrac{1}{2}(\sigma_{22} - \sigma_{11})\sin 2\theta + \sigma_{12}\cos 2\theta & \sigma_{11}\sin^2\theta + \sigma_{22}\cos^2\theta - \sigma_{12}\sin 2\theta \end{pmatrix}$$

Since $\sigma'_{21} = \sigma'_{12}$, the θ value needed to make $\sigma'_{21} = 0$, makes $\sigma'_{12} = 0$ also. The degree of symmetry required is an orthogonal rotation of axes to equalize quadrants. This approach also works in three or more dimensions, because the covariance matrix is always symmetric.

Of course, a suitable θ may be found by solving for $\sigma'_{12} = 0$, or

$$\theta = \frac{1}{2} \arctan\left(\frac{2\sigma_{12}}{\sigma_{11} - \sigma_{22}}\right)$$

But this technique is useful only in two dimensions. In more dimensions at least three angles are involved, and the formulas become much more cumbersome. To gain insight into a more general method, matrix algebra may be used. If two matrices **A** and **B** are related by

$$\mathbf{A} = \mathbf{P}\mathbf{B}\mathbf{P}^T$$

where **P** is an orthogonal matrix and T denotes transposition, then determinant **A** = determinant **B**; **A** and **B** have the same eigenvalues; and the eigenvectors of **B** and **A** are identical. In particular, if **A** is diagonal, then the eigenvalues of **B** are the diagonal entries of **A** and the eigenvectors of **B** are orthogonal. For the scatter plot considered, the rotation of axes is an orthogonal transformation and the (u, v) axes lie in the unique positions of the widest and narrowest spread of the scatter plot. Hence, the question arises of whether this relationship holds between Γ, Γ', and the orthogonal rotation matrix

$$\mathbf{R} = \begin{pmatrix} \cos\theta & \sin\theta \\ -\sin\theta & \cos\theta \end{pmatrix}$$

The answer is affirmative, because a matrix multiplication will verify that

$$\Gamma' = \mathbf{R}\Gamma\mathbf{R}^T$$

Now eigenvector techniques may be brought to bear on the problem. A method that will produce the eigenvalues and eigenvectors of a matrix will give the σ'_{ii} values and the actual axes of the coordinate system that equalize the quadrants. The σ'_{ii} values, being variances, indicate the spread of the points along the new axes. To find the axis of the widest spread, the eigenvector of the largest eigenvalue (largest σ'_{ii}) is used. To find best-fit ellipses, semimajor and semiminor axes are chosen proportional to the values $\sigma'_i = \sqrt{\sigma'_{ii}}$ (standard deviations) and with values such that π times their product equals the area being fitted.

An illustration of the above remarks is afforded by the bivariate normal distribution suggested by Court (ref. 13) and applied by Amorocho (ref. 2). Its density is given by

$$\frac{(1/2\pi\sigma_x\sigma_y\sqrt{1-\rho^2})\exp\left\{-\left[(x/\sigma_x)^2 - 2\rho(x/\sigma_x)(y/\sigma_y) + (y/\sigma_y)^2\right]\right\}}{2(1-\rho^2)}$$

where the correlation coefficient $\rho = \sigma_{xy}/\sigma_x\sigma_y$. Points of equal probability density lie on ellipses

$$K = \left(\frac{x}{\sigma_x}\right)^2 - 2\rho\frac{x}{\sigma_x}\frac{y}{\sigma_y} + \left(\frac{y}{\sigma_y}\right)^2$$

$$= \frac{x^2}{\sigma_{xx}} - 2\sigma_{xy}\frac{x}{\sigma_{xx}}\frac{y}{\sigma_{yy}} + \frac{y^2}{\sigma_{yy}}$$

where $K > 0$. These ellipses have the same shape as an ellipse with semiaxes σ_x and σ_y, and their orientation θ with respect to the (x, y) coordinate lines may be found from these formulas.

The error of fit for two figures of the same area must consider shape. The measure used originally was $(A_o/A_f) \times 100$, where A_f is the figure area and A_o is the area of the boxes with centers outside the ellipse. It was later found that a more general mathematical concept, the symmetric difference metric, which is twice the above for equal areas, was used for this purpose by Lee and Sallee (ref. 15). Thus, $[1 - (A_f - A_o)/(A_e + A_o)] \times 100$ is now used for generality, where A_e is the ellipse area.

4.3 FITTING SETS OF ELLIPSES

The individual-ellipse fits to storm cell data as displayed at the left of figure 4-1 indicate the reasonableness of using the average of all thetas (TAV) and of all ratios of minor/major axes (RAV) for all ellipses of a given set. It is also seen that the centers are not far from uniformly spaced on a straight line. This line may be found from a three-dimensional version of fitting a line to a group of points so that the sum of the squares of the errors is minimized, assuming that $\log Z$ or Z is the third dimension. As the points being fitted are the centers of gravity or centroids of the individual ellipses, the resulting line is called the centroid line. It is specified by the three block coordinates of a point on the line and two angles.

It remains to examine how ellipse area varies with $\log Z$. If $\log Z$ is considered as a third dimension, the problem may be visualized as finding the shape of the appropriate solid. It will first be shown analytically that the two simplest alternatives are the cone and the paraboloid.

Assuming for simplicity that the ellipses have their major axes along the y axis, their equations are

$$\frac{x^2}{a^2} + \frac{y^2}{b^2} = 1$$

But $\pi ab = A$ = area and $a/b = R$ = axis ratio, so

$$a^2 = \frac{A}{\pi}$$

$$b^2 = \frac{A}{\pi R}$$

$$x^2 + R^2 y^2 = \frac{A}{\pi} = \frac{A}{K^2}$$

where

$$K^2 = \pi.$$

If the *square root of the area* is a linear function of $\log Z$

$$A = (B - S \log Z)^2$$

where

B = intercept of line with $\sqrt{A}$ axis

S = slope of line

then the cross section in the plane $y = 0$ is

$$\pm Kx = B - S \log Z$$

This is a linear function, so the surface is a cone. Similarly, if the *area* is a linear function of $\log Z$

$$a = b - s \log Z$$

then the cross section at $y = 0$ is

$$K^2x^2 = b - s \log Z$$

This is a parabola, so the surface is a paraboloid.

Both of these alternatives are displayed in figure 4-1. The paraboloid at the center displays two features of interest: First, it does not come to a point like a cone, but has a blunt top which may not quite reach the $\log Z = 5$ level. This is not important because the equations are available for scatter or attenuation calculations up to the fitted peak of perhaps $\log Z = 4.9$. It is probably more accurate to determine the shape of the top from the main portion of the data and not to place too much weight on the two boxes with $\log Z = 5$. Second, and most important, the paraboloid models the asymmetry found in nature by means of its crowded contours along one edge. It may be noted that the two lowest contours touch in both the individual fits and in the paraboloid. The preference for this model is reinforced by discussions with meteorologists such as A. J. Chisholm and Ralph Donaldson studying severe storms and by data such as appear in figure 4-2, taken from Shaw (ref. 4). The outline of the cloud is shown as a thin line; the heavy lines within the shading (denoting radar-detected precipitation) are isopleths of $Z = 2 \times 10^2$, 2×10^4, and 2×10^6 mm^6 m^{-3}. Outlines are shown at time t of 10, 30, and 50 min after the storm first appears.

For the results reported in sections 5 and 7, the few points with $\log Z = 5$ were ignored to avoid the possible large quantizing errors associated with the smallest areas, and the area profiles were offset as required to pass through the points at $\log Z \geqslant 4$. This action was intended to give stronger weight to the higher reflectivities. It was found later, however, as reported in section 6, that comparisons of attenuations on paths through the centers of the actual cells and the corresponding models indicated that the offset and omission of the points for $\log Z = 5$ increased the errors. The result is believed to be critical only for this measure and the central paths. It may also be advisable in this case to set the common ellipse orientation to that of the highest level instead of to the average of all. For other uses, these details may not be significant.

4.4 FITTING RELATED SETS OF ELLIPSES

The sets of ellipses considered so far have each been derived from data taken almost simultaneously at a given time and tilt or elevation angle. The question now arises of relations between sets derived from the same cell but made at different elevation angles or at the same elevation angle but at different times. These are clearly related and storm modeling should demonstrate this stability in time and space, or any major lack of continuity such as caused by wind shear with height or by splitting. Conceptually, this part of the study is also curve- or line-fitting as above, such as noting constancy of orientation, or linearity of motion.

In line with this discussion, the only effort made to fit related sets of ellipses was for different elevations in the same storm cell. It would be of advantage to model the three-dimensional cell as not just a stack of unrelated ellipse sets but as an elliptical cylinder or an ellipsoid. Alternatively, the approach may be taken of finding the errors resulting if one of these assumptions is made. The computer program was made interactive so that similarities could be forced between the ellipse sets at different elevations to show these effects. The significance of the results is difficult to interpret. It was found, for example, that the same ellipse sets can be used at elevations from 2° to 4.5°, with differences only in translation and rotation of complete, otherwise identical, sets at the different levels. This translation and rotation may have a great deal of interest for the meteorologist, but would not be significant for a horizontal radio ray from a random direction. It is perhaps advisable to gather more data before formulating more hypotheses or conclusions.

The interactive procedure for relating sets of ellipses is as follows. The data pertaining to all levels of a cell must be isolated, stored, and culled. Using appropriate switches on the computer console, a preliminary run may be made with or without ellipse plotting, as desired. Then on a second round, some levels may be given the same centroid lines as others that are closely similar. The same line at different locations and orientations may be tried for all the echoes between selected levels. On a last run, the area sets may be equalized at all levels. On all runs the parameters including error are tabulated and plots made. Results are presented in the next section.

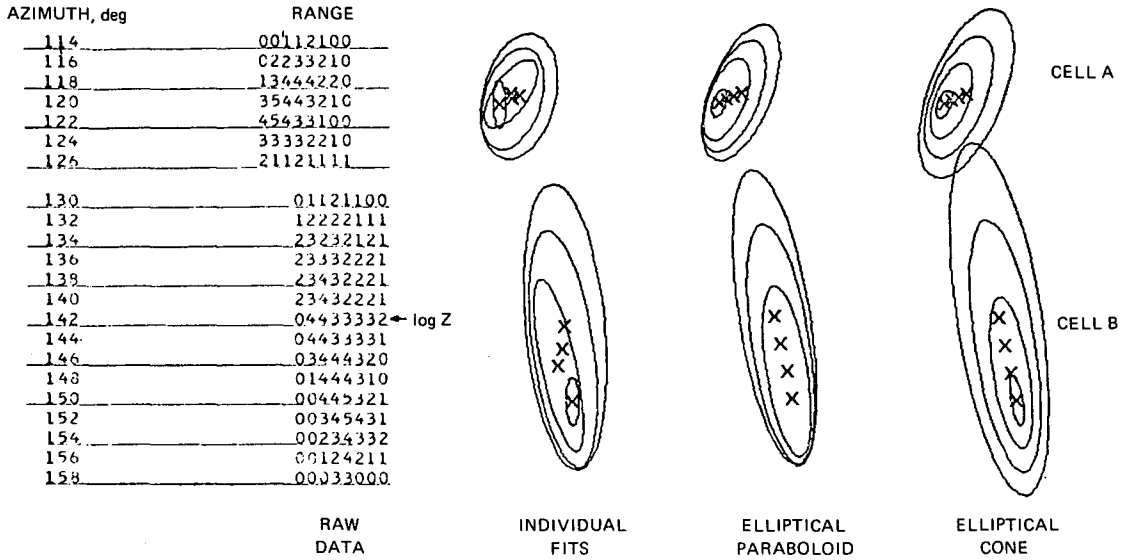

Figure 4-1.—Typical ellipse fits to NSSL data.

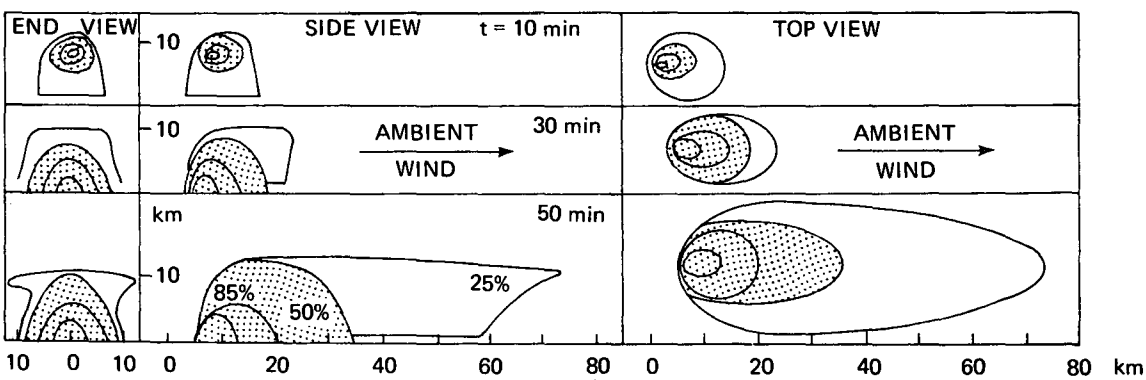

Figure 4-2.—McGill reflectivity contours.

Section 5
EXAMPLE OF MODEL FITTING

5.1 INTRODUCTION

Because of the complexity of the model-fitting techniques, and because several sources and types of data are involved, it seems wise to present the results in two separate ways. In this section, log Z data from one storm cell, MIT-LL cell A, are considered in detail to clarify the methodology and the terms and formats used. In the next section, other cells, linear Z data, and NSSL temporal sequences are considered, and standardized results are compared to bring out similarities and differences.

The basic results are all presented in the form of computer printouts. The abbreviations used in the printouts are explained in table 5-1 and a typical printout is shown in table 5-2. The printout format is as follows, keyed to table 5-2.

(1) An overall header contains a date group and labels for the five columns corresponding to the contours of minimum log $Z = 1$, etc., as displayed in the table.

(2) The tabulation of data for each time is headed by the time and data relating to the individual contours.

(3) Below the header extending across a whole line, more data for individual ellipses are shown for comparisons with data for related ellipses, in following lines.

(4) The first data line starting at the left margin describes the ellipse family automatically fitted using the assumptions of section 2.5.

(5) Following lines under the same time header note the results of changes of many possible types, generally with the object of showing uniformity between successive related sets.

The same time header may be repeated for additional cells from the same block, or for splits. In this case, data for related sets become separated.

5.2 FITTING SETS OF ELLIPSES

An example of the raw logarithmic data to be fitted has been shown in figure 3-6. It provides four contours, around the digits 1 or greater, 2 or greater, etc., as shown at the top of figure 5-1. These are fitted with ellipses with the results printed on the top lines for time = 2322 of table 5-2 under the headings Min $Z = 1$, 2, 3, and 4. To help in following further processing, these parameters are plotted on the X, Y plane in figure 5-2(a) with the semimajor and semiminor axes at the correct orientation of the former, THTA. Note that the

Table 5-1.—Abbreviations for Tables 5-2 and 7-3 to 7-5

Abbreviation	Definition
MODAYR	Date–MOnth DAy YeaR
MINZ=1	Refers to contour including log $Z \geqslant 1$
TIME	Time 0 to 2400
THTA	Theta–azimuth of upper semimajor axis, ccw from north in degrees (MIT); subtract AZ for NSSL
MAJ	Length of semimajor axis in boxes (MIT) or RU (NSSL)[a]
MIN	Length of semiminor axis in boxes (MIT) or RU (NSSL)
RAT	Ratio of MIN/MAJ
CFA	Centroid azimuth $-90°$ (NSSL) or Y in boxes (MIT)
CFR	Centroid range in RU (NSSL) or X in boxes (MIT)
CFZ	Centroid log Z
TRZ	True azimuth of centroid line projection (MIT); subtract CFA for NSSL
PRJ	Projected spacing between log $Z = I$ and log $Z = I + 2$
TAV	Average theta or true azimuth (MIT); subtract CFA for NSSL
RAV	Average ratio of MIN/MAJ
CG-AZ	Center-of-gravity azimuth (NSSL) or Y in boxes (MIT)
CG-RU	Center-of-gravity range (NSSL) or X in boxes (MIT)
AREA	Ellipse area in RU deg (NSSL) or square boxes (MIT)
ER	Error of fit in percent (see sec. 4.2)

[a]Range units (RU) = 2.624 km (1.417 n. mi.); 1 box = 0.7814 km. (See sec. 3.2.)

scale for the axes is not the same as for the rest of the figure. The centers of gravity, or centroids, are projected on the X-log Z plane in figure 5-2(b), showing the dashed centroid line, CENLN, fitted for least-square error. PRJ gives a measure of the slope of this line, the projection of the CENLN between X, Y planes log $Z = I$ and log $Z = I + 2$. The CENLN is shown projected on an X, Y plane in figure 5-2(c). The nominal c.g. coordinates for Min Z = 1 to 4 and 2.5 are printed in the first full line for time = 2322, but the values are truncated by dropping hundredths, so they do not agree precisely with the figure. The CENLN azimuth, TRZ, is shown as well as the average THTA, TAV, common to all major axes. The areas within the contours, from the same printout line, are plotted versus Min Z in figure 5-2(d). A profile is fitted for least-square error, as shown, with the apex marked at the maximum log Z, for which the area is zero. The slope is arbitrarily defined as

$$s = 100 \times \frac{\max \log Z}{\max \text{ area}}$$

$$= 100 \frac{4.75}{140}$$

$$= \frac{100}{DA} = \frac{100}{29.5} = 3.4$$

Table 5-2.–MIT-LL Ellipse Data Printout

```
(1)  MODAYR                                MINZ=1                MINZ=2                MINZ=3                MINZ=4                MINZ=5
      72970

(2)  TIME                                  THTA MAJ MIN RAT      THTA MAJ MIN RAT      THTA MAJ MIN RAT      THTA MAJ MIN RAT      THTA MAJ MIN RAT
     2316                                  85.  4.6 2.9 0.64     -65.  3.1 2.7 0.84
(3)  CFA  CFR  CFZ TRZ PRJ TAV RAV         AZ-CG-RU AREA ER      AZ-CG-RU AREA ER      AZ-CG-RU AREA ER      AZ-CG-RU AREA ER      AZ-CG-RU AREA ER
                                           32.7 24.8  43 13      32.6 25.2  27 13

(4)  32.6 25.0 1.5 102 0.9 -79 0.7         32.7 24.8  43 17      32.6 25.2  27 20

(5)  32.6 25.2 2.0 100 0.6 -79 0.7         32.6 24.8  43 13      32.6 25.2  27 20

     32.6 25.2 2.0 100 0.6 -80 0.6         32.6 24.8  43 13      32.6 25.2  27 25

     TIME                                  THTA MAJ MIN RAT      THTA MAJ MIN RAT      THTA MAJ MIN RAT      THTA MAJ MIN RAT      THTA MAJ MIN RAT
     2322                                 -51.  8.0 5.4 0.68     -61.  6.3 4.1 0.64     -62.  5.7 2.8 0.49     -74.  3.9 1.7 0.44
     CFA  CFR  CFZ TRZ PRJ TAV RAV         AZ-CG-RU AREA ER      AZ-CG-RU AREA ER      AZ-CG-RU AREA ER      AZ-CG-RU AREA ER      AZ-CG-RU AREA ER
                                           33.4 26.1 138 23      33.7 25.9  83 25      33.5 25.4  51 11      33.8 25.2  22  8

     33.6 25.6 2.5 -72 0.6 -66 0.5         33.4 26.1 113 30      33.5 25.8  83 21      33.6 25.5  52 16      33.7 25.2  22 24

     33.8 25.2 4.0 -70 0.6 -66 0.5         33.4 26.1 113 30      33.5 25.8  83 21      33.6 25.5  52 16      33.8 25.2  22 24

     33.8 25.2 4.0 -70 0.6 -65 0.6         33.4 26.1 113 32      33.5 25.8  83 17      33.6 25.5  52 20      33.8 25.2  22 30

     TIME                                  THTA MAJ MIN RAT      THTA MAJ MIN RAT      THTA MAJ MIN RAT      THTA MAJ MIN RAT      THTA MAJ MIN RAT
     2328                                 -55.  7.2 4.6 0.64     -60.  7.1 3.9 0.54     -64.  4.8 3.1 0.65     -71.  3.0 1.9 0.65
     CFA  CFR  CFZ TRZ PRJ TAV RAV         AZ-CG-RU AREA ER      AZ-CG-RU AREA ER      AZ-CG-RU AREA ER      AZ-CG-RU AREA ER      AZ-CG-RU AREA ER
                                           32.1 25.6 106 12      32.4 25.7  88  8      32.3 25.6  49 15      31.5 26.8  19  0

     32.1 25.9 2.5 121 0.9 -65 0.6         32.4 25.3 123 21      32.2 25.7  88 15      31.9 26.1  53 22      31.7 26.5  19  0

     31.8 26.5 4.0 120 0.6 -65 0.6         32.3 25.5 123 21      32.1 25.8  88 15      31.9 26.1  53 22      31.8 26.5  19 10

     31.8 26.5 4.0 120 0.6 -65 0.6         32.3 25.5 123 19      32.1 25.8  88 15      31.9 26.1  53 22      31.8 26.5  19 10

     TIME                                  THTA MAJ MIN RAT      THTA MAJ MIN RAT      THTA MAJ MIN RAT      THTA MAJ MIN RAT      THTA MAJ MIN RAT
     2334                                 -45.  9.2 5.7 0.61     -40.  7.8 5.1 0.66     -11.  5.1 4.2 0.82     -65.  3.0 2.2 0.74       0.  0.5 0.5 1.00
     CFA  CFR  CFZ TRZ PRJ TAV RAV         AZ-CG-RU AREA ER      AZ-CG-RU AREA ER      AZ-CG-RU AREA ER      AZ-CG-RU AREA ER      AZ-CG-RU AREA ER
                                           32.0 25.6 167 13      31.6 26.1 128 15      31.8 26.5  68 18      31.3 26.8  22 24

     31.7 26.3 2.5 114 0.8 -38 0.7         31.9 25.7 181 18      31.8 26.1 128 21      31.6 26.5  75 21      31.4 26.8  22 24

     31.5 26.9 4.0 115 0.6 -38 0.7         31.9 25.9 181 18      31.7 26.2 128 23      31.6 26.5  75 21      31.5 26.9  22 24

     31.5 26.9 4.0 115 0.6 -40 0.6         31.9 25.9 181 15      31.7 26.2 128 14      31.6 26.5  75 25      31.5 26.9  22 24

     TIME                                  THTA MAJ MIN RAT      THTA MAJ MIN RAT      THTA MAJ MIN RAT      THTA MAJ MIN RAT      THTA MAJ MIN RAT
     2340                                 -26.  8.9 5.8 0.65     -9.  7.0 4.9 0.70     -14.  4.4 3.5 0.79     -71.  2.9 1.8 0.64
```

Table 5-2.–Concluded

CFA	CFR	CFZ	TRZ	PRJ	TAV	RAV	AZ-CG-RU	AREA	ER	AZ-CG-RU	AREA	ER	AZ-CG-RU	AREA	ER	AZ-CG-RU	AREA	ER	AZ-CG-RU	AREA	ER
							32.6	26.2	165 18	32.0	26.8	110 21	31.2	26.2	50 18	31.6	26.8	17 11			
31.8	26.5	2.5	164	0.8	-31	0.7	32.4	26.3	160 17	32.0	26.5	112 24	31.6	26.6	64 30	31.3	26.7	17 45			
31.3	26.7	4.0	165	0.6	-31	0.7	32.3	26.4	160 18	31.9	26.5	112 24	31.6	26.6	64 30	31.3	26.7	17 45			
31.3	26.7	4.0	165	0.6	-30	0.6	32.3	26.4	160 15	31.9	26.5	112 25	31.6	26.6	64 30	31.3	26.7	17 45			
TIME							THTA	MAJ	MIN RAT	THTA	MAJ	MIN RAT	THTA	MAJ	MIN RAT	THTA	MAJ	MIN RAT	THTA	MAJ	MIN RAT
2345							7.	7.2	6.2 0.86	11.	6.5	5.1 0.79	-57.	4.5	3.3 0.73	-45.	1.8	1.5 0.81			
CFA	CFR	CFZ	TRZ	PRJ	TAV	RAV	AZ-CG-RU	AREA	ER	AZ-CG-RU	AREA	ER	AZ-CG-RU	AREA	ER	AZ-CG-RU	AREA	ER	AZ-CG-RU	AREA	ER
							33.0	28.3	142 13	32.6	28.5	107 23	31.0	28.0	48 18	31.7	28.2	9 36			
32.1	28.2	2.5	191	1.3	-30	0.7	33.0	28.4	158 19	32.4	28.3	108 26	31.7	28.2	58 32	31.1	28.1	9 50			
31.1	28.1	4.0	190	0.6	-30	0.7	32.1	28.2	158 23	31.7	28.2	108 29	31.4	28.1	58 32	31.1	28.1	9 50			
31.1	28.1	4.0	190	0.6	-30	0.6	32.1	28.2	158 29	31.7	28.2	108 34	31.4	28.1	58 29	31.1	28.1	9 50			
TIME							THTA	MAJ	MIN RAT	THTA	MAJ	MIN RAT	THTA	MAJ	MIN RAT	THTA	MAJ	MIN RAT	THTA	MAJ	MIN RAT
2351							35.	8.0	5.1 0.64	63.	5.2	4.5 0.85	44.	3.6	3.1 0.85						
CFA	CFR	CFZ	TRZ	PRJ	TAV	RAV	AZ-CG-RU	AREA	ER	AZ-CG-RU	AREA	ER	AZ-CG-RU	AREA	ER	AZ-CG-RU	AREA	ER	AZ-CG-RU	AREA	ER
							33.4	29.2	130 18	32.3	28.9	75 17	32.3	29.1	36 15						
32.7	29.0	2.0	185	1.1	54	0.7	33.3	29.1	130 25	32.7	29.0	83 20	32.1	29.0	36 10						
32.1	29.0	3.0	180	0.6	54	0.7	32.8	29.0	130 23	32.4	29.0	83 18	32.1	29.0	36 15						
32.1	29.0	3.0	180	0.6	500	0.6	32.8	29.0	130 45	32.4	29.0	83 32	32.1	29.0	36 40						
32.1	29.0	3.0	180	0.6	50	0.6	32.8	29.0	130 19	32.4	29.0	83 22	32.1	29.0	36 24						
TIME							THTA	MAJ	MIN RAT	THTA	MAJ	MIN RAT	THTA	MAJ	MIN RAT	THTA	MAJ	MIN RAT	THTA	MAJ	MIN RAT
2357							51.	7.8	4.2 0.53	52.	3.0	0.6 0.21									
CFA	CFR	CFZ	TRZ	PRJ	TAV	RAV	AZ-CG-RU	AREA	ER	AZ-CG-RU	AREA	ER	AZ-CG-RU	AREA	ER	AZ-CG-RU	AREA	ER	AZ-CG-RU	AREA	ER
							34.9	34.8	105 29	32.6	32.6	6 80									
33.8	33.7	1.5	224	6.3	51	0.3	34.9	34.8	105 29	32.6	32.6	6 90									
32.7	32.7	2.0	225	0.6	51	0.3	32.9	32.9	105 44	32.7	32.7	6 90									
32.7	32.7	2.0	225	0.6	50	0.6	32.9	32.9	105 48	32.7	32.7	6 90									

where DA = differential area per unit log Z. The last items printed are the errors of fit. To give this unconventional measure discussed in section 4.2 some physical significance, the original contours and the fitted ellipses have been superposed in figure 5-1. The computed errors (in percent) are–

Min Z	1	2	3	4
Cell A	23	25	11	8
Cell B	17	28	10	37

Table 5-3 summarizes not only some of the data already presented, but also the averages and standard deviations of the fits for MIT-LL cell A. The figures must be interpreted with some care. For RAV, the average ratio of minor to major ellipse axes, a coefficient of variation of 0.057/0.70, or about 0.08, is obtained. For TAV, however, the base should not be the average azimuth, but 360°, for a coefficient of about 0.05. For the centroid lines, the rms error is in linear box units of 0.78 km, and for the area in square box units. The uniformity of many of the parameters, such as TAV, RAV, and max log Z, is quite remarkable if data from erratic top and bottom levels are ignored.

5.3 FITTING RELATED SETS OF ELLIPSES

In figure 5-3 the sets of fitted ellipses for horizontal cross sections at all heights of cell A are shown. The columns from left to right are raw data contours, individually fitted ellipses, and ellipse sets as described above. The fitting errors are collected in table 5-4. Only two of the individual fit errors are over 30 percent. Min Z = 4 at 2345 has note a in the table and figure. It is seen that the high error is due to the ragged shape of the contour and to its small size, which leads to high quantizing error. Note b shows a high error from a split at the cell top. Set fit errors more than 10 percent higher than the individual fit errors are also noted. Notes c, e, and g refer to Min Z = 4 cores maintaining the same orientation at all cell heights even though the lower reflectivity structures rotate increasingly ccw with height. Notes d and f seem due to a random orientation of Min Z = 3 contours.

Figure 5-3 illustrates the effects of changes forced on the ellipse parameters by the interactive procedure. The method is in general to average parameter values from all levels, and to force all levels to the same value. This reduces the number of parameters required to describe the cell and leads to the simplified elliptical cylinder model. The first, least significant, change was to set all CENLN projections PRJ equal to 0.70 as indicated at the head of a column of the figure and at one line in the table by the abbreviation **P** = .70. As expected, the ellipse centers are now all uniformly spaced, and the only significant error increase is at note h because of the large original projection. The common value of MIN/MAJ = RAV = **R** = .65 caused no error increases over 10 percent. Forcing a common major axis orientation 65° right of north produced large error increases at notes j to n, only

Table 5-3.—MIT-LL Ellipse Set Data

MIT-LL cell A			σ/TAV, deg	σ/RAV	Centroid line Log $Z = F(X, Y)$			Area line Area = b − (log Z/DA)		
Time	Elevation, deg	Height, km			rms error	PRJ	TRZ, deg	rms error	Max log Z	Slope
2316	1½	4	15/-69	0/0.79	–	0.9	102	–	[a]3.7	[a]6.3
2322	2	5	6/-66	.087/.53	0.20	.6	[a]-72	0.7	4.7	3.3
2328	2½	6	5/-66	.049/.62	.49	.9	121	2.1	4.5	2.9
2334	3	7	22/-39	.063/.74	.26	.8	114	3.3	4.4	1.9
2340	3½	8	28/-32	.064/.72	.44	.8	164	6.5	4.3	2.1
2345	4	9	30/-31	.034/.78	.63	1.3	191	4.7	4.2	2.0
2351	4½	10	10/[a]54	.099/.78	.30	1.1	185	3.8	3.8	2.1
Averages			17/-56	.057/.70	.39	.9	149	3.5	4.3	2.4

[a]Excluded from averages.

Table 5-4.–MIT-LL Ellipse Fitting Errors

Model	Time = 2316		Time = 2322				Time = 2328				Time = 2334			
	Min Z		Min Z				Min Z				Min Z			
	1	2	1	2	3	4	1	2	3	4	1	2	3	4
Individual	13	13	23	25	11	8	12	18	15	0	13	15	18	24
Set	17	20	30	21	16	[c]24	21	15	22	0	18	21	21	24
P = .70	13	20	30	21	16	24	21	15	22	0	18	23	21	18
R = .65	13	25	32	17	20	30	19	15	22	10	15	14	25	24
$T = -65°$	[j]28	25	32	17	20	30	19	17	22	10	23	24	32	[k]37
A = **A′**	[p]46	32	26	20	20	38	27	15	24	5	30	34	29	32
A	[r]37	13	2	17	9	2	[r]34	12	11	1	27	28	8	2

Model	Time = 2340				Time = 2345				Time = 2351			Time = 2357		Number of notes
	Min Z				Min Z				Min Z			Min Z		
	1	2	3	4	1	2	3	4	1	2	3	1	2	
Individual	18	21	18	11	13	23	18	[a]36	18	17	15	29	[b]80	2
Set	17	24	[d]30	[e]45	19	26	[f]32	[g]50	25	20	10	29	90	5
P = .70	18	24	30	45	23	29	32	50	23	18	15	[h]44	90	1
R = .65	15	25	30	45	29	34	29	50	19	22	24	48	90	0
$T = -65°$	[m]36	35	37	30	30	40	35	50	[n]46	32	32	52	90	4
A = **A′**	36	38	33	23	34	40	31	55	49	26	[q]52	53	90	2
A	15	10	10	3	2	7	12	11	[r]30	15	16	25	[r]34	4

Note.–See text for explanation of letter notes.

k occurring at Min $Z = 4$. In the right-hand column of the figure, **R** = .65, $T = -65°$, and the area profile has been chosen for best fit for time 2322 to 2340 as

$$\text{Area} = 180 - 40 \log Z$$

This caused large errors at notes p, q, and r at the top and bottom of the cell, as expected, but it is seen that the proposed model of sheared, nested, elliptical cylinders is validated.

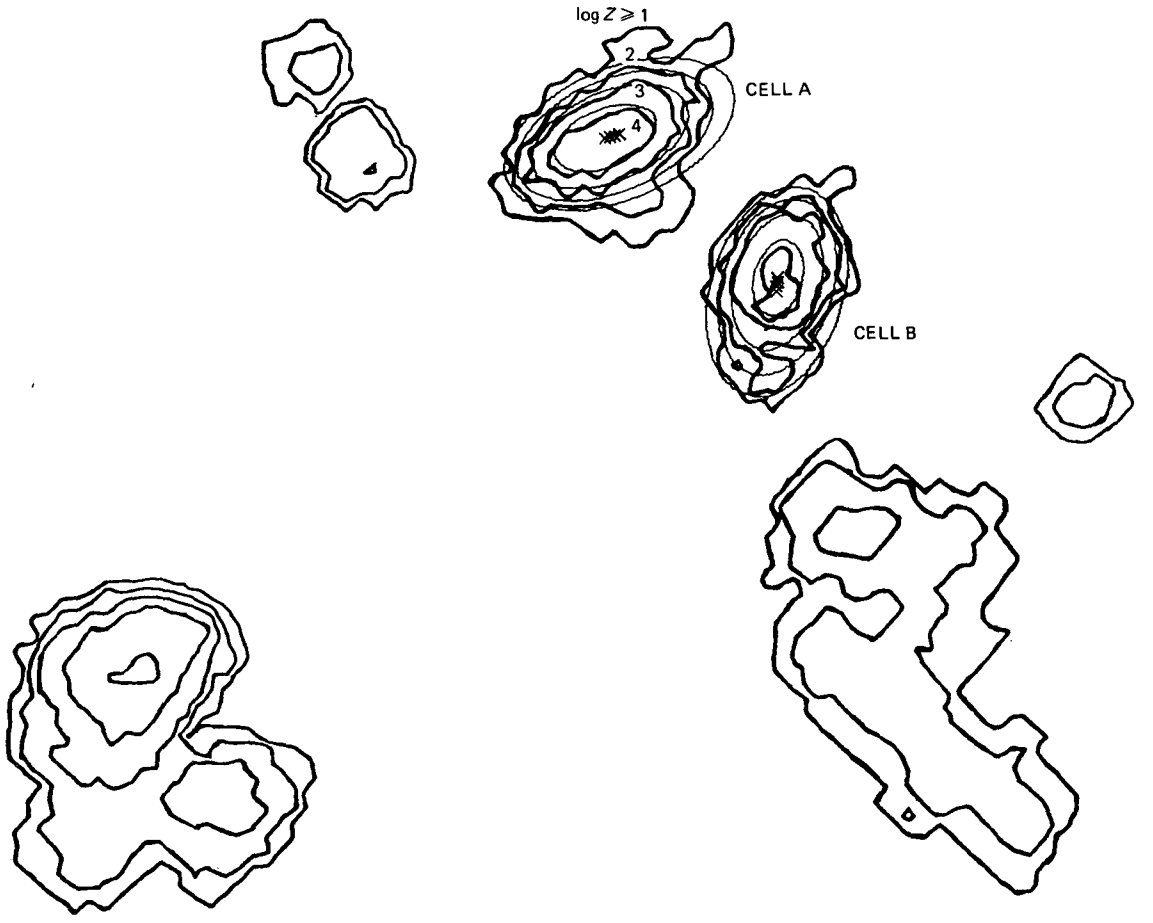

Figure 5-1.—MIT-LL fitted ellipses.

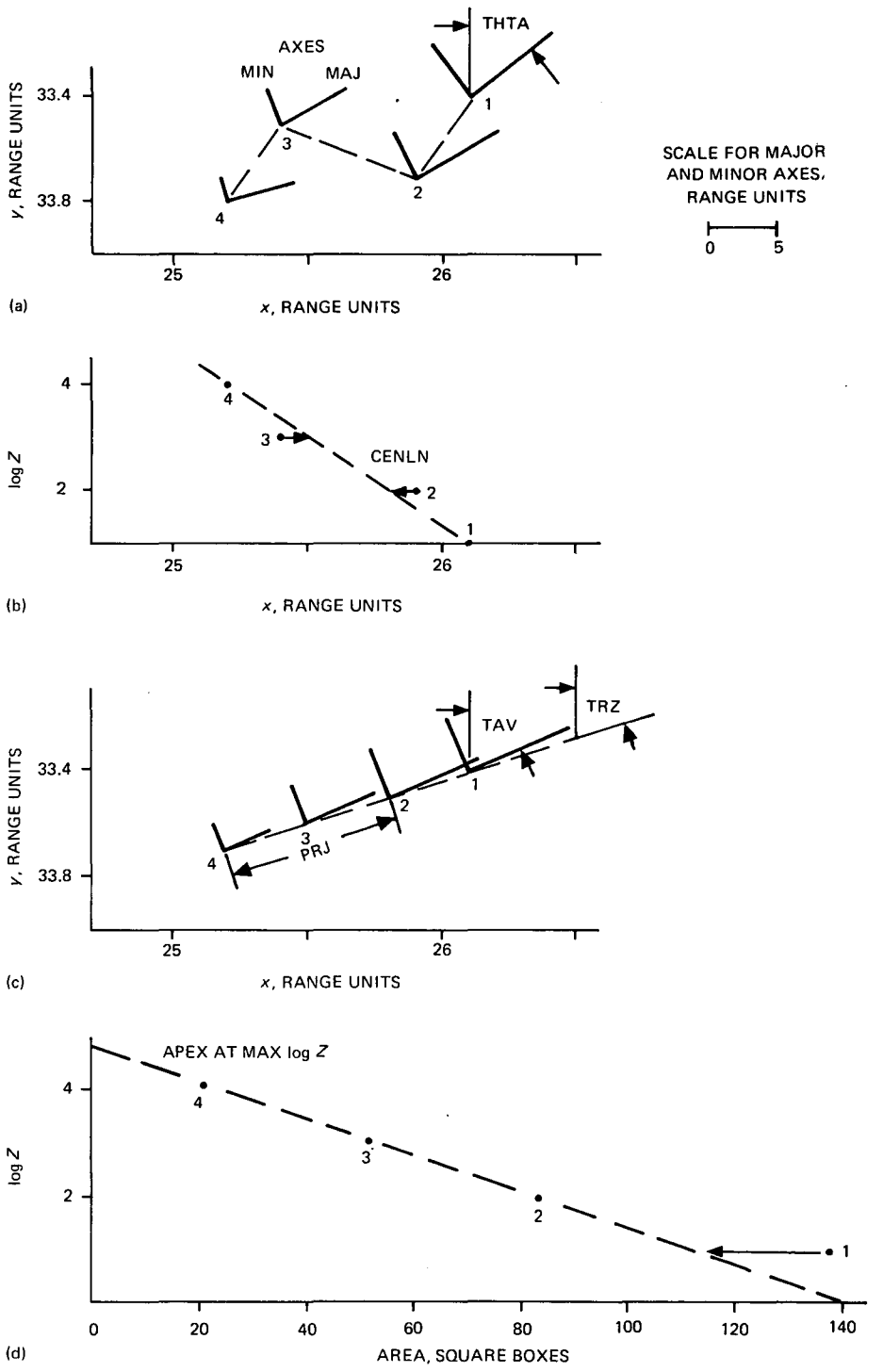

Figure 5-2.—MIT-LL plotted ellipse data. (a) Individual ellipses. (b) Centroid line fit. (c) Ellipse set fit. (d) Area profiles.

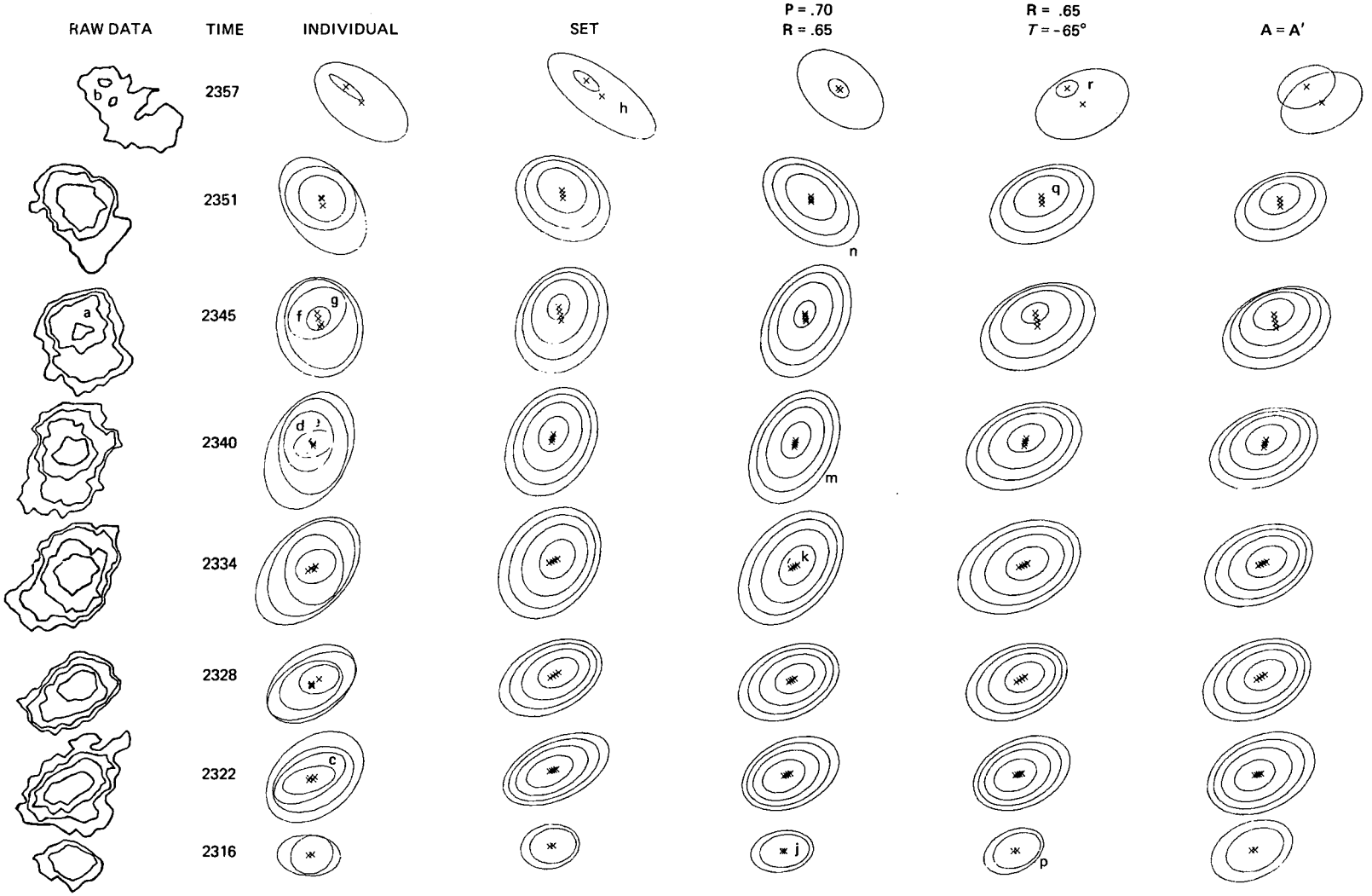

Figure 5-3.—MIT-LL ellipse set plots.

Section 6
TEST OF STORM MODEL

6.1 TEST METHOD

For the development of the storm model, error of fit was estimated using geometric criteria as discussed above. Its intended application, however, involves transmission of electromagnetic energy, so a more relevant criterion of usefulness is desirable. Therefore, the attenuation of a radio wave through the observed reflectivity pattern has been compared with that through a storm cell reconstructed from the model parameters. This is facilitated by using east-west or north-south paths parallel to the X and Y axes of the MIT-LL data. For these paths, precise values of reflectivity are available for each increment of 0.78 km. It will be shown for the three east-west central paths through five cross sections of the MIT-LL cell A, that Z sums by the two methods generally differ by about 5 percent.

6.2 CALCULATION OF ATTENUATION

With certain usual assumptions about the dropsize spectrum, the attenuation A in decibels through a storm cell may be expressed as

$$A = K \int Z^a \, ds$$

where

K = a function of frequency, dB km^{-1}

a = constant to be discussed

Z = reflectivity, mm^6 m^{-3}

ds = distance along path, here 0.78 km

For greatest accuracy, the constant a should be considered to vary as in table 6-1, taken from Zawadski and Rogers (ref. 16), but if the values of K shown are used, a may be taken as unity without large errors, for Z values of most interest, around 10^4. The last two rows show the attenuation corresponding to a typical $Z\,ds$ of 10^5 and the attenuation error for 5 percent error in the integral as a function of frequency.

6.3 RESULTS

A computer program was written to construct digitized horizontal cross sections of cells similar to those in figure 3-1 from the fitted ellipse parameters, and to sum the values of Z in the rows in the X direction. When these sums were compared with similar sums

Table 6-1.–Attenuation at Various Frequencies

Attenuation factors	Frequency, GHz			
	10	20	30	40
Best a	0.78	0.70	0.66	0.63
Best K for a=1	2×10^{-5}	10^{-4}	3×10^{-4}	5×10^{-4}
A for $\int Z\, ds = 10^5$, dB	2	10	30	50
0.05 A, dB	0.1	0.5	1.5	2.5

Table 6-2.–Highest Values of $\int Z\, ds/1000$

Time	From data			From model			Error for highest peak, percent
2322	149	199	125	181	206	129	3
2328	87	129	139	88	122	132	5
2334	219	348	266	168	217	203	38
2340	83	111	72	63	70	63	37
2345	43	50	42	52	53	43	6

derived from the raw data, it was found that agreement was improved by using area profiles without the offset to produce equal areas at the $\log Z \geqslant 4$ level, which is described in section 4.3. It was also found essential to use the point at $\log Z = 5$ in fitting the area profile for time 2334. In table 6-2, the paths with the three highest sums are compared for MIT-LL cell A at all elevations at which $\log Z \geqslant 4$ was observed. The errors are high at 2334 and 2340 because the ellipses for $\log Z \geqslant 4$ are not alined with the others in the sets. If north-south paths were considered as well as east-west, and the highest integrals of both sets considered, this error would be reduced. In any case, most of the errors are small at low frequencies.

Section 7
RESULTS

7.1 INTRODUCTION

The storm modeling results presented are based on data of three types:

(1) MIT-LL elevation sequence—logarithmic

(2) MIT-LL elevation sequence—linear

(3) NSSL time sequence—logarithmic

The first type provides spatial characteristics in three dimensions from successive radar sweeps at increasing elevation angles. The second considers distributions of reflectivity Z instead of log Z to focus on the high-intensity cell cores. The third type provides temporal characteristics by following several cells for several hours in two dimensions with a horizontal radar scan.

To facilitate comparisons, all three types are considered in the same order used previously; data first, then fits to individual ellipses, sets of ellipses, and finally related sets of ellipses.

7.2 DATA

7.2.1 Logarithmic MIT-LL Data

Before considering results, the data used will be reviewed and displayed in the more convenient form of figure 7-1. Here the portions of figure 3-4 containing cells A and B have been used in the form of digital maps like figure 3-6. Contours have been drawn about the 1's, 4's, and 5's, etc., and placed side by side for comparison. There is a common Y grid, the displaced X references are labeled, and the horizontal scale is marked. Cell A, in the upper half of the figure, displays intensity levels 1 to 4 from 2° to 4° in elevation, or from about 5 to 9 km in height. Only a single log Z = 5 box appears, at 3°. The bottom tapers down symmetrically but the top shows a split at the log Z = 2 level. The centers of the 1° to 3½° levels are close to a vertical line; higher levels have drifted to the east. The time required for scanning is not negligible, so the 36 min intervening between the 1° and 4° scans may be significant.

Cell B, also shown logarithmically, does not display much vertical uniformity. In fact, a split is indicated by the peninsula at the bottom at 2° and is definite at 1½°. Only the northern part shows at 1°. More and faster scans such as those of NSSL for 1969 and later

are required to separate fully the effects of time and elevation in a case like this. Without an extended time sequence, the two effects may easily be confused.

Another aspect of splitting is evident in cell C, shown logarithmically in figure 7-1. Definite splits exist at both the top and bottom. Small internal peaks at 1½° to 2½° are disregarded, and the 1½° and 2° levels are split near the peninsulas, and consistent with this at 2½° as shown. The part called C2 is fairly weak and uniform from 1½° to 3°. The other part, C1, probably continues below 1°, or a height of about 3 km.

7.2.2 Linear MIT-LL Data

The cell A linear data are plotted below the logarithmic cell A data in figure 7-1. The significance of the shades used in the figure may be seen from table 7-1. The right-hand column applies for time 2334. In the logarithmic data, the digit 4 is used for $40 \leqslant 10 \log Z < 50$, or in this case, for 40 to 50, whereas the linear presentation uses five levels to provide greater detail in the small intense area responsible for most scattering and attenuation.

7.2.3 NSSL Data

NSSL data are used as well as MIT data because the former include long time sequences giving preliminary information on cell velocities, lives, splits, etc. The automatically blocked data of figure 3-1 were manually culled to remove trivial echoes, and significant related echoes were identified as shown and grouped for best display of their characteristics in figure 7-2. Cell scans each 15 min between 1735 and 2020 of May 3, 1968, were studied. Elongated cell B split into cells B and C between 1820 and 1835.

7.3 INDIVIDUAL ELLIPSE FITS

7.3.1 Fitting Errors

The results of the individual ellipse fitting as described above are included in tables 7-3 to 7-5 (presented subsequently), which use abbreviations explained in table 5-1. To facilitate understanding the results, these are extracted and presented in various ways. The first question of interest is the accuracy of the fits. Using the error measure discussed at the end of section 4.2, figure 7-3(a) characterizes the fit errors in a histogram format giving the number of cases in each error category. The errors over 50 percent are due to splits, as are many of those from 40 to 50 percent.

Data sets for two NSSL storm cells are shown in figure 7-2 with the left-hand sets of ellipses showing the individual fits. For example, in the upper cell there are two 5's, one above the other, so there is a vertically oriented central ellipse. The 4's ellipse is sharply tilted to the right, and the 3's and 2's ellipses have a slight tilt. The 1's have not been used because they are insignificant electromagnetically, pruned arbitrarily, and often in a very ragged configuration, as in a plume at the top of a storm. The apparent misalinement of the 5's ellipse

Table 7-1.—Linear Scale Equivalents

Shade (fig. 7-1)	Z/Z_{max} linear	$10 \log (Z/Z_{max}) \times 10$	Typical dBZ
5	0.8 to 1.0	9 to 10	50
4	.6 to .8	8 to 9	49
3	.4 to .6	6 to 8	47, 48
2	.2 to .4	3 to 6	44, 45, 46
1	.1 to .2	0 to 3	41, 42, 43
0	0 to .1	0	<40

ccw of the average azimuth and of the 4's clockwise (cw) is probably due to quantizing error. That is, there are too few samples (boxes too large—low resolution) to define the contour accurately.

7.3.2 Cell Sizes

As a preliminary estimate of cell size for the ellipses fitted to the contours of $\log Z = 4$ for the MIT logarithmic data and the contours $Z = 0.6Z_{max}$ for the MIT linear data, the average semiaxis lengths are as follows:

Cell	Semimajor axis length	Semiminor axis length
MIT A (logarithmic)	2.9	1.8
MIT B	2.7	1.8
MIT C	4.5	2.5
MIT A (linear)	2.0	1.1
MIT C	2.2	1.7

As the lengths are given in units of 0.78 km, a typical cell at the $\log Z = 4$ level has major and minor axes of about 4.5 and 2.8 km, respectively. The geometrical mean, or radius of the equivalent circle, is 3.5 km, as noted in various CCIR reports. The cell sizes can be found for other levels, but the highest levels tend to be the most irregular, thus it is well to derive such data from the lines fitted to several levels, or sets of ellipses, as will be discussed. The many other individual cell characteristics may properly be ignored after it is shown that they are adequately represented by the set parameters.

7.4 SETS OF ELLIPSES

7.4.1 Fitting Errors

Figure 7-4 graphically portrays the individual ellipse parameters for MIT-LL cell A as in figure 5-2(a). Inspection of the diagram for the different elevation angles shows both regularity and irregularity. The diagrams for 2.5°, 3°, and 3.5° are very similar, taking account of the expanded scale. Those for 1.5° and 2° appear somewhat similar until it is noted that the 2° centroid line points in the direction opposite to those of the other four. The 4° and 4.5° diagrams form a small rough group, but it seems reasonable that the bottoms and tops of the cells would be most irregular. To emphasize this, the log $Z = 4$ ellipses at 2.5°, 3°, and 3.5° are closely identical, whereas the 1° and 5° levels shown in figures 3-4(a) and 3-4(i) are highly irregular. Fortunately, they are also very weak, an inverse of the basic rule postulated previously that intensity and order go together. Similar plots for the fitted sets of ellipses are shown in figure 7-5, but only one ellipse axis is shown for each set, as they all have the same orientation.

The errors of fitting the ellipses to the basic contours are shown later in tables 7-3 to 7-5. It is of interest to study the increase in error between the individual fits and the set fits. These are shown in histogram form in figure 7-3(b). The differential error due to set fitting, that is, alining orientations and eccentricities, and fitting centroid and area lines has a median value of about 5 percent. This remarkably low figure indicates the basic orderly structure of the cell, even though the individual contours are not precisely elliptical. It is strongly implied that the basic assumption of elliptical shapes is reasonable.

7.4.2 Set Characteristics

The characteristics of the ellipse sets for a given time or elevation are best considered along with those for the related sets, but a few points are worth noting separately. For example, the cell size at one-half peak reflectivity may be found by averaging the areas from table 7-4 for Min $Z = 3$, as this corresponds to $Z/Z_{max} = 0.5$ according to table 7-1. Attention is restricted at first to those times when a peak of 40 dBZ occurred, that is, 2322 to 2345 for MIT cell A and 2316 for MIT cell B. For cell A the average area is 14 square boxes, or an effective diameter of 3.3 km, close to that noted in section 7.3.2 for 40 dBZ. For times and cells with lower peak intensities, the areas are generally much larger and of little interest.

From the tabulated areas fitted to each contour of log Z it is easy to obtain the apex or log Z at zero area. The peak values found are listed in table 7-2 along with the precise peak values from the MIT-LL tape, converted to dBZ. It may be seen that even though the logarithmic data are quantized in 10-dBZ steps, the use of several levels and a good model has more effect on accuracy than the quantizing interval. In other words, the model is a sufficiently good representation of the cell that a peak at 46 dBZ can be predicted from inputs at 10, 20, 30, and 40 dBZ. A detailed plot using 1-dB steps shows that the large difference at 2334 is due to the coincidence that a notch in the distribution fell at 40 dBZ, shifting the best-fit profile using that point.

Table 7-2.–Peak Values of Log Z

Time	Derived, dBZ	Precise, dBZ	Difference
2322	47	46.4	0.6
2328	45.5	45.8	-.3
2334	[a]47.5	50.0	-2.5
2340	44	44.3	-.3
2345	42	40.9	-1.1

[a]Found using point at log $Z = 5$.

7.5 RELATED SETS OF ELLIPSES

Tables 7-3 to 7-5 give the results of ellipse fitting operations. The following information is presented in this section with regard to related sets:

Data source	Raw data	Ellipse data	Data plots
MIT logarithmic	Figure 7-1	Table 7-3	Figures 7-4 and 7-5
MIT linear	Figure 7-1	Table 7-4	
NSSL	Figure 7-2	Table 7-5	Figure 7-2

Figure 5-3 has presented horizontal cross sections through MIT-LL cell A, supporting the use of a vertical, cylindrical cell model. Figure 7-6 shows vertical sections through MIT-LL cells A, B, and C along lines shown in figure 3-4(c). The tapered tops and split bottoms are evident in cells B and C. The distributions of the parameters of the ellipses, TAV and TRZ, are shown in figures 7-3(c) and 7-3(d). The histogram for NSSL ellipse set orientation, TAV, shows the predominant northeast-to-southwest direction assumed by Rogers and Rao (ref. 1), but the MIT-LL results do not. However, the latter storm cells are weaker, with only a single box with log $Z = 5$. They are also nearly round, with an average minor/major axis ratio of about 0.75 and about the same value for centroid line slope PRJ. The NSSL storm, on the other hand, showed a maximum intensity of log $Z = 5$ from 1735 to 1820 and was highly elliptical, with a larger PRJ. The histogram for centroid line azimuth, TRZ minus TAV, shows that the line of ellipse centers was displaced about 20° ccw from the major axis line in data from all sources.

The NSSL time sequence of figure 7-2 and additional data from table 5-4 are summarized in figure 7-7. The azimuth (AZ) and range (RU) coordinates can be seen to vary smoothly, with the azimuth fairly constant and the range increasing slowly in a southeasterly direction at about 12 km s^{-1} (23 knots). The average orientation, TAV, runs northeast to southwest, as assumed by Rogers and Rao (ref. 1), except for one point. The angle between the centroid line, TRZ, and TAV remained small until the cell split a second time. The area profile intercept dBZ_{max} fell slowly and the slope remained fairly constant, although

the area for log $Z = 4$, AREA (4), dropped sharply after the split. The weakening of the storm is also indicated by decreasing ellipticity (increasing RAV) and increasing symmetry or concentricity (decreasing PRJ). The intensity, long life, and major axis of about 37 km (20 miles) indicate that this may be the type of supercell associated with tornadoes and/or hailstorms.

Table 7-3.–MIT-LL Logarithmic Ellipse Data. (a) Cell A

MOCAYR 7297C							MINZ=1				MINZ=2				MINZ=3				MINZ=4				MINZ=5			
TIME							THTA	MAJ	MIN	RAT	THTA	MAJ	MIN	RAT	THTA	MAJ	MIN	RAT	THTA	MAJ	MIN	RAT	THTA	MAJ	MIN	RAT
2316							85.	4.6	2.9	0.64	-65.	3.1	2.7	0.84												
CFA	CFR	CFZ	TRZ	PRJ	TAV	RAV	AZ-CG-RU		AREA	ER	AZ-CG-RU		AREA	ER	AZ-CG-RU		AREA	ER	AZ-CG-RU		AREA	ER	AZ-CG-RU		AREA	ER
							32.7	24.8	43	13	32.6	25.2	27	13												
32.6	25.0	1.5	102	C.9	-79	0.7	32.7	24.8	43	17	32.6	25.2	27	20												
32.6	25.0	1.5	102	C.9	-80	0.6	32.7	24.8	43	13	32.6	25.2	27	25												
TIME							THTA	MAJ	MIN	RAT	THTA	MAJ	MIN	RAT	THTA	MAJ	MIN	RAT	THTA	MAJ	MIN	RAT	THTA	MAJ	MIN	RAT
2322							-51.	8.0	5.4	0.68	-61.	6.3	4.1	C.64	-62.	5.7	2.8	0.49	-74.	3.9	1.7	0.44				
CFA	CFR	CFZ	TRZ	PRJ	TAV	RAV	AZ-CG-RU		AREA	ER	AZ-CG-RU		AREA	ER	AZ-CG-RU		AREA	ER	AZ-CG-RU		AREA	ER	AZ-CG-RU		AREA	ER
							33.4	26.1	138	23	33.7	25.9	83	25	33.5	25.4	51	11	33.8	25.2	22	8				
33.6	25.6	2.5	-72	C.6	-66	0.5	33.4	26.1	113	30	33.5	25.8	83	21	33.6	25.5	52	16	33.7	25.2	22	24				
33.6	25.6	2.5	-72	C.6	-650	0.6	33.4	26.1	113	41	33.5	25.8	83	37	33.6	25.5	52	42	33.7	25.2	22	48				
33.6	25.6	2.5	-72	C.6	-65	0.6	33.4	26.1	113	32	33.5	25.8	83	21	33.6	25.5	52	20	33.7	25.2	22	30				
TIME							THTA	MAJ	MIN	RAT	THTA	MAJ	MIN	RAT	THTA	MAJ	MIN	RAT	THTA	MAJ	MIN	RAT	THTA	MAJ	MIN	RAT
2328							-55.	7.2	4.6	0.64	-60.	7.1	3.9	C.54	-64.	4.8	3.1	0.65	-71.	3.0	1.9	0.65				
CFA	CFR	CFZ	TRZ	PRJ	TAV	RAV	AZ-CG-RU		AREA	ER	AZ-CG-RU		AREA	ER	AZ-CG-RU		AREA	ER	AZ-CG-RU		AREA	ER	AZ-CG-RU		AREA	ER
							32.1	25.6	106	12	32.4	25.7	88	8	32.3	25.6	49	15	31.5	26.8	19	0				
32.1	25.9	2.5	121	C.9	-65	0.6	32.4	25.3	123	21	32.2	25.7	88	15	31.9	26.1	53	22	31.7	26.5	19	0				
32.1	25.9	2.5	121	C.9	-65	0.6	32.4	25.3	123	19	32.2	25.7	88	17	31.9	26.1	53	22	31.7	26.5	19	10				
TIME							THTA	MAJ	MIN	RAT	THTA	MAJ	MIN	RAT	THTA	MAJ	MIN	RAT	THTA	MAJ	MIN	RAT	THTA	MAJ	MIN	RAT
2334							-45.	9.2	5.7	0.61	-40.	7.8	5.1	0.66	-11.	5.1	4.2	0.82	-65.	3.0	2.2	0.74	0.	0.5	0.5	1.00
CFA	CFR	CFZ	TRZ	PRJ	TAV	RAV	AZ-CG-RU		AREA	ER	AZ-CG-RU		AREA	ER	AZ-CG-RU		AREA	ER	AZ-CG-RU		AREA	ER	AZ-CG-RU		AREA	ER
							32.C	25.6	167	13	31.6	26.1	128	15	31.8	26.5	68	18	31.3	26.8	22	24				
31.7	26.3	2.5	114	C.8	-38	0.7	31.9	25.7	181	18	31.8	26.1	128	21	31.6	26.5	75	21	31.4	26.8	22	24				
31.7	26.3	2.5	114	0.8	-40	0.6	31.9	25.7	181	15	31.8	26.1	128	14	31.6	26.5	75	25	31.4	26.8	22	24				
TIME							THTA	MAJ	MIN	RAT	THTA	MAJ	MIN	RAT	THTA	MAJ	MIN	RAT	THTA	MAJ	MIN	RAT	THTA	MAJ	MIN	RAT
2340							-26.	8.9	5.8	0.65	-9.	7.0	4.9	C.70	-14.	4.4	3.5	0.79	-71.	2.9	1.8	0.64				
CFA	CFR	CFZ	TRZ	PRJ	TAV	RAV	AZ-CG-RU		AREA	ER	AZ-CG-RU		AREA	ER	AZ-CG-RU		AREA	ER	AZ-CG-RU		AREA	ER	AZ-CG-RU		AREA	ER
							32.6	26.2	165	18	32.0	26.8	11C	21	31.2	26.2	50	18	31.6	26.8	17	11				
31.8	26.5	2.5	164	C.8	-31	0.7	32.4	26.3	160	17	32.0	26.5	112	24	31.6	26.6	64	30	31.3	26.7	17	45				
31.8	26.5	2.5	164	C.8	-30	0.6	32.4	26.3	160	15	32.0	26.5	112	25	31.6	26.6	64	30	31.3	26.7	17	45				

Table 7-3.–(a) Continued

TIME							THTA MAJ MIN RAT	THTA MAJ MIN RAT	THTA MAJ MIN RAT	THTA MAJ MIN RAT	THTA MAJ MIN RAT
2345							7. 7.2 6.2 0.86	11. 6.5 5.1 0.79	-57. 4.5 3.3 0.73	-45. 1.8 1.5 0.81	
CFA	CFR	CFZ	TRZ	PRJ	TAV	RAV	AZ-CG-RU AREA ER	AZ-CG-RU AREA ER	AZ-CG-RU AREA ER	AZ-CG-RU AREA ER	AZ-CG-RU AREA ER
							33.0 28.3 142 13	32.6 28.5 107 23	31.0 28.0 48 18	31.7 28.2 9 36	
32.1	28.2	2.5	191	1.3	-30	0.7	33.0 28.4 158 19	32.4 28.3 108 26	31.7 28.2 58 32	31.1 28.1 9 50	
32.1	28.2	2.5	191	1.3	-30	0.6	33.0 28.4 158 27	32.4 28.3 108 29	31.7 28.2 58 35	31.1 28.1 9 50	
TIME							THTA MAJ MIN RAT	THTA MAJ MIN RAT	THTA MAJ MIN RAT	THTA MAJ MIN RAT	THTA MAJ MIN RAT
2351							35. 8.0 5.1 0.64	63. 5.2 4.5 0.85	44. 3.6 3.1 0.85		
CFA	CFR	CFZ	TRZ	PRJ	TAV	RAV	AZ-CG-RU AREA ER	AZ-CG-RU AREA ER	AZ-CG-RU AREA ER	AZ-CG-RU AREA ER	AZ-CG-RU AREA ER
							33.4 29.2 130 18	32.3 28.9 75 17	32.3 29.1 36 15		
32.7	29.0	2.0	185	1.1	54	0.7	33.3 29.1 130 25	32.7 29.0 83 20	32.1 29.0 36 10		
32.7	29.0	2.0	185	1.1	50	0.6	33.3 29.1 130 17	32.7 29.0 83 22	32.1 29.0 36 24		
TIME							THTA MAJ MIN RAT	THTA MAJ MIN RAT	THTA MAJ MIN RAT	THTA MAJ MIN RAT	THTA MAJ MIN RAT
2357							51. 7.8 4.2 0.53	52. 3.0 0.6 0.21			
CFA	CFR	CFZ	TRZ	PRJ	TAV	RAV	AZ-CG-RU AREA ER	AZ-CG-RU AREA ER	AZ-CG-RU AREA ER	AZ-CG-RU AREA ER	AZ-CG-RU AREA ER
							34.9 34.8 105 29	32.6 32.6 6 80			
33.8	33.7	1.5	224	6.3	51	0.3	34.9 34.8 105 29	32.6 32.6 6 90			
33.8	33.7	1.5	224	6.3	50	0.6	34.9 34.8 105 29	32.6 32.6 6 90			
TIME							THTA MAJ MIN RAT	THTA MAJ MIN RAT	THTA MAJ MIN RAT	THTA MAJ MIN RAT	THTA MAJ MIN RAT
2316							85. 4.6 2.9 0.64	-65. 3.1 2.7 0.84			
CFA	CFR	CFZ	TRZ	PRJ	TAV	RAV	AZ-CG-RU AREA ER	AZ-CG-RU AREA ER	AZ-CG-RU AREA ER	AZ-CG-RU AREA ER	AZ-CG-RU AREA ER
							32.7 24.8 43 13	32.6 25.2 27 13			
32.6	25.0	1.5	102	0.9	-80	0.6	32.7 24.8 80 46	32.6 25.2 40 32			
TIME							THTA MAJ MIN RAT	THTA MAJ MIN RAT	THTA MAJ MIN RAT	THTA MAJ MIN RAT	THTA MAJ MIN RAT
2322							-51. 8.0 5.4 0.68	-61. 6.3 4.1 0.64	-62. 5.7 2.8 0.49	-74. 3.9 1.7 0.44	
CFA	CFR	CFZ	TRZ	PRJ	TAV	RAV	AZ-CG-RU AREA ER	AZ-CG-RU AREA ER	AZ-CG-RU AREA ER	AZ-CG-RU AREA ER	AZ-CG-RU AREA ER
							33.4 26.1 138 23	33.7 25.9 83 25	33.5 25.4 51 11	33.8 25.2 22 8	
33.6	25.6	2.5	-72	0.6	-65	0.6	33.4 26.1 140 26	33.5 25.8 100 20	33.6 25.5 60 20	33.7 25.2 20 38	
TIME							THTA MAJ MIN RAT	THTA MAJ MIN RAT	THTA MAJ MIN RAT	THTA MAJ MIN RAT	THTA MAJ MIN RAT
2328							-55. 7.2 4.6 0.64	-60. 7.1 3.9 0.54	-64. 4.8 3.1 0.65	-71. 3.0 1.9 0.65	
CFA	CFR	CFZ	TRZ	PRJ	TAV	RAV	AZ-CG-RU AREA ER	AZ-CG-RU AREA ER	AZ-CG-RU AREA ER	AZ-CG-RU AREA ER	AZ-CG-RU AREA ER
							32.1 25.6 106 12	32.4 25.7 88 8	32.3 25.6 49 15	31.5 26.8 19 0	
32.1	25.9	2.5	121	0.9	-65	0.6	32.4 25.3 140 27	32.2 25.7 100 15	31.9 26.1 60 24	31.7 26.5 20 5	

Table 7-3.–(a) Concluded

TIME							THTA MAJ MIN RAT	THTA MAJ MIN RAT	THTA MAJ MIN RAT	THTA MAJ MIN RAT	THTA MAJ MIN RAT
2334							-45. 9.2 5.7 0.61	-40. 7.8 5.1 0.66	-11. 5.1 4.2 0.82	-65. 3.0 2.2 0.74	0. 0.5 0.5 1.00
CFA	CFR	CFZ	TRZ	PRJ	TAV	RAV	AZ-CG-RU AREA ER	AZ-CG-RU AREA ER	AZ-CG-RU AREA ER	AZ-CG-RU AREA ER	AZ-CG-RU AREA ER
							32.0 25.6 167 13	31.6 26.1 128 15	31.8 26.5 68 18	31.3 26.8 22 24	
31.7	26.3	2.5	114	0.8	-40	0.6	31.9 25.7 140 19	31.8 26.1 100 25	31.6 26.5 60 31	31.4 26.8 20 17	
TIME							THTA MAJ MIN RAT	THTA MAJ MIN RAT	THTA MAJ MIN RAT	THTA MAJ MIN RAT	THTA MAJ MIN RAT
2340							-26. 8.9 5.8 0.65	-9. 7.0 4.9 0.70	-14. 4.4 3.5 0.79	-71. 2.9 1.8 0.64	
CFA	CFR	CFZ	TRZ	PRJ	TAV	RAV	AZ-CG-RU AREA ER	AZ-CG-RU AREA ER	AZ-CG-RU AREA ER	AZ-CG-RU AREA ER	AZ-CG-RU AREA ER
							32.6 26.2 165 18	32.0 26.8 110 21	31.2 26.2 50 18	31.6 26.8 17 11	
31.8	26.5	2.5	164	0.8	-30	0.6	32.4 26.3 140 21	32.0 26.5 100 23	31.6 26.6 60 28	31.3 26.7 20 31	
TIME							THTA MAJ MIN RAT	THTA MAJ MIN RAT	THTA MAJ MIN RAT	THTA MAJ MIN RAT	THTA MAJ MIN RAT
2345							7. 7.2 6.2 0.86	11. 6.5 5.1 0.79	-57. 4.5 3.3 0.73	-45. 1.8 1.5 0.81	
CFA	CFR	CFZ	TRZ	PRJ	TAV	RAV	AZ-CG-RU AREA ER	AZ-CG-RU AREA ER	AZ-CG-RU AREA ER	AZ-CG-RU AREA ER	AZ-CG-RU AREA ER
							33.0 28.3 142 13	32.6 28.5 107 23	31.0 28.0 48 18	31.7 28.2 9 36	
32.1	28.2	2.5	191	1.3	-30	0.6	33.0 28.4 140 23	32.4 28.3 100 28	31.7 28.2 60 36	31.1 28.1 20 61	
TIME							THTA MAJ MIN RAT	THTA MAJ MIN RAT	THTA MAJ MIN RAT	THTA MAJ MIN RAT	THTA MAJ MIN RAT
2351							35. 8.0 5.1 0.64	63. 5.2 4.5 0.85	44. 3.6 3.1 0.85		
CFA	CFR	CFZ	TRZ	PRJ	TAV	RAV	AZ-CG-RU AREA ER	AZ-CG-RU AREA ER	AZ-CG-RU AREA ER	AZ-CG-RU AREA ER	AZ-CG-RU AREA ER
							33.4 29.2 130 18	32.3 28.9 75 17	32.3 29.1 36 15		
32.7	29.0	2.0	185	1.1	50	0.6	33.3 29.1 100 29	32.7 29.0 60 26	32.1 29.0 20 48		
TIME							THTA MAJ MIN RAT	THTA MAJ MIN RAT	THTA MAJ MIN RAT	THTA MAJ MIN RAT	THTA MAJ MIN RAT
2357							51. 7.8 4.2 0.53	52. 3.0 0.6 0.21			
CFA	CFR	CFZ	TRZ	PRJ	TAV	RAV	AZ-CG-RU AREA ER	AZ-CG-RU AREA ER	AZ-CG-RU AREA ER	AZ-CG-RU AREA ER	AZ-CG-RU AREA ER
							34.9 34.8 105 29	32.6 32.6 6 80			
33.8	33.7	1.5	224	6.3	50	0.6	34.9 34.8 80 40	32.6 32.6 40 87			

Table 7-3.–(b) Cell B

MODAYR 72970							MINZ=1					MINZ=2					MINZ=3					MINZ=4					MINZ=5				
TIME 2316							THTA	MAJ	MIN	RAT		THTA	MAJ	MIN	RAT		THTA	MAJ	MIN	RAT		THTA	MAJ	MIN	RAT		THTA	MAJ	MIN	RAT	
							4.	6.8	3.3	0.48		0.	3.7	1.2	0.34																
CFA	CFR	CFZ	TRZ	PRJ	TAV	RAV	AZ-CG-RU		AREA	ER		AZ-CG-RU		AREA	ER		AZ-CG-RU		AREA	ER		AZ-CG-RU		AREA	ER		AZ-CG-RU		AREA	ER	
							42.9	34.7	71	48		42.4	35.2	15	69																
42.6	35.0	1.5	136	1.4	2	0.4	42.9	34.7	71	48		42.3	35.2	15	63																
42.6	35.0	1.5	136	1.4	0	0.6	42.9	34.7	71	56		42.3	35.2	15	63																
TIME 2322							THTA	MAJ	MIN	RAT		THTA	MAJ	MIN	RAT		THTA	MAJ	MIN	RAT		THTA	MAJ	MIN	RAT		THTA	MAJ	MIN	RAT	
							-12.	6.9	4.3	0.62		-15.	6.2	3.6	0.58		-21.	4.0	2.9	0.74		-12.	2.8	1.4	0.51						
CFA	CFR	CFZ	TRZ	PRJ	TAV	RAV	AZ-CG-RU		AREA	ER		AZ-CG-RU		AREA	ER		AZ-CG-RU		AREA	ER		AZ-CG-RU		AREA	ER		AZ-CG-RU		AREA	ER	
							44.0	36.7	96	17		43.7	36.9	71	28		42.6	37.1	38	10		43.5	36.7	13	37						
43.5	36.8	2.5	174	0.6	-16	0.6	43.9	36.8	100	17		43.6	36.8	71	25		43.3	36.9	42	26		43.0	36.9	13	37						
43.5	36.8	2.5	174	0.6	-20	0.6	43.9	36.8	100	20		43.6	36.8	71	25		43.3	36.9	42	26		43.0	36.9	13	37						
TIME 2328							THTA	MAJ	MIN	RAT		THTA	MAJ	MIN	RAT		THTA	MAJ	MIN	RAT		THTA	MAJ	MIN	RAT		THTA	MAJ	MIN	RAT	
							-47.	6.1	4.6	0.75		-31.	5.2	4.0	0.76		-65.	3.8	2.9	0.77		7.	2.5	2.1	0.83						
CFA	CFR	CFZ	TRZ	PRJ	TAV	RAV	AZ-CG-RU		AREA	ER		AZ-CG-RU		AREA	ER		AZ-CG-RU		AREA	ER		AZ-CG-RU		AREA	ER		AZ-CG-RU		AREA	ER	
							43.0	37.0	89	18		43.4	36.3	67	8		42.3	36.5	36	20		42.4	37.1	17	11						
42.8	36.7	2.5	169	0.6	-29	0.7	43.3	36.6	93	21		43.0	36.7	67	19		42.6	36.8	42	31		42.3	36.8	17	21						
42.8	36.7	2.5	169	0.6	-30	0.6	43.3	36.6	93	21		43.0	36.7	67	19		42.6	36.8	42	27		42.3	36.8	17	45						
TIME 2334							THTA	MAJ	MIN	RAT		THTA	MAJ	MIN	RAT		THTA	MAJ	MIN	RAT		THTA	MAJ	MIN	RAT		THTA	MAJ	MIN	RAT	
							-16.	4.5	4.4	0.96		15.	4.0	3.1	0.77		5.	2.4	1.4	0.59											
CFA	CFR	CFZ	TRZ	PRJ	TAV	RAV	AZ-CG-RU		AREA	ER		AZ-CG-RU		AREA	ER		AZ-CG-RU		AREA	ER		AZ-CG-RU		AREA	ER		AZ-CG-RU		AREA	ER	
							44.5	36.7	64	17		44.1	37.3	40	13		44.5	37.2	11	53											
44.4	37.1	2.0	92	0.5	10	0.7	44.4	36.8	64	17		44.4	37.1	37	13		44.4	37.3	11	42											
44.4	37.1	2.0	92	0.5	10	0.6	44.4	36.8	64	27		44.4	37.1	37	26		44.4	37.3	11	53											
TIME 2340							THTA	MAJ	MIN	RAT		THTA	MAJ	MIN	RAT		THTA	MAJ	MIN	RAT		THTA	MAJ	MIN	RAT		THTA	MAJ	MIN	RAT	
							-30.	3.0	2.5	0.84																					
CFA	CFR	CFZ	TRZ	PRJ	TAV	RAV	AZ-CG-RU		AREA	ER		AZ-CG-RU		AREA	ER		AZ-CG-RU		AREA	ER		AZ-CG-RU		AREA	ER		AZ-CG-RU		AREA	ER	
							43.9	37.6	25	27																					
TIME 2345							THTA	MAJ	MIN	RAT		THTA	MAJ	MIN	RAT		THTA	MAJ	MIN	RAT		THTA	MAJ	MIN	RAT		THTA	MAJ	MIN	RAT	
							-59.	2.0	0.9	0.43																					
CFA	CFR	CFZ	TRZ	PRJ	TAV	RAV	AZ-CG-RU		AREA	ER		AZ-CG-RU		AREA	ER		AZ-CG-RU		AREA	ER		AZ-CG-RU		AREA	ER		AZ-CG-RU		AREA	ER	
							44.8	38.5	6	0																					

Table 7-3.–(b) Concluded

TIME							THTA MAJ MIN RAT	THTA MAJ MIN RAT	THTA MAJ MIN RAT	THTA MAJ MIN RAT	THTA MAJ MIN RAT
2316							4. 6.8 3.3 0.48	0. 3.7 1.2 0.34			
CFA	CFR	CFZ	TRZ	PRJ	TAV	RAV	AZ-CG-RU AREA ER	AZ-CG-RU AREA ER	AZ-CG-RU AREA ER	AZ-CG-RU AREA ER	AZ-CG-RU AREA ER
							42.9 34.7 71 48	42.4 35.2 15 69			
42.6	35.0	1.5	136	1.4	0	0.6	42.9 34.7 55 58	42.3 35.2 24 70			

TIME							THTA MAJ MIN RAT	THTA MAJ MIN RAT	THTA MAJ MIN RAT	THTA MAJ MIN RAT	THTA MAJ MIN RAT
2322							-12. 6.9 4.3 0.62	-15. 6.2 3.6 0.58	-21. 4.0 2.9 0.74	-12. 2.8 1.4 0.51	
CFA	CFR	CFZ	TRZ	PRJ	TAV	RAV	AZ-CG-RU AREA ER	AZ-CG-RU AREA ER	AZ-CG-RU AREA ER	AZ-CG-RU AREA ER	AZ-CG-RU AREA ER
							44.0 36.7 96 17	43.7 36.9 71 28	42.6 37.1 38 10	43.5 36.7 13 37	
43.5	36.8	2.5	174	0.6	-20	0.6	43.9 36.8 100 20	43.6 36.8 70 25	43.3 36.9 40 26	43.0 36.9 9 35	

TIME							THTA MAJ MIN RAT	THTA MAJ MIN RAT	THTA MAJ MIN RAT	THTA MAJ MIN RAT	THTA MAJ MIN RAT
2328							-47. 6.1 4.6 0.75	-31. 5.2 4.0 0.76	-65. 3.8 2.9 0.77	7. 2.5 2.1 0.83	
CFA	CFR	CFZ	TRZ	PRJ	TAV	RAV	AZ-CG-RU AREA ER	AZ-CG-RU AREA ER	AZ-CG-RU AREA ER	AZ-CG-RU AREA ER	AZ-CG-RU AREA ER
							43.0 37.0 89 18	43.4 36.3 67 8	42.3 36.5 36 20	42.4 37.1 17 11	
42.8	36.7	2.5	169	0.6	-30	0.6	43.3 36.6 100 25	43.0 36.7 70 19	42.6 36.8 40 27	42.3 36.8 9 41	

TIME							THTA MAJ MIN RAT	THTA MAJ MIN RAT	THTA MAJ MIN RAT	THTA MAJ MIN RAT	THTA MAJ MIN RAT
2334							-16. 4.5 4.4 0.96	15. 4.0 3.1 0.77	5. 2.4 1.4 0.59		
CFA	CFR	CFZ	TRZ	PRJ	TAV	RAV	AZ-CG-RU AREA ER	AZ-CG-RU AREA ER	AZ-CG-RU AREA ER	AZ-CG-RU AREA ER	AZ-CG-RU AREA ER
							44.5 36.7 64 17	44.1 37.3 40 13	44.5 37.2 11 53		
44.4	37.1	2.0	92	0.5	10	0.6	44.4 36.8 70 32	44.4 37.1 40 29	44.4 37.3 9 49		

TIME							THTA MAJ MIN RAT	THTA MAJ MIN RAT	THTA MAJ MIN RAT	THTA MAJ MIN RAT	THTA MAJ MIN RAT
2340							-30. 3.0 2.5 0.84				
CFA	CFR	CFZ	TRZ	PRJ	TAV	RAV	AZ-CG-RU AREA ER	AZ-CG-RU AREA ER	AZ-CG-RU AREA ER	AZ-CG-RU AREA ER	AZ-CG-RU AREA ER
							43.9 37.6 25 27				

TIME							THTA MAJ MIN RAT	THTA MAJ MIN RAT	THTA MAJ MIN RAT	THTA MAJ MIN RAT	THTA MAJ MIN RAT
2345							-59. 2.0 0.9 0.43				
CFA	CFR	CFZ	TRZ	PRJ	TAV	RAV	AZ-CG-RU AREA ER	AZ-CG-RU AREA ER	AZ-CG-RU AREA ER	AZ-CG-RU AREA ER	AZ-CG-RU AREA ER
							44.8 38.5 6 0				

Table 7-3.–(c) Cell C

	MCDAYR 72970							MINZ=1	MINZ=2	MINZ=3	MINZ=4	MINZ=5
Cell C1	TIME 2310							THTA MAJ MIN RAT -13.11.5 8.7 0.76	THTA MAJ MIN RAT -10.10.0 7.4 0.74	THTA MAJ MIN RAT -11. 7.1 6.2 0.88	THTA MAJ MIN RAT -59. 5.3 2.0 0.37	THTA MAJ MIN RAT
	CFA	CFR	CFZ	TRZ	PRJ	TAV	RAV	AZ-CG-RU AREA ER	AZ-CG-RU AREA ER	AZ-CG-RU AREA ER	AZ-CG-RU AREA ER	AZ-CG-RU AREA ER
								12.4 25.2 319 33	11.9 24.6 235 32	10.4 23.8 140 25	10.3 24.9 34 21	
	11.2	24.6	2.5	196	1.6	-26	0.6	12.5 25.0 335 33	11.6 24.7 235 32	10.8 24.5 134 29	10.0 24.2 34 45	
	TIME 2316							THTA MAJ MIN RAT 36.11.0 8.6 0.78	THTA MAJ MIN RAT 30. 9.8 7.2 0.73	THTA MAJ MIN RAT 50. 7.0 4.4 0.63	THTA MAJ MIN RAT 35. 3.7 2.9 0.79	THTA MAJ MIN RAT
	CFA	CFR	CFZ	TRZ	PRJ	TAV	RAV	AZ-CG-RU AREA ER	AZ-CG-RU AREA ER	AZ-CG-RU AREA ER	AZ-CG-RU AREA ER	AZ-CG-RU AREA ER
								13.4 23.8 298 19	12.1 23.5 224 20	9.5 22.6 99 29	7.8 20.7 35 15	
	10.7	22.6	2.5	208	4.4	38	0.7	13.7 24.2 328 20	11.7 23.1 230 20	9.7 22.1 132 34	7.8 21.1 35 25	
	TIME 2322							THTA MAJ MIN RAT 60. 8.3 8.1 0.98	THTA MAJ MIN RAT -0. 7.2 5.8 0.80	THTA MAJ MIN RAT -64. 3.1 1.6 0.51	THTA MAJ MIN RAT	THTA MAJ MIN RAT
	CFA	CFR	CFZ	TRZ	PRJ	TAV	RAV	AZ-CG-RU AREA ER	AZ-CG-RU AREA ER	AZ-CG-RU AREA ER	AZ-CG-RU AREA ER	AZ-CG-RU AREA ER
								13.0 24.0 214 19	12.9 23.4 132 35	9.6 22.3 16 0		
	11.8	23.3	2.0	204	4.4	-32	0.7	13.9 24.2 215 25	11.8 23.3 115 46	9.8 22.3 16 31		
	TIME 2328							THTA MAJ MIN RAT 86. 8.1 6.2 0.76	THTA MAJ MIN RAT 51. 6.1 4.7 0.77	THTA MAJ MIN RAT	THTA MAJ MIN RAT	THTA MAJ MIN RAT
	CFA	CFR	CFZ	TRZ	PRJ	TAV	RAV	AZ-CG-RU AREA ER	AZ-CG-RU AREA ER	AZ-CG-RU AREA ER	AZ-CG-RU AREA ER	AZ-CG-RU AREA ER
								12.8 24.1 159 16	13.4 23.1 93 17			
	13.1	23.6	1.5	-56	2.4	69	0.7	12.8 24.1 159 21	13.4 23.1 93 19			
	TIME 2334							THTA MAJ MIN RAT 87. 5.2 3.3 0.63	THTA MAJ MIN RAT 71. 3.1 2.1 0.67	THTA MAJ MIN RAT	THTA MAJ MIN RAT	THTA MAJ MIN RAT
	CFA	CFR	CFZ	TRZ	PRJ	TAV	RAV	AZ-CG-RU AREA ER	AZ-CG-RU AREA ER	AZ-CG-RU AREA ER	AZ-CG-RU AREA ER	AZ-CG-RU AREA ER
								12.4 23.9 55 16	13.3 24.0 21 9			
	12.9	23.9	1.5	3	1.8	79	0.6	12.4 23.9 55 22	13.3 24.0 21 9			
Cell C2	TIME 2310							THTA MAJ MIN RAT 37. 5.5 4.5 0.81	THTA MAJ MIN RAT 63. 2.9 2.1 0.73	THTA MAJ MIN RAT	THTA MAJ MIN RAT	THTA MAJ MIN RAT
	CFA	CFR	CFZ	TRZ	PRJ	TAV	RAV	AZ-CG-RU AREA ER	AZ-CG-RU AREA ER	AZ-CG-RU AREA ER	AZ-CG-RU AREA ER	AZ-CG-RU AREA ER
								31.1 31.3 80 40	31.7 32.1 20 33			
	31.4	31.7	1.5	56	1.8	50	0.7	31.1 31.3 80 41	31.6 32.1 20 33			
	TIME 2316							THTA MAJ MIN RAT 48. 8.9 5.7 0.64	THTA MAJ MIN RAT 40. 7.8 4.7 0.60	THTA MAJ MIN RAT 0. 3.0 0.9 0.30	THTA MAJ MIN RAT	THTA MAJ MIN RAT
	CFA	CFR	CFZ	TRZ	PRJ	TAV	RAV	AZ-CG-RU AREA ER	AZ-CG-RU AREA ER	AZ-CG-RU AREA ER	AZ-CG-RU AREA ER	AZ-CG-RU AREA ER
								30.3 29.5 162 20	30.0 29.8 118 21	33.0 31.0 9 71		
	31.1	30.1	2.0	26	3.8	20	0.5	29.3 29.2 171 36	31.1 30.1 90 33	32.8 30.9 9 80		

Table 7-3.—(c) Concluded

TIME							THTA MAJ MIN RAT	THTA MAJ MIN RAT	THTA MAJ MIN RAT	THTA MAJ MIN RAT	THTA MAJ MIN RAT
2322							55. 9.2 4.6 0.49	50. 8.0 2.8 0.35			
CFA	CFR	CFZ	TRZ	PRJ	TAV	RAV	AZ-CG-RU AREA ER	AZ-CG-RU AREA ER	AZ-CG-RU AREA ER	AZ-CG-RU AREA ER	AZ-CG-RU AREA ER
							26.3 28.2 135 23	25.6 28.0 73 26			
25.9	28.1	1.5	198	1.4	53	0.4	26.3 28.2 135 23	25.6 28.0 73 28			
TIME							THTA MAJ MIN RAT	THTA MAJ MIN RAT	THTA MAJ MIN RAT	THTA MAJ MIN RAT	THTA MAJ MIN RAT
2328							58.11.0 6.0 0.54	48.10.0 4.4 0.44			
CFA	CFR	CFZ	TRZ	PRJ	TAV	RAV	AZ-CG-RU AREA ER	AZ-CG-RU AREA ER	AZ-CG-RU AREA ER	AZ-CG-RU AREA ER	AZ-CG-RU AREA ER
							25.7 28.9 211 21	25.5 28.6 142 25			
25.6	28.8	1.5	225	0.7	53	0.4	25.7 28.9 211 24	25.5 28.6 142 24			
TIME							THTA MAJ MIN RAT	THTA MAJ MIN RAT	THTA MAJ MIN RAT	THTA MAJ MIN RAT	THTA MAJ MIN RAT
2334							41.13.4 6.9 0.51	43.10.9 5.2 0.48			
CFA	CFR	CFZ	TRZ	PRJ	TAV	RAV	AZ-CG-RU AREA ER	AZ-CG-RU AREA ER	AZ-CG-RU AREA ER	AZ-CG-RU AREA ER	AZ-CG-RU AREA ER
							25.8 32.8 291 18	25.4 32.8 182 19			
25.6	32.8	1.5	188	0.6	42	0.4	25.8 32.8 291 18	25.4 32.8 182 20			
TIME							THTA MAJ MIN RAT	THTA MAJ MIN RAT	THTA MAJ MIN RAT	THTA MAJ MIN RAT	THTA MAJ MIN RAT
2340							54. 8.0 5.0 0.62	59. 5.6 2.9 0.52			
CFA	CFR	CFZ	TRZ	PRJ	TAV	RAV	AZ-CG-RU AREA ER	AZ-CG-RU AREA ER	AZ-CG-RU AREA ER	AZ-CG-RU AREA ER	AZ-CG-RU AREA ER
							28.0 40.0 128 25	27.3 40.1 53 29			
27.7	40.0	1.5	175	1.4	56	0.5	28.0 40.0 128 27	27.3 40.1 53 29			
TIME							THTA MAJ MIN RAT	THTA MAJ MIN RAT	THTA MAJ MIN RAT	THTA MAJ MIN RAT	THTA MAJ MIN RAT
2345							37. 4.2 3.9 0.93				
CFA	CFR	CFZ	TRZ	PRJ	TAV	RAV	AZ-CG-RU AREA ER	AZ-CG-RU AREA ER	AZ-CG-RU AREA ER	AZ-CG-RU AREA ER	AZ-CG-RU AREA ER
							29.6 47.0 52 40				

Table 7-4.–MIT-LL Linear Ellipse Data. (a) Cell A

	MCCAYR 7297C							MINZ=1				MINZ=2				MINZ=3				MINZ=4				MINZ=5			
Cell A	TIME							THTA	MAJ	MIN	RAT	THTA	MAJ	MIN	RAT	THTA	MAJ	MIN	RAT	THTA	MAJ	MIN	RAT	THTA	MAJ	MIN	RAT
	2316							-83.	3.7	2.9	0.78	-64.	3.1	2.6	C.84	-83.	2.8	1.7	0.60	-71.	1.5	1.4	0.89	-45.	1.2	0.7	0.57
	CFA	CFR	CFZ	TRZ	PRJ	TAV	RAV	AZ-CG-RU	AREA	ER		AZ-CG-RU	AREA	ER		AZ-CG-RU	AREA	ER		AZ-CG-RU	AREA	ER		AZ-CG-RL	AREA	ER	
								32.6	24.8	34	21	32.6	25.2	26	14	32.8	25.1	16	22	32.5	24.8	7	60				
	32.6	25.0	2.5	19C	C.C	-73	0.7	32.6	25.0	35	28	32.6	25.0	26	26	32.6	25.0	16	33	32.6	25.0	7	72				
	TIME							THTA	MAJ	MIN	RAT	THTA	MAJ	MIN	RAT	THTA	MAJ	MIN	RAT	THTA	MAJ	MIN	RAT	THTA	MAJ	MIN	RAT
	2322							-68.	4.2	1.9	0.45	-70.	3.8	1.8	C.48	-68.	3.0	1.3	0.43	-66.	1.9	0.9	0.49	-61.	2.0	0.4	0.22
	CFA	CFR	CFZ	TRZ	PRJ	TAV	RAV	AZ-CG-RU	AREA	ER		AZ-CG-RU	AREA	ER		AZ-CG-RU	AREA	ER		AZ-CG-RU	AREA	ER		AZ-CG-RU	AREA	ER	
								33.6	25.1	26	20	33.8	25.1	23	23	34.0	24.9	13	47	34.1	25.1	6	28				
	33.9	25.0	2.5	-6	C.3	-68	0.4	33.6	25.1	31	38	33.8	25.1	23	23	33.9	25.0	14	43	34.1	25.0	6	66				
	TIME							THTA	MAJ	MIN	RAT	THTA	MAJ	MIN	RAT	THTA	MAJ	MIN	RAT	THTA	MAJ	MIN	RAT	THTA	MAJ	MIN	RAT
	2328							-62.	4.1	2.6	0.63	-83.	3.3	1.9	C.59	-59.	2.9	1.4	0.48	0.	1.4	0.8	0.61	0.	0.5	0.5	1.00
	CFA	CFR	CFZ	TRZ	PRJ	TAV	RAV	AZ-CG-RU	AREA	ER		AZ-CG-RU	AREA	ER		AZ-CG-RU	AREA	ER		AZ-CG-RU	AREA	ER		AZ-CG-RU	AREA	ER	
								32.C	26.3	34	21	31.5	26.8	21	9	31.4	26.6	13	26	31.0	26.7	4	0				
	31.5	26.6	2.5	160	C.6	-47	0.5	32.C	26.4	29	3C	31.6	26.5	21	25	31.3	26.7	12	35	31.0	26.8	4	40				
	TIME							THTA	MAJ	MIN	RAT	THTA	MAJ	MIN	RAT	THTA	MAJ	MIN	RAT	THTA	MAJ	MIN	RAT	THTA	MAJ	MIN	RAT
	2334							-65.	3.0	2.2	C.74	-51.	2.9	1.9	C.66	-51.	1.8	1.5	0.83	-22.	0.7	0.0	0.00	0.	0.5	0.5	1.00
	CFA	CFR	CFZ	TRZ	PRJ	TAV	RAV	AZ-CG-RU	AREA	ER		AZ-CG-RU	AREA	ER		AZ-CG-RU	AREA	ER		AZ-CG-RU	AREA	ER		AZ-CG-RU	AREA	ER	
								31.3	26.8	21	32	31.3	26.6	18	28	31.4	26.1	9	36	31.5	25.5	2	0				
	31.4	26.2	2.5	-85	C.9	-41	0.5	31.3	26.9	26	43	31.4	26.4	18	36	31.4	26.0	10	42	31.4	25.5	2	67				
	TIME							THTA	MAJ	MIN	RAT	THTA	MAJ	MIN	RAT	THTA	MAJ	MIN	RAT	THTA	MAJ	MIN	RAT	THTA	MAJ	MIN	RAT
	2340							-23.	3.8	3.0	C.79	-23.	3.1	2.4	C.77	-77.	2.6	1.8	0.68	-71.	1.4	1.1	0.77	0.	0.5	0.5	1.00
	CFA	CFR	CFZ	TRZ	PRJ	TAV	RAV	AZ-CG-RU	AREA	ER		AZ-CG-RU	AREA	ER		AZ-CG-RU	AREA	ER		AZ-CG-RU	AREA	ER		AZ-CG-RU	AREA	ER	
								31.1	26.4	37	31	31.0	26.7	24	28	31.7	26.6	15	23	31.6	27.2	5	75				
	31.3	26.7	2.5	45	C.6	-57	0.7	31.C	26.4	33	38	31.2	26.6	24	34	31.4	26.8	14	40	31.6	27.0	5	88				
	TIME							THTA	MAJ	MIN	RAT	THTA	MAJ	MIN	RAT	THTA	MAJ	MIN	RAT	THTA	MAJ	MIN	RAT	THTA	MAJ	MIN	RAT
	2345							-51.	4.2	3.1	C.73	24.	3.2	2.4	C.76	5.	2.9	2.3	0.81	24.	2.2	1.9	0.86	-71.	2.0	1.0	0.53
	CFA	CFR	CFZ	TRZ	PRJ	TAV	RAV	AZ-CG-RU	AREA	ER		AZ-CG-RU	AREA	ER		AZ-CG-RU	AREA	ER		AZ-CG-RU	AREA	ER		AZ-CG-RU	AREA	ER	
								30.8	27.9	42	35	30.7	28.0	25	33	30.8	28.0	22	37	30.9	27.8	14	25				
	30.8	27.9	2.5	-26	C.C	18	0.8	30.7	27.9	31	42	30.8	27.9	25	40	30.8	27.9	19	38	30.8	27.9	14	35				
	TIME							THTA	MAJ	MIN	RAT	THTA	MAJ	MIN	RAT	THTA	MAJ	MIN	RAT	THTA	MAJ	MIN	RAT	THTA	MAJ	MIN	RAT
	2351							37.	4.6	3.1	0.68	44.	4.1	2.9	C.71	56.	3.0	2.9	0.98	9.	2.6	1.5	0.58	22.	0.7	0.0	C.00
	CFA	CFR	CFZ	TRZ	PRJ	TAV	RAV	AZ-CG-RU	AREA	ER		AZ-CG-RU	AREA	ER		AZ-CG-RU	AREA	ER		AZ-CG-RU	AREA	ER		AZ-CG-RU	AREA	ER	
								32.2	29.0	46	16	32.2	28.9	39	22	32.5	29.0	28	19	32.7	29.0	13	37				
	32.4	29.0	2.5	6	C.3	36	0.7	32.1	29.0	52	28	32.3	29.0	39	23	32.5	29.0	26	31	32.7	29.0	13	55				
	TIME							THTA	MAJ	MIN	RAT	THTA	MAJ	MIN	RAT	THTA	MAJ	MIN	RAT	THTA	MAJ	MIN	RAT	THTA	MAJ	MIN	RAT
	2357							5C.	7.9	4.1	C.52	53.	7.0	3.4	0.49	48.	5.8	2.3	0.39	47.	4.6	1.1	0.25	31.	2.0	0.7	C.36
	CFA	CFR	CFZ	TRZ	PRJ	TAV	RAV	AZ-CG-RU	AREA	ER		AZ-CG-RU	AREA	ER		AZ-CG-RU	AREA	ER		AZ-CG-RU	AREA	ER		AZ-CG-RL	AREA	ER	
								35.C	34.8	1C4	3C	35.C	34.8	77	41	34.5	34.4	43	65	34.1	34.1	17	82				
	34.7	34.5	2.5	216	C.7	49	0.3	35.1	34.9	1C7	3C	34.8	34.6	77	43	34.5	34.4	47	69	34.2	34.2	17	86				

Table 7-4.–(b) Cell C

Cell C

TIME							THTA MAJ MIN RAT	THTA MAJ MIN RAT	THTA MAJ MIN RAT	THTA MAJ MIN RAT	THTA MAJ MIN RAT
2316							60. 3.8 3.1 0.82	41. 3.6 2.8 0.78	40. 2.7 2.2 0.81	85. 2.4 1.2 0.52	-70. 2.0 0.6 0.29
CFA	CFR	CFZ	TRZ	PRJ	TAV	RAV	AZ-CG-RU AREA ER	AZ-CG-RU AREA ER	AZ-CG-RU AREA ER	AZ-CG-RU AREA ER	AZ-CG-RU AREA ER
							7.8 14.7 39 22	7.7 14.7 33 21	7.7 15.0 19 34	8.4 15.4 10 46	
7.9	14.9	2.5	51	0.5	55	0.7	7.6 14.6 45 28	7.8 14.8 33 22	8.0 15.1 21 47	8.1 15.3 10 57	

TIME							THTA MAJ MIN RAT	THTA MAJ MIN RAT	THTA MAJ MIN RAT	THTA MAJ MIN RAT	THTA MAJ MIN RAT
2322							67. 4.2 2.4 0.58	-70. 2.8 2.1 0.75	-58. 2.2 1.2 0.56	-50. 2.3 1.0 0.45	0. 0.5 0.5 1.00
CFA	CFR	CFZ	TRZ	PRJ	TAV	RAV	AZ-CG-RU AREA ER	AZ-CG-RU AREA ER	AZ-CG-RU AREA ER	AZ-CG-RU AREA ER	AZ-CG-RU AREA ER
							9.5 15.8 33 16	9.7 16.4 19 19	9.4 16.4 9 20	9.5 16.6 8 0	
9.5	16.3	2.5	99	0.4	-60	0.5	9.6 15.9 28 47	9.5 16.2 21 27	9.5 16.4 14 39	9.5 16.6 8 40	

TIME							THTA MAJ MIN RAT	THTA MAJ MIN RAT	THTA MAJ MIN RAT	THTA MAJ MIN RAT	THTA MAJ MIN RAT
2328							77. 5.4 4.3 0.79	58. 4.8 4.2 0.88	-29. 4.0 3.3 0.82	-60. 2.7 2.3 0.86	-71. 1.6 0.9 0.57
CFA	CFR	CFZ	TRZ	PRJ	TAV	RAV	AZ-CG-RU AREA ER	AZ-CG-RU AREA ER	AZ-CG-RU AREA ER	AZ-CG-RU AREA ER	AZ-CG-RU AREA ER
							19.5 18.7 76 23	19.6 18.8 64 24	20.0 18.5 42 38	20.6 18.7 20 26	
19.9	18.7	2.5	-4	0.7	49	0.8	19.4 18.7 86 23	19.8 18.7 64 27	20.1 18.7 42 35	20.5 18.6 20 26	

TIME							THTA MAJ MIN RAT	THTA MAJ MIN RAT	THTA MAJ MIN RAT	THTA MAJ MIN RAT	THTA MAJ MIN RAT
2334							77. 8.0 5.0 0.62	76. 7.3 4.7 0.64	60. 5.6 3.7 0.67	77. 3.9 3.2 0.81	82. 2.7 1.9 0.69
CFA	CFR	CFZ	TRZ	PRJ	TAV	RAV	AZ-CG-RU AREA ER	AZ-CG-RU AREA ER	AZ-CG-RU AREA ER	AZ-CG-RU AREA ER	AZ-CG-RU AREA ER
							22.0 24.2 127 18	22.1 24.5 110 21	22.4 24.5 67 18	22.1 23.2 40 22	
22.2	24.1	2.5	-80	0.6	71	0.7	22.1 24.6 146 24	22.1 24.3 111 24	22.2 23.9 75 25	22.3 23.6 40 26	

TIME							THTA MAJ MIN RAT	THTA MAJ MIN RAT	THTA MAJ MIN RAT	THTA MAJ MIN RAT	THTA MAJ MIN RAT
2340							65. 6.7 4.6 0.68	58. 6.2 3.8 0.61	59. 5.5 2.9 0.52	67. 4.8 1.9 0.40	65. 3.8 1.4 0.37
CFA	CFR	CFZ	TRZ	PRJ	TAV	RAV	AZ-CG-RU AREA ER	AZ-CG-RU AREA ER	AZ-CG-RU AREA ER	AZ-CG-RU AREA ER	AZ-CG-RU AREA ER
							27.3 33.8 97 18	27.2 34.0 76 23	27.3 34.0 52 29	27.0 33.7 30 37	
27.2	33.9	2.5	200	0.1	61	0.5	27.3 33.9 99 28	27.2 33.9 76 23	27.1 33.8 53 35	27.1 33.8 30 50	

TIME							THTA MAJ MIN RAT	THTA MAJ MIN RAT	THTA MAJ MIN RAT	THTA MAJ MIN RAT	THTA MAJ MIN RAT
2345							49. 4.1 3.9 0.95	85. 4.1 3.6 0.86	28. 2.3 1.6 0.68	-90. 1.5 0.8 0.54	0. 0.5 0.5 1.00
CFA	CFR	CFZ	TRZ	PRJ	TAV	RAV	AZ-CG-RU AREA ER	AZ-CG-RU AREA ER	AZ-CG-RU AREA ER	AZ-CG-RU AREA ER	AZ-CG-RU AREA ER
							29.6 41.1 52 40	29.8 41.2 48 42	28.5 39.6 12 73	28.0 39.7 4 85	
29.0	40.4	2.5	224	1.8	67	0.6	29.9 41.4 78 43	29.3 40.7 53 43	28.6 40.1 28 71	28.0 39.4 4100	

TIME							THTA MAJ MIN RAT	THTA MAJ MIN RAT	THTA MAJ MIN RAT	THTA MAJ MIN RAT	THTA MAJ MIN RAT
2345							49. 4.1 3.9 0.95	85. 4.1 3.6 0.86	28. 2.3 1.6 0.68	0. 1.8 0.5 0.29	0. 0.5 0.5 1.00
CFA	CFR	CFZ	TRZ	PRJ	TAV	RAV	AZ-CG-RU AREA ER	AZ-CG-RU AREA ER	AZ-CG-RU AREA ER	AZ-CG-RU AREA ER	AZ-CG-RU AREA ER
							29.6 41.1 52 40	29.8 41.2 48 42	28.5 39.6 12 73	28.0 39.0 3 0	
29.0	40.2	2.5	233	2.1	37	0.6	29.9 41.5 78 49	29.3 40.6 53 51	28.6 39.8 28 71	28.0 38.9 3100	

TIME							THTA MAJ MIN RAT	THTA MAJ MIN RAT	THTA MAJ MIN RAT	THTA MAJ MIN RAT	THTA MAJ MIN RAT
2345							49. 4.1 3.9 0.95	85. 4.1 3.6 0.86	28. 2.3 1.6 0.68	0. 0.5 0.5 1.00	0. 0.5 0.5 1.00
CFA	CFR	CFZ	TRZ	PRJ	TAV	RAV	AZ-CG-RU AREA ER	AZ-CG-RU AREA ER	AZ-CG-RU AREA ER	AZ-CG-RU AREA ER	AZ-CG-RU AREA ER
							29.6 41.1 52 40	29.8 41.2 48 42	28.5 39.6 12 73	28.0 42.0 1 0	
29.0	41.0	2.5	167	1.3	37	0.8	29.9 40.7 78 41	29.3 40.9 52 48	28.6 41.0 26 77	28.0 41.2 1166	

Table 7-5.–NSSL Ellipse Data

	MODAYR							MINZ=1				MINZ=2				MINZ=3				MINZ=4				MINZ=5			
	5 368																										
Cell A	TIME							THTA	MAJ	MIN	RAT	THTA	MAJ	MIN	RAT	THTA	MAJ	MIN	RAT	THTA	MAJ	MIN	RAT	THTA	MAJ	MIN	RAT
	1735							-1.	7.5	3.7	0.49	-10.	6.4	3.0	0.48	-14.	5.2	2.4	0.46	-29.	3.8	1.5	0.39	0.	2.4	0.5	0.21
	CFA	CFR	CFZ	TRZ	PRJ	TAV	RAV	AZ-CG-RU	AREA	ER		AZ-CG-RU	AREA	ER		AZ-CG-RU	AREA	ER		AZ-CG-RU	AREA	ER		AZ-CG-RU	AREA	ER	
								30.5	21.1	90	14	30.2	20.6	62	25	30.5	20.1	40	9	30.0	20.0	18	20				
	30.3	20.4	2.5	249	0.8	-18	0.4	30.5	21.0	84	26	30.4	20.6	62	20	30.2	20.2	40	13	30.1	19.8	18	36				
	TIME							THTA	MAJ	MIN	RAT	THTA	MAJ	MIN	RAT	THTA	MAJ	MIN	RAT	THTA	MAJ	MIN	RAT	THTA	MAJ	MIN	RAT
	1750							-5.	10.3	3.0	0.29	-6.	9.0	2.5	0.28	-2.	7.8	1.7	0.21	-2.	6.5	1.3	0.20	-12.	2.2	0.8	0.37
	CFA	CFR	CFZ	TRZ	PRJ	TAV	RAV	AZ-CG-RU	AREA	ER		AZ-CG-RU	AREA	ER		AZ-CG-RU	AREA	ER		AZ-CG-RU	AREA	ER		AZ-CG-RU	AREA	ER	
								28.1	22.4	100	11	27.9	22.1	74	27	28.8	21.3	42	13	29.2	21.2	28	6				
	28.5	21.8	2.5	-43	1.2	-3	0.2	27.8	22.4	100	15	28.3	22.0	76	21	28.7	21.6	52	26	29.2	21.1	28	19				
	TIME							THTA	MAJ	MIN	RAT	THTA	MAJ	MIN	RAT	THTA	MAJ	MIN	RAT	THTA	MAJ	MIN	RAT	THTA	MAJ	MIN	RAT
	1805							-3.	10.3	3.3	0.32	-0.	8.8	2.6	0.30	-14.	6.6	1.8	0.27	0.	2.3	1.0	0.44	0.	1.1	0.5	0.44
	CFA	CFR	CFZ	TRZ	PRJ	TAV	RAV	AZ-CG-RU	AREA	ER		AZ-CG-RU	AREA	ER		AZ-CG-RU	AREA	ER		AZ-CG-RU	AREA	ER		AZ-CG-RU	AREA	ER	
								27.4	24.6	108	22	28.3	24.0	74	42	28.8	23.3	38	23	31.0	22.5	8	0				
	28.9	23.6	2.5	-31	2.7	-4	0.3	27.1	24.7	107	23	28.3	23.9	74	42	29.4	23.2	41	38	30.6	22.5	8	0				
	TIME							THTA	MAJ	MIN	RAT	THTA	MAJ	MIN	RAT	THTA	MAJ	MIN	RAT	THTA	MAJ	MIN	RAT	THTA	MAJ	MIN	RAT
	1820							-16.	5.3	2.2	0.42	-14.	5.3	1.8	0.35	-15.	4.4	1.4	0.31	-26.	2.4	1.0	0.40				
	CFA	CFR	CFZ	TRZ	PRJ	TAV	RAV	AZ-CG-RU	AREA	ER		AZ-CG-RU	AREA	ER		AZ-CG-RU	AREA	ER		AZ-CG-RU	AREA	ER		AZ-CG-RU	AREA	ER	
								30.2	25.1	38	10	29.8	25.3	32	17	30.6	25.1	20	26	31.0	25.0	8	0				
	30.4	25.1	2.5	-13	0.6	-18	0.3	29.9	25.2	44	21	30.2	25.1	32	6	30.5	25.1	20	9	30.9	25.0	8	0				
	TIME							THTA	MAJ	MIN	RAT	THTA	MAJ	MIN	RAT	THTA	MAJ	MIN	RAT	THTA	MAJ	MIN	RAT	THTA	MAJ	MIN	RAT
	1835							-13.	5.5	2.2	0.41	-14.	5.2	1.9	0.36	-15.	3.5	1.4	0.39	-12.	2.2	0.8	0.37				
	CFA	CFR	CFZ	TRZ	PRJ	TAV	RAV	AZ-CG-RU	AREA	ER		AZ-CG-RU	AREA	ER		AZ-CG-RU	AREA	ER		AZ-CG-RU	AREA	ER		AZ-CG-RU	AREA	ER	
								29.8	27.9	40	4	30.3	27.8	32	11	31.0	27.0	16	40	31.3	26.6	6	0				
	30.6	27.3	2.5	-42	1.4	-14	0.3	29.8	28.0	45	16	30.3	27.5	32	27	30.8	27.1	19	16	31.4	26.6	6	0				
Cell B	TIME							THTA	MAJ	MIN	RAT	THTA	MAJ	MIN	RAT	THTA	MAJ	MIN	RAT	THTA	MAJ	MIN	RAT	THTA	MAJ	MIN	RAT
	1735							2.	15.7	3.9	0.24	3.	14.4	3.3	0.23	6.	12.0	2.5	0.21	9.	8.7	1.4	0.16	0.	2.4	0.5	0.21
	CFA	CFR	CFZ	TRZ	PRJ	TAV	RAV	AZ-CG-RU	AREA	ER		AZ-CG-RU	AREA	ER		AZ-CG-RU	AREA	ER		AZ-CG-RU	AREA	ER		AZ-CG-RU	AREA	ER	
								52.7	24.7	194	16	53.4	24.4	152	19	55.7	24.2	96	23	57.4	23.8	40	26				
	54.8	24.3	2.5	-10	3.3	6	0.2	52.3	24.7	208	22	54.0	24.4	152	22	55.6	24.1	96	22	57.3	23.8	40	40				
	TIME							THTA	MAJ	MIN	RAT	THTA	MAJ	MIN	RAT	THTA	MAJ	MIN	RAT	THTA	MAJ	MIN	RAT	THTA	MAJ	MIN	RAT
	1750							5.	18.3	3.6	0.19	7.	16.8	3.0	0.18	9.	12.2	2.3	0.18	13.	7.9	1.7	0.22	0.	1.1	0.5	0.44
	CFA	CFR	CFZ	TRZ	PRJ	TAV	RAV	AZ-CG-RU	AREA	ER		AZ-CG-RU	AREA	ER		AZ-CG-RU	AREA	ER		AZ-CG-RU	AREA	ER		AZ-CG-RU	AREA	ER	
								59.4	27.5	208	15	60.0	27.1	162	18	62.3	27.0	90	23	64.3	27.0	44	48				
	61.5	27.1	2.5	-5	3.5	10	0.1	58.9	27.4	223	26	60.6	27.2	163	21	62.4	27.1	103	21	64.1	26.9	44	45				

Table 7-5.–Continued

TIME							THTA MAJ MIN RAT	THTA MAJ MIN RAT	THTA MAJ MIN RAT	THTA MAJ MIN RAT	THTA MAJ MIN RAT
1805							9.16.1 4.2 0.26	11.14.2 3.3 0.23	12.11.4 2.8 0.24	21. 8.7 2.1 0.24	14. 5.1 0.3 0.07
CFA	CFR	CFZ	TRZ	PRJ	TAV	RAV	AZ-CG-RU AREA ER	AZ-CG-RU AREA ER	AZ-CG-RU AREA ER	AZ-CG-RU AREA ER	AZ-CG-RU AREA ER
							63.0 29.5 216 10	65.3 29.6 150 23	67.3 29.6 102 25	70.4 30.1 58 12	
66.5	29.7	2.5	4	4.8	14	0.2	62.8 29.5 196 21	65.3 29.6 150 22	67.7 29.8 104 20	70.1 30.0 58 36	
TIME							THTA MAJ MIN RAT	THTA MAJ MIN RAT	THTA MAJ MIN RAT	THTA MAJ MIN RAT	THTA MAJ MIN RAT
1820							15.16.0 4.9 0.30	17.14.2 4.0 0.28	18.11.8 3.3 0.28	18. 7.7 2.3 0.29	25. 3.6 0.3 0.09
CFA	CFR	CFZ	TRZ	PRJ	TAV	RAV	AZ-CG-RU AREA ER	AZ-CG-RU AREA ER	AZ-CG-RU AREA ER	AZ-CG-RU AREA ER	AZ-CG-RU AREA ER
							70.3 33.2 248 19	71.7 33.3 182 25	72.7 33.1 126 26	74.5 33.7 56 44	
72.3	33.3	2.5	6	2.7	18	0.2	70.2 33.1 245 21	71.6 33.2 182 25	73.0 33.4 119 29	74.4 33.5 56 44	
TIME							THTA MAJ MIN RAT	THTA MAJ MIN RAT	THTA MAJ MIN RAT	THTA MAJ MIN RAT	THTA MAJ MIN RAT
1835							19.14.6 5.0 0.34	19.13.2 4.5 0.34	23. 9.9 3.7 0.37	20. 7.4 2.3 0.31	
CFA	CFR	CFZ	TRZ	PRJ	TAV	RAV	AZ-CG-RU AREA ER	AZ-CG-RU AREA ER	AZ-CG-RU AREA ER	AZ-CG-RU AREA ER	AZ-CG-RU AREA ER
							74.1 36.1 234 15	75.3 36.4 190 23	77.4 37.3 118 31	79.7 38.3 54 31	
76.6	37.0	2.5	21	4.1	21	0.3	73.7 35.9 258 19	75.6 36.6 190 24	77.6 37.4 122 32	79.5 38.2 54 31	
TIME							THTA MAJ MIN RAT	THTA MAJ MIN RAT	THTA MAJ MIN RAT	THTA MAJ MIN RAT	THTA MAJ MIN RAT
1850							25.11.9 5.3 0.44	21.11.0 4.6 0.41	16. 9.4 3.3 0.35	10. 5.5 1.3 0.25	
CFA	CFR	CFZ	TRZ	PRJ	TAV	RAV	AZ-CG-RU AREA ER	AZ-CG-RU AREA ER	AZ-CG-RU AREA ER	AZ-CG-RU AREA ER	AZ-CG-RU AREA ER
							76.6 39.5 200 16	77.1 40.2 160 21	78.3 41.1 98 32	80.6 42.6 24 54	
78.2	40.8	2.5	38	3.5	16	0.3	76.1 39.2 228 28	77.5 40.3 160 28	78.9 41.4 92 33	80.3 42.4 24 50	
TIME							THTA MAJ MIN RAT	THTA MAJ MIN RAT	THTA MAJ MIN RAT	THTA MAJ MIN RAT	THTA MAJ MIN RAT
1905							28.10.1 6.1 0.60	26. 9.4 5.1 0.54	19. 7.9 4.0 0.50	5. 5.5 1.3 0.24	
CFA	CFR	CFZ	TRZ	PRJ	TAV	RAV	AZ-CG-RU AREA ER	AZ-CG-RU AREA ER	AZ-CG-RU AREA ER	AZ-CG-RU AREA ER	AZ-CG-RU AREA ER
							79.5 44.5 196 16	80.0 45.0 154 25	80.3 45.5 100 31	80.5 47.0 24 62	
80.0	45.5	2.5	69	1.7	17	0.4	79.6 44.3 220 29	79.9 45.1 155 29	80.2 45.9 89 33	80.5 46.7 24 82	
TIME							THTA MAJ MIN RAT	THTA MAJ MIN RAT	THTA MAJ MIN RAT	THTA MAJ MIN RAT	THTA MAJ MIN RAT
1920							13. 9.8 6.0 0.61	14. 9.1 5.0 0.54	2. 6.9 3.4 0.49	3. 5.7 0.7 0.13	
CFA	CFR	CFZ	TRZ	PRJ	TAV	RAV	AZ-CG-RU AREA ER	AZ-CG-RU AREA ER	AZ-CG-RU AREA ER	AZ-CG-RU AREA ER	AZ-CG-RU AREA ER
							79.2 48.8 186 20	79.3 48.6 146 31	80.0 49.8 74 42	80.0 51.0 14 83	
79.6	49.5	2.5	69	1.7	6	0.3	79.1 48.3 212 36	79.5 49.1 146 34	79.8 49.9 80 44	80.1 50.8 14 83	
TIME							THTA MAJ MIN RAT	THTA MAJ MIN RAT	THTA MAJ MIN RAT	THTA MAJ MIN RAT	THTA MAJ MIN RAT
1935							-3.10.4 5.2 0.50	-0. 8.5 4.7 0.55	-3. 6.8 3.1 0.46	3. 3.9 0.9 0.24	0. 1.1 0.5 0.44
CFA	CFR	CFZ	TRZ	PRJ	TAV	RAV	AZ-CG-RU AREA ER	AZ-CG-RU AREA ER	AZ-CG-RU AREA ER	AZ-CG-RU AREA ER	AZ-CG-RU AREA ER
							78.3 52.4 174 9	78.9 52.7 126 27	79.5 53.4 68 34	76.3 54.8 12 58	
78.3	53.3	2.5	139	2.7	0	0.4	79.8 52.0 183 23	78.8 52.9 126 26	77.8 53.8 69 34	76.7 54.7 12 58	
TIME							THTA MAJ MIN RAT	THTA MAJ MIN RAT	THTA MAJ MIN RAT	THTA MAJ MIN RAT	THTA MAJ MIN RAT
1950							-12. 9.1 5.6 0.61	-10. 8.1 4.9 0.60	-4. 6.0 3.6 0.61	-43. 3.8 1.6 0.41	
CFA	CFR	CFZ	TRZ	PRJ	TAV	RAV	AZ-CG-RU AREA ER	AZ-CG-RU AREA ER	AZ-CG-RU AREA ER	AZ-CG-RU AREA ER	AZ-CG-RU AREA ER
							77.5 56.9 164 24	77.3 57.0 126 37	75.6 58.0 70 47	74.0 57.9 20 33	

Table 7-5.–Concluded

	76.1	57.4	2.5	163	2.7	-19	0.5	78.1	56.9	179	26	76.8	57.2	126	36	75.4	57.6	73	37	74.1	58.0	20	40
	TIME									THTA	MAJ	MIN	RAT	THTA	MAJ	MIN	RAT	THTA	MAJ	MIN	RAT	THTA	MAJ	MIN	RAT
	2005									21.	9.3	6.5	0.69	25.	7.6	5.2	0.68	20.	6.1	3.2	0.52	2.	2.5	1.2	0.47
	CFA	CFR	CFZ	TRZ	PRJ	TAV	RAV	AZ-CG-RU		AREA	ER	AZ-CG-RU		AREA	ER	AZ-CG-RU		AREA	ER	AZ-CG-RU		AREA	ER	AZ-CG-RU	AREA	ER
								75.3	61.3	192	23	75.4	61.4	126	36	75.0	62.8	62	63	72.4	62.8	10	57			
	74.5	62.0	2.5	154	2.5	16	0.5	76.2	61.2	184	30	75.1	61.8	126	42	74.0	62.3	68	61	72.9	62.9	10	46			
	TIME									THTA	MAJ	MIN	RAT	THTA	MAJ	MIN	RAT	THTA	MAJ	MIN	RAT	THTA	MAJ	MIN	RAT	THTA	MAJ	MIN	RAT
	2020									14.	9.3	5.0	0.54	6.	7.2	4.6	0.65	-13.	5.2	2.6	0.49	0.	3.2	0.3	0.12				
	CFA	CFR	CFZ	TRZ	PRJ	TAV	RAV	AZ-CG-RU		AREA	ER	AZ-CG-RU		AREA	ER	AZ-CG-RU		AREA	ER	AZ-CG-RU		AREA	ER	AZ-CG-RU	AREA	ER
								73.4	65.7	148	22	73.9	65.9	106	31	73.0	66.4	44	45	72.0	67.0	4	100			
	73.1	66.2	2.5	142	1.4	-2	0.4	73.9	65.5	159	33	73.4	66.0	107	40	72.8	66.4	55	48	72.2	66.9	4	85			
Cell C	TIME									THTA	MAJ	MIN	RAT	THTA	MAJ	MIN	RAT	THTA	MAJ	MIN	RAT	THTA	MAJ	MIN	RAT	THTA	MAJ	MIN	RAT
	1835									2.	8.3	3.2	0.38	5.	7.4	2.7	0.36	8.	5.6	2.4	0.43	15.	3.1	1.6	0.51				
	CFA	CFR	CFZ	TRZ	PRJ	TAV	RAV	AZ-CG-RU		AREA	ER	AZ-CG-RU		AREA	ER	AZ-CG-RU		AREA	ER	AZ-CG-RU		AREA	ER	AZ-CG-RU	AREA	ER
								57.0	20.3	84	17	56.9	19.9	64	31	57.5	19.6	44	30	58.5	19.2	16	81			
	57.4	19.7	2.5	-33	1.2	9	0.4	56.6	20.2	88	19	57.2	19.9	64	31	57.7	19.6	40	35	58.2	19.2	16	81			
	TIME									THTA	MAJ	MIN	RAT	THTA	MAJ	MIN	RAT	THTA	MAJ	MIN	RAT	THTA	MAJ	MIN	RAT	THTA	MAJ	MIN	RAT
	1850									-0.	8.6	2.5	0.29	2.	7.8	2.1	0.28	2.	5.8	1.5	0.25	0.	4.8	0.5	0.10				
	CFA	CFR	CFZ	TRZ	PRJ	TAV	RAV	AZ-CG-RU		AREA	ER	AZ-CG-RU		AREA	ER	AZ-CG-RU		AREA	ER	AZ-CG-RU		AREA	ER	AZ-CG-RU	AREA	ER
								54.2	20.9	70	15	54.5	20.7	54	28	56.2	20.5	28	25	57.0	20.0	8	0			
	55.5	20.5	2.5	-16	2.1	1	0.2	53.9	21.0	77	18	54.9	20.7	54	23	56.0	20.4	31	44	57.0	20.1	8	40			
	TIME									THTA	MAJ	MIN	RAT	THTA	MAJ	MIN	RAT	THTA	MAJ	MIN	RAT	THTA	MAJ	MIN	RAT	THTA	MAJ	MIN	RAT
	1905									0.	7.2	1.0	0.14	0.	7.2	1.0	0.14	1.	5.0	0.8	0.17								
	CFA	CFR	CFZ	TRZ	PRJ	TAV	RAV	AZ-CG-RU		AREA	ER	AZ-CG-RU		AREA	ER	AZ-CG-RU		AREA	ER	AZ-CG-RU		AREA	ER	AZ-CG-RU	AREA	ER
								55.0	22.5	24	0	55.0	22.5	24	0	56.2	22.2	14	0							
	55.4	22.4	2.0	-9	1.4	0	0.1	54.7	22.5	27	0	55.4	22.4	20	-6	56.1	22.3	14	0							

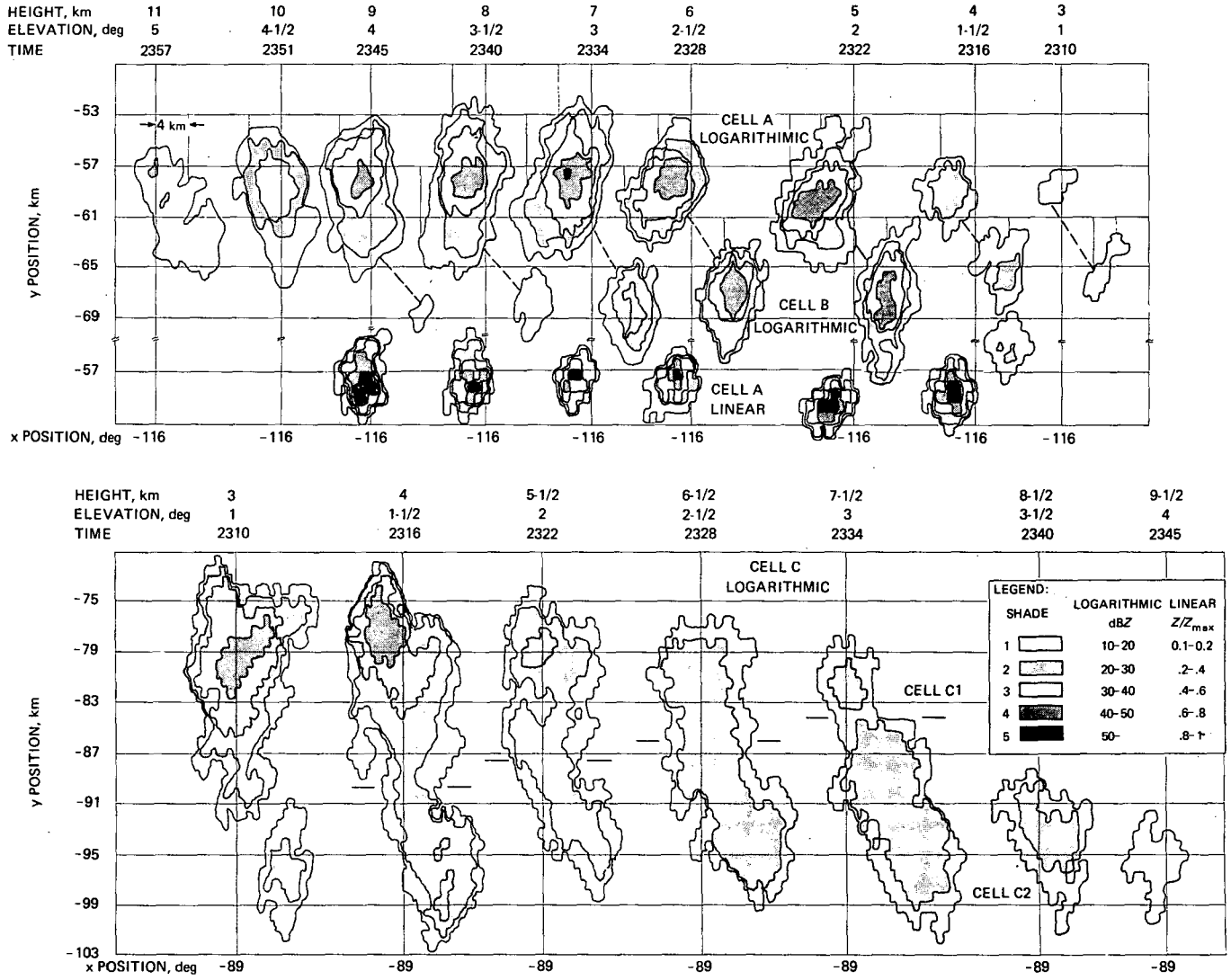

Figure 7-1.—MIT-LL preprocessed-data map versus elevation.

AZIMUTH	RAW DATA
114	00112100
116	02233210
118	13444220
120	35443210
122	45433100
124	33332210
126	21121111
130	01121100
132	12222111
134	23232121
136	23332221
138	23432221
140	23432221
142	04433332
144	04433331
146	03444320
148	01444310
150	00445321
152	00345431
154	00234332
156	00124211
158	00033000

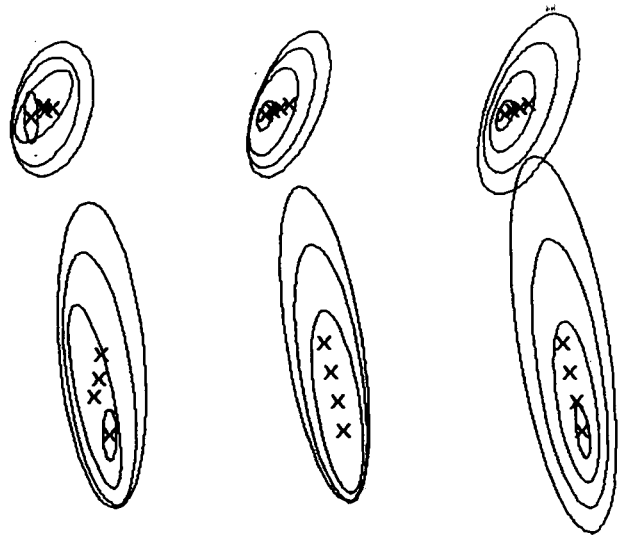

(a)

110	022111
112	033222
114	144221
116	144322
118	354322
120	554221
122	444211
124	344100
126	123100
128	021000
134	22110000
136	22211110
138	23221110
140	23222120
142	23222210
144	13332200
146	24333200
148	24343210
150	34344310
152	14444310
154	04443210
156	02453221
158	00343331
160	00244442
162	00022442
164	00001331
166	00000122
168	00000012

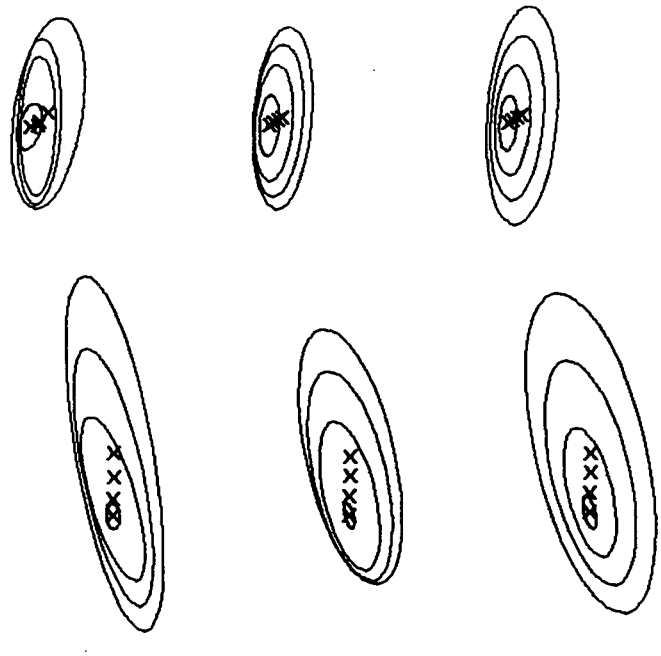

(b)

Figure 7-2.—NSSL data and plots. (a) Time 1735. (b) Time 1750.

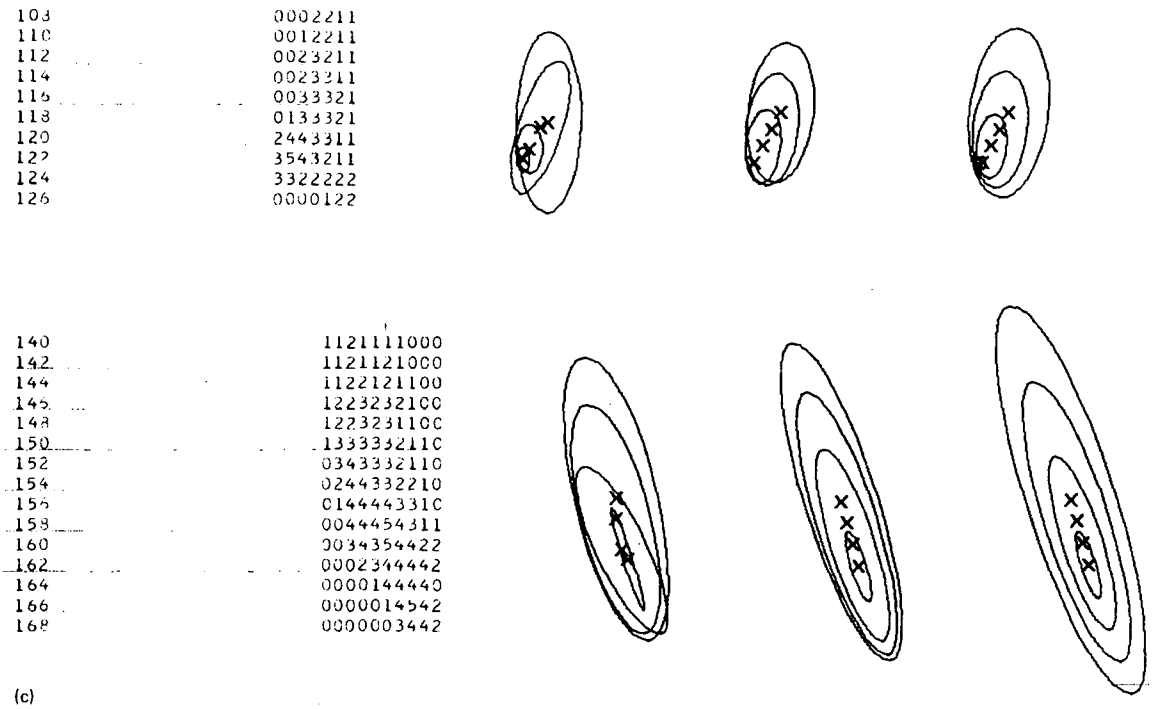

(c)

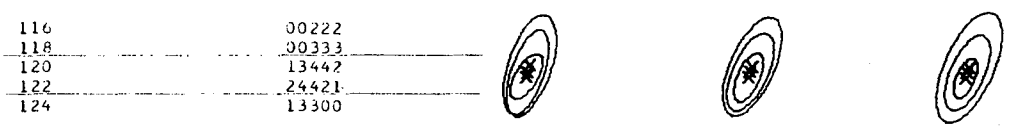

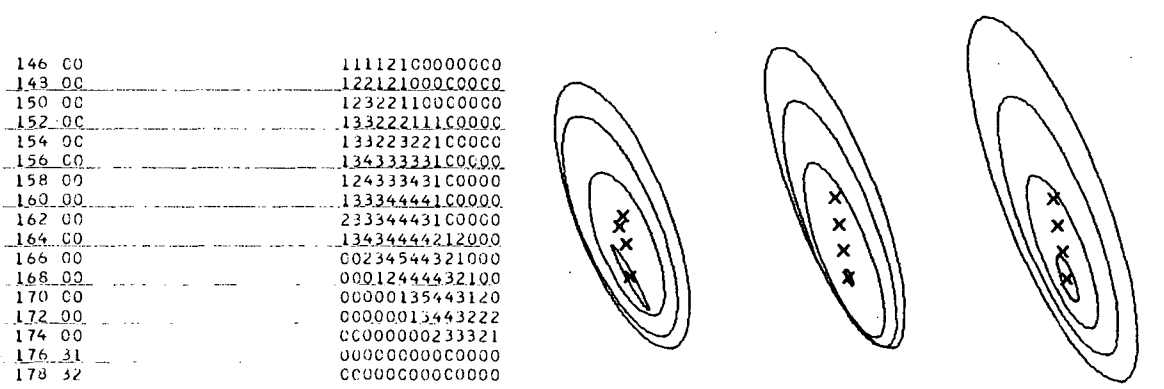

(d)

Figure 7-2 (continued).—(c) Time 1805. (d) Time 1820.

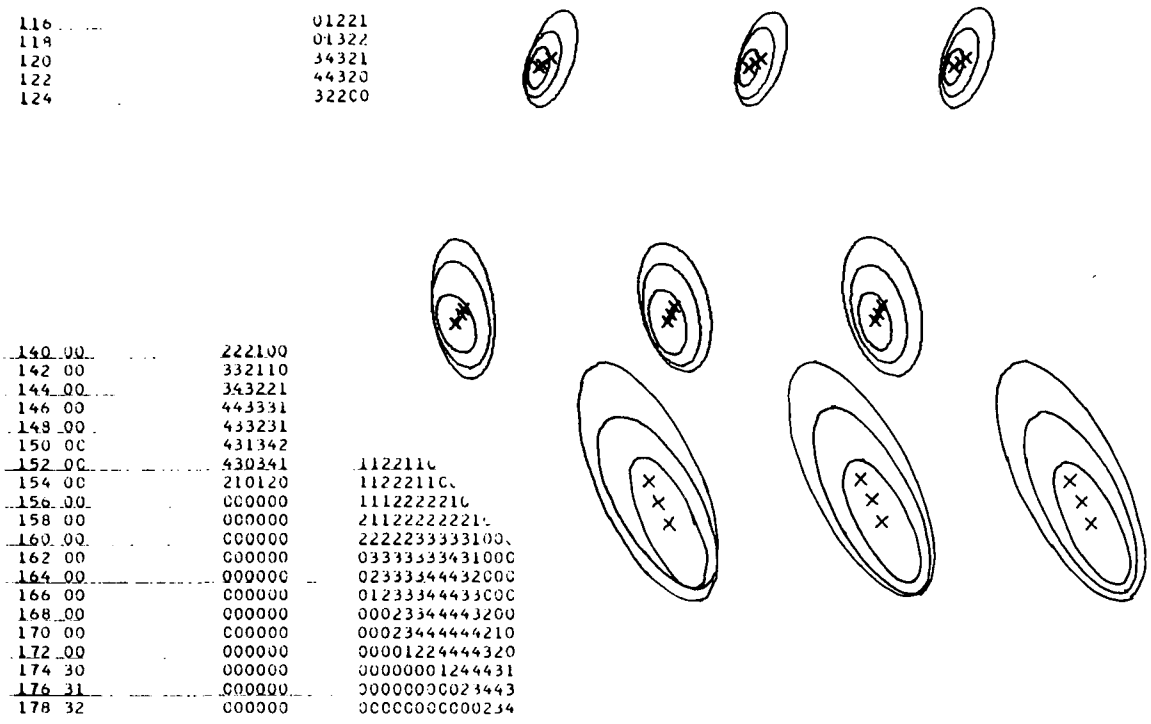

(e)

Figure 7-2 (concluded).—(e) Time 1835.

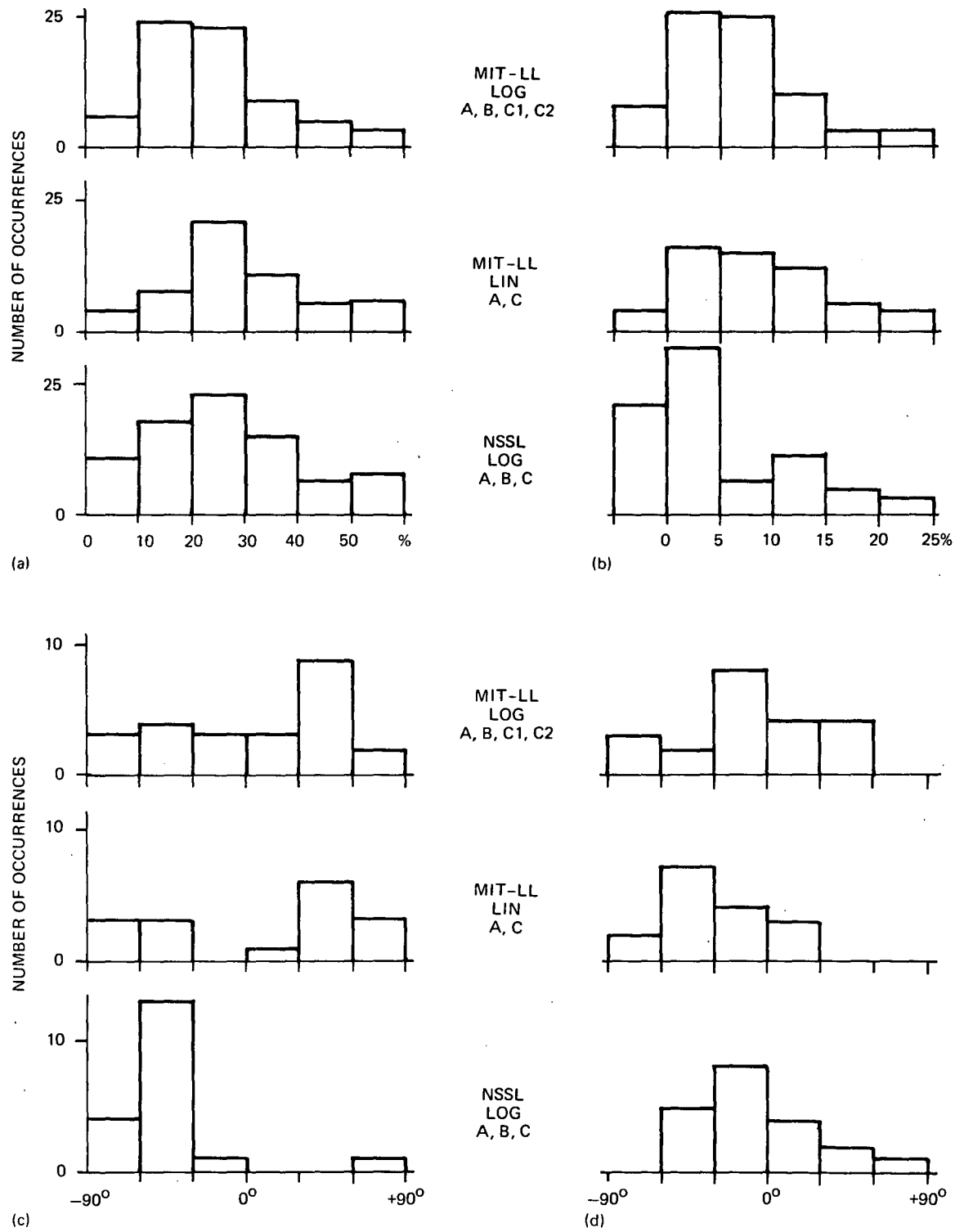

Figure 7.3.—Histograms of error measures. (a) Individual errors. (b) Set minus individual errors. (c) TAV. (d) TRZ minus TAV.

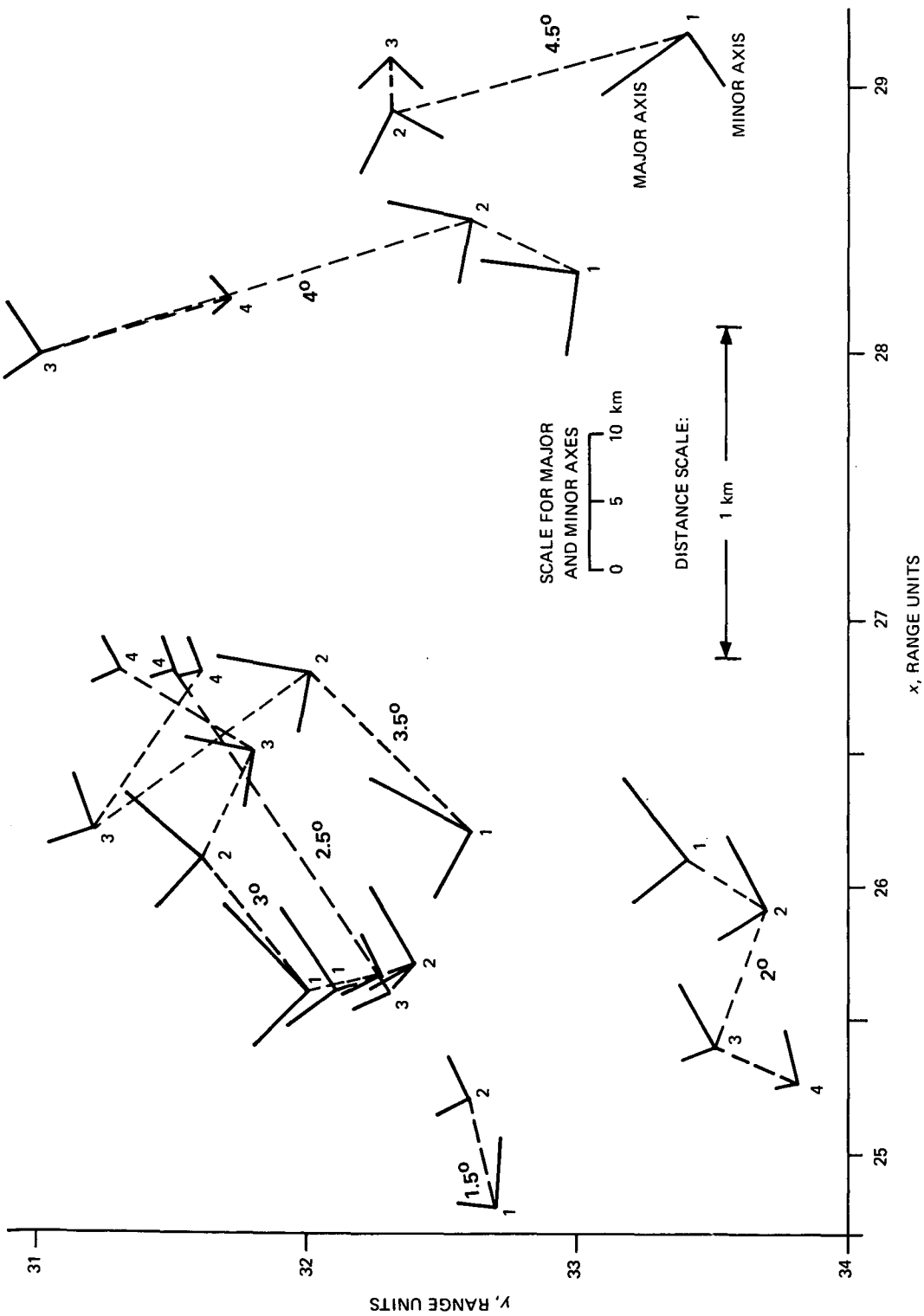

Figure 7-4.–MIT-LL cell A plotted individual-ellipse data.

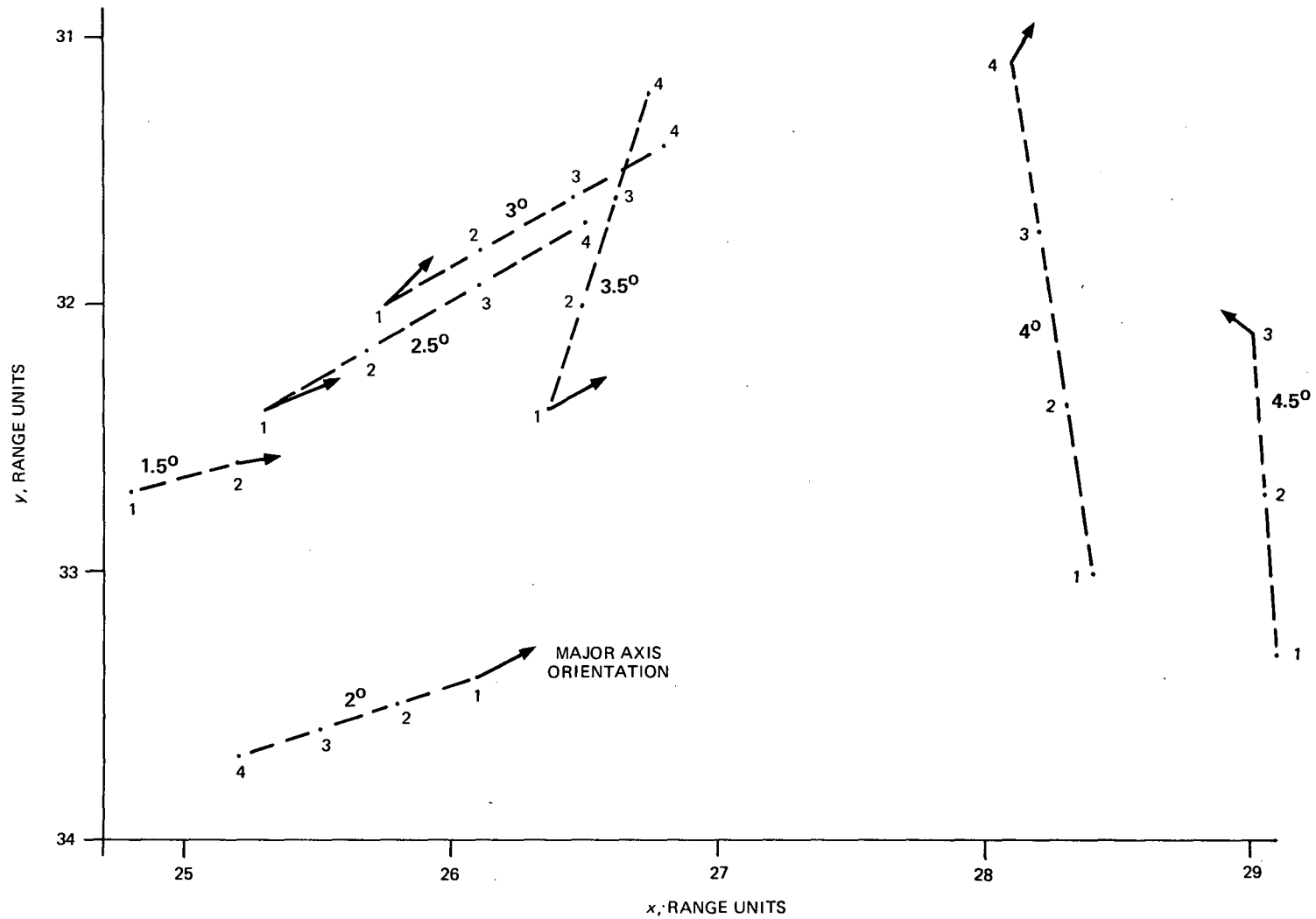

Figure 7-5.—MIT-LL cell A plotted ellipse-set data.

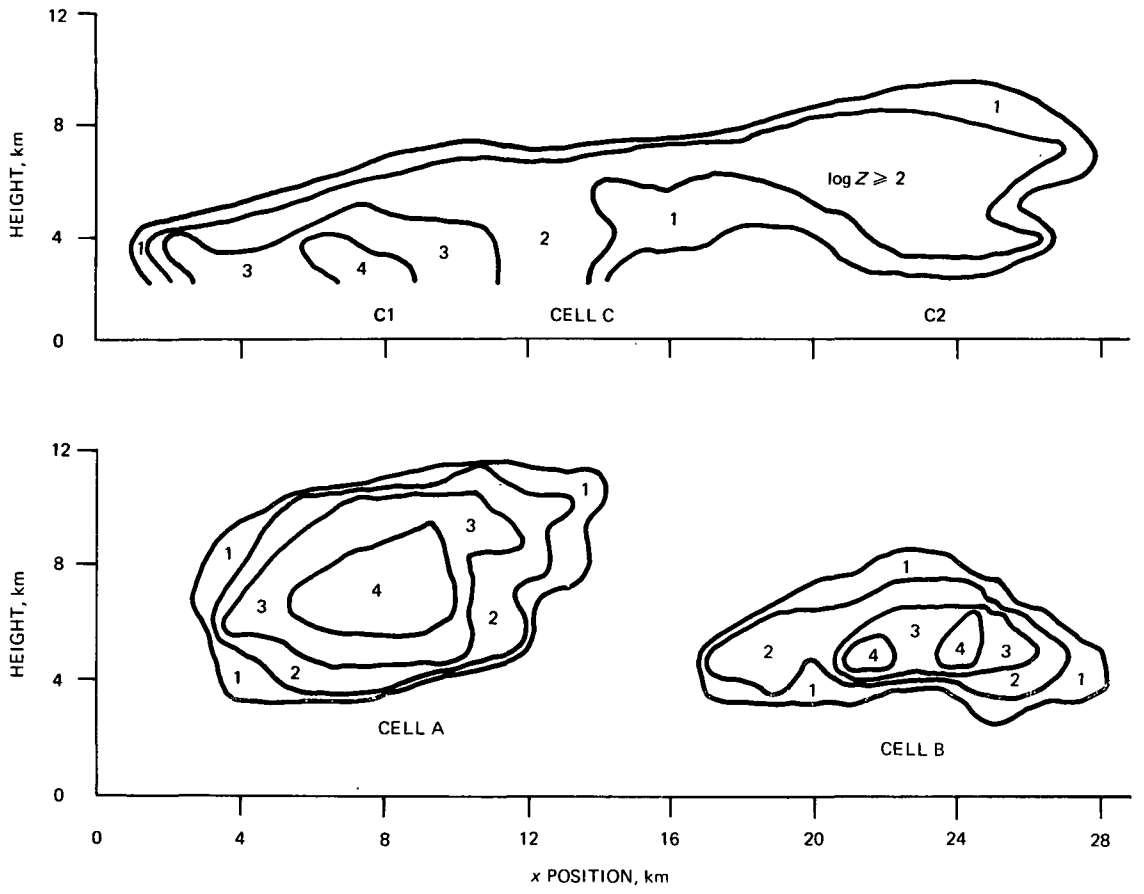

Figure 7-6.—Vertical sections through MIT-LL cells A, B, and C.

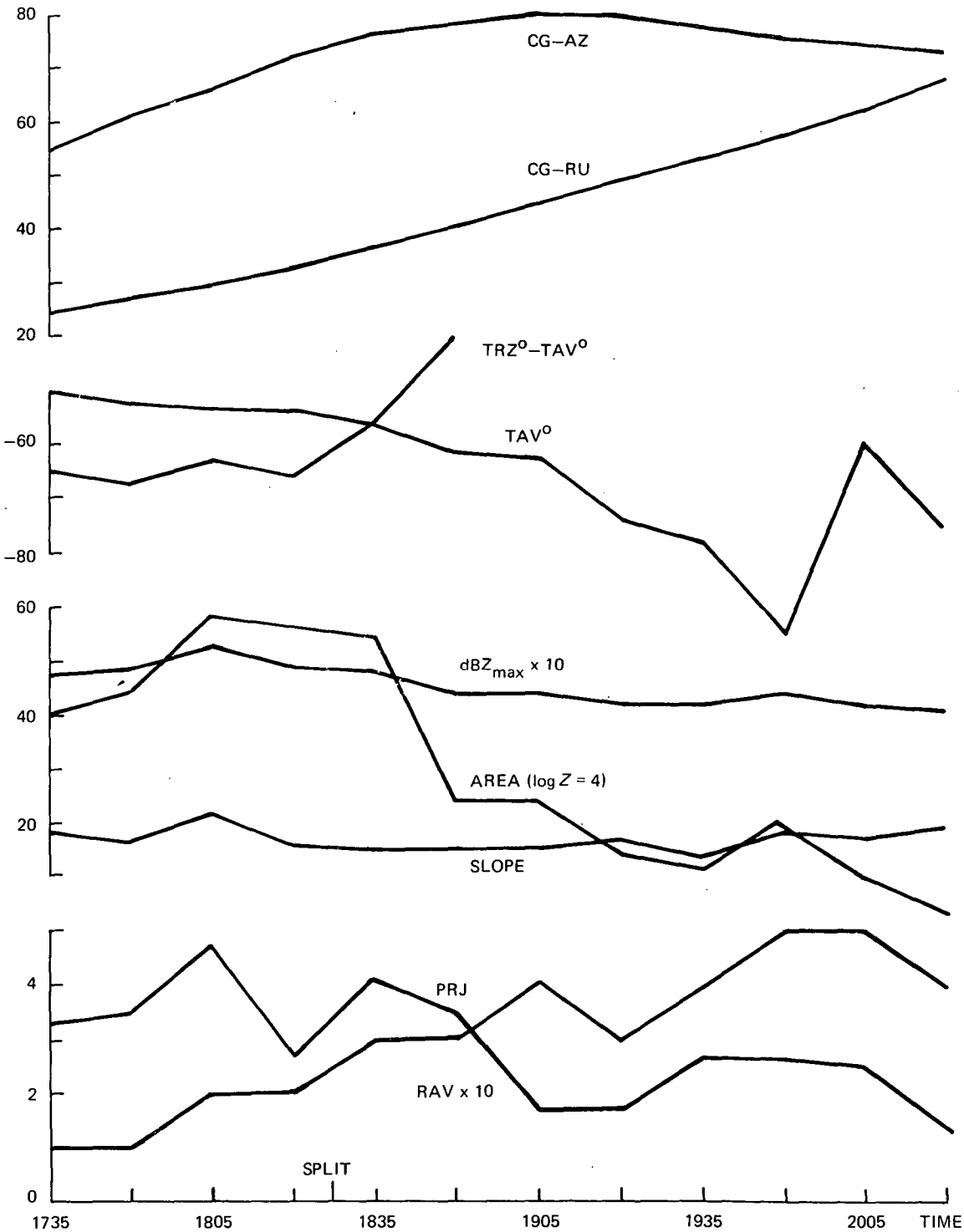

Figure 7-7.—Temporal characteristics of NSSL cell B.

Section 8
CONCLUSIONS

It has been shown that intense storm cells can be usefully represented by digitized weather data with a resolution of 1 to 2 km. Any deficiency in such resolution is partly compensated by the interpolation and extrapolation from adjacent data using the models summarized below. This is important in reducing the quantity of input data required and the number of parameters needed by the model. Height slices 2 km apart and a repetition rate of four scans per hour seem adequate, but this judgment may be based on inadequate sampling. Linear stratification in Z instead of log Z is useful for detailed storm core studies but requires a large number of intensity levels in the input data unless only the most intense cells are of interest. This may not be the case as higher frequencies come into use, which are subject to greater attenuation by the lower intensity areas within a storm.

Using the above data and contours of constant reflectivity, it was found that–

(1) Individual horizontal contours of log Z are fairly well fitted by ellipses.

(2) Sets of contours for different reflectivities at a given time and height are very well fitted by assumption of constant ellipse orientation, ellipticity, and uniform spacing of ellipse centers on a straight line, about 20° ccw from the major axes.

(3) The ellipse areas in a set were found to vary directly with log Z, in agreement with results of other observers.

(4) For related sets at different heights or lateral positions, fitted ellipse parameters were found to vary slowly and uniformly except for the effect of vertical wind shear, so that the best model appears to be nested, vertical elliptical cylinders.

Too few cells were studied to generalize the results, but an effective core diameter of about 3.5 km was indicated with a favored ellipse orientation of northeast to southwest for the strongest storm studied.

A comparison was made of the attenuations along paths through the centers of five horizontal sections of MIT-LL cell A as observed and as modeled by ellipse sets. The agreement at three of the levels was excellent, but at two levels it was degraded because the orientation of the core log $Z = 4$ ellipse remained relatively constant with height, whereas the average rotated ccw. It may therefore improve the model for some purposes to use the core orientation for the ellipse set instead of the average of the individual orientations.

Many more storm cells should be processed to verify the model parameters derived and to suggest appropriate methods for treating splitting cells, or at least to indicate the magnitude of the problem.

REFERENCES

1. Rogers, R. R.; and Rao, K. M.: "Attenuation Statistics for Application to Microwave Communication Links." *Proc. 13th Radar Meteorol. Conf.*, Aug. 1968, pp. 286-289. (Also published as McGill Univ. Stormy Weather Group Tech. Rept. MW-52, Jan. 1968.)

2. Amorocho, J.; and Morgan, Don: "Convective Storm Field Simulation for Distributed Catchment Models." Paper presented at Int. Symp. Math. Models in Hydrology (Warsaw), 1971.

3. Hudlow, Michael: "Three-Dimensional Model of Precipitation Echoes for X-Band Radar Data Collected During Bomex." *Bomex Bull. no.10,* National Oceanic and Atmospheric Administration, June 1971, pp. 51-62.

4. Shaw, R. W.: "Motion of Radar Echoes Within a Cloud Envelope." *14th Radar Meteorol. Conf.,* Amer. Meteorol. Soc. (Boston), 1970.

5. Bilham, E. G.: *Classification of Heavy Falls of Rain in Short Periods.* HMSO (London), 1962.

6. Altman, F. J.: *Precipitation Scatter Interference Between Space and Terrestrial Communication Systems.* Rept. 453340, Communication Systems, Inc. (now Computer Sciences Corp.), Oct. 1967. (Also published as NASA CR-90108, Oct. 1967.)

7. Altman, F. J.: *Prediction of Hydrometeor Reflectivity Profiles.* Rept. 6012-1, Computer Sciences Corp., Sept. 1970.

8. Altman, F. J.: *Rainfall Distribution Models.* Rept. 6012-2, Computer Sciences Corp., Apr. 1971.

9. Huff, F. A.: "Spatial Distribution of Heavy Storm Rainfalls in Illinois." *Water Resour. Res.* 4(1): 47-54, Feb. 1968.

10. Browning, K. A.; and Fujita, T.: *A Family Outbreak of Severe Local Storms—A Comprehensive Study of the Storms in Oklahoma on 26 May 1963.* Rept. 65-695(1), Air Force Cambridge Res. Labs., 1965.

11. Dennis, A. S.: *Rainfall Determinations by Meteorological Satellite Radar.* Final Report, Project 4080, Stanford Res. Inst., 1963.

12. Wilk, K. E.; Watts, W. L.; Sirmans, D.; Lhermitte, R. M.; Kessler, E.; and Gray, K. C.: *Weather Radar Data System at the National Severe Storms Laboratory.* Tech. Circ. no 4, National Severe Storms Lab., Norman, Okla., Oct. 1967.

13. Court, A.: "Area-Depth Rainfall Formulas." *J. Geophys. Res.* 66(6): 1823-1831, 1961.

14. Eagleson, P. S.: *Dynamic Hydrology*. McGraw-Hill Book Co., Inc., 1970.

15. Lee, David R; and Sallee, G. Thomas: "A Method of Measuring Shape." *Geog. Rev.* 60(4): 555-563, Oct. 1970.

16. Zawadski, I. I.; and Rogers, R. R.: *ADA: An Instrument for Real-Time Display of Microwave Attenuation Due to Rain*. McGill Univ. Stormy Weather Group Tech. Rept. MWT-6, Sept. 1969.

NASA–GSFC